FUNCTIONS OF DELETED IN LIVER CANCER 1 (DLC1)
IN CELL DYNAMICS

ZHONG DANDAN

(B.Sc, Xiamen University, China)

A THESIS SUBMITTED

FOR THE DEGREE OF DOCTOR OF PHILOSOPHY

DEPARTMENT OF BIOLOGICAL SCIENCES

NATIONAL UNIVERSITY OF SINGAPORE

2008

ACKNOWLEDGEMENTS

Zhong Dandan

Jan.2008

TABLE OF CONTENTS

CHAPTER 1 INTRODUCTION

CHAPTER 2 MATERIALS AND METHODS

CHAPTER 3 RESULTS

SUMMARY

Deleted in Liver Cancer-1 (DLC1) is a multi-modular Rho GTPase-activating Protein (RhoGAP) and a tumor suppressor. In this study, the identification of eukaryotic elongation factor-1A1 (EF1A1) and BNIP-2 similar isoform alpha (BNIP-Sα) as two novel interacting partners of DLC1, the molecular mechanism and the functional significance of the interaction between EF1A1 and DLC1 will be presented.

DLC1 harbors 3 distinctive domains, i.e. the Sterile-Alpha Motif (SAM) at its N-terminus, the Steroidogenic Acute Regulatory-related Lipid Transfer (START) domain at the C-terminus and a conserved RhoGAP (GAP) domain close to the middle of the protein. Besides its RhoGAP domain, functions of other domains in DLC1 remain largely unknown. In my current study, EF1A1 was identified as a novel binding partner of DLC1-SAM domain by protein precipitation and mass spectrometry. Residues F38 and L39 within a hydrophobic patch on DLC1-SAM domain were identified as an indispensable EF1A1-interacting motif. DLC1-SAM recruits EF1A1 to membrane periphery and ruffles which plays an auxiliary role in DLC1's function in cell motility suppression. My current study also presents the novel interacting activity between the BNIP-2 and Cdc42GAP homology (BCH) domain of BNIP-Sα and DLC1. Three BNIP-Sα-interacting regions on DLC1 were delineated, including the START domain and two N-terminus regions between the SAM domain and the GAP domain. These findings shed light on the mechanisms of how other motifs of DLC1 cooperate with the RhoGAP activity to modulate DLC1's function in cell dynamic control.

membrane periphery and membrane ruffles.

LIST OF TABLES

LIST OF ABBREVIATIONS

BCH domain: BNIP-2 and Cdc42GAP homology domain

BNIP-2: Bcl2/adenovirus E1B 19D interacting Protein 2

BNIP-H: BNIP-2 Homology

BNIP-Sα: BNIP-2 Similar alpha

bp: base pair

BSA: bovine serum albumin

Cdc42: Cell Division Cycle 42

DAG: diacylglycerol

DLC1: Deleted in Liver Cancer 1

DMEM: Dulbecco's modified eagle medium

DNA: deoxyribonucleic acid

EF1A1: Elongation Factor 1A1

F-actin: filamentous actin

G-actin: globular actin

GAP: GTPase Activating Protein

GFP: Green Fluorescent Protein

GST: Glutathion S-transferase

GTP: Guanosine Triphosphate

HCC: hepatocellular carcinoma

IP: immunoprecipitation

IP$_3$, inositol-3,4,5-triphosphate

IPTG: isopropyl-thiogalactoside

Kb: kilobase

kD: kilodalton

l: litre

M: molarity, moles/dm^3

mg: milligram

min: minute

ml: millitre

mM: molarity, millimoles/dm^3

MW: molecular weight

OD: optical density

PAGE: polyacrylamide gel electrophoresis

PBS: phosphate buffered saline

PCR: polymerase chain reaction

PD: pull-down

PI(4)P: phosphatidylinositol-4-phopshate

PI(4,5)P_2: phosphatidylinositol-4,5-bisphopshate

PIP$_3$: phosphatidylinositol-3,4,5-bisphopshate

PLC: phospholipase C

Rac1: Ras-related C3 Botulinum Toxin Substrate 1

RhoA: Ras homologous member A

rpm: rotation per minute

SAM: Sterile Alpha Motif

SDS: sodium dodecyl sulfate

Sec: second

START: STAR-related lipid-Transfer

U: unit

µg: microgram

µl: microlitre

v/v: volumn by volumn

w/v: weight by volumn

WCL: whole cell lysate

X-gal: 5-bromo-4-chloro-3-indolyl-β-D-galactopyranoside

SYMPOSIA PRESENTATION

1. Zhong D, Low BC. Dissecting the Molecular Mechanism Underlying Cell Dynamics Control by Deleted in Liver Cancer 1 Protein (DLC1). Oral presentation. 9th Biological Science Graduate Congress, Chulalongkorn University, Bangkok, Thailand, December 16-18th, 2004.

2. Zhong D, Low BC. Dissecting the Molecular Mechanism Underlying Cell Dynamics Control by Deleted in Liver Cancer 1 Protein (DLC1). Third International Conference on Structural biology & Functional Genomics, Singapore, December 2-4th, 2004.

3. Zhong D, Low BC. Understanding the Role of Sterile Alpha Motif (SAM) Domain for the Function of DLC-1. 8th Biological Science Graduate Congress, Department of Biological Sciences, National University of Singapore, Singapore, December 3-6th, 2003.

Chapter 1

Introduction

1.1 Rho GTPase family

 Ras homologous (Rho) GTPases comprise a family of small guanosine triphosphatases (GTPases), which belong to the Ras GTPases monomeric G protein superfamily. To date, more than 20 members of Rho GTPases have been identified in humans (Wennerberg *et al.,* 2005). Based on their primary sequences and known functions, Rho GTPases can be roughly divided into 5 groups, the Rho-like, Rac-like, Cdc42-like, Rnd, and RhoBTB subfamilies (Figure 1.1) (Burridge and Wennerberg, 2004). RhoA, Rac1, and Cdc42 are the three best studied Rho GTPases (Hall, 2005). The following parts in the introduction will focus on their functions and the underlying molecular mechanisms in cell dynamic control.
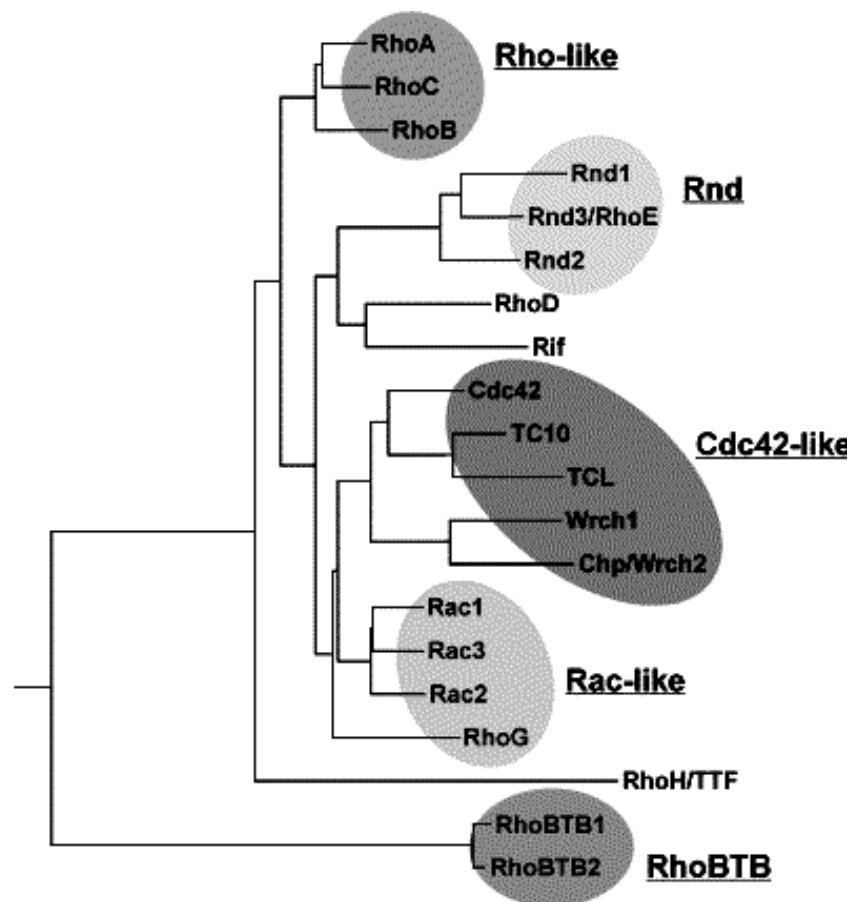
Figure 1.1 20 Rho GTPases can be divided into five subfamilies, Rho-like, Rnd, Cdc42-like, Rac-like, and RhoBTB. (Adapted from Burridge and Wennerberg, 2004.)

1.1.1 The Rho GTPase cycle

1.1.1.1 Mechanism of the Rho GTPase cycle

Each Rho GTPase contains one conserved G domain of around 20kDa, which can bind to GDP/GTP. With their G-domains, Rho GTPases can cycle between active GTP-bound state and inactive GDP-bound state like binary molecular switches (Figure 1.2) (Vetter and Wittinghofer, 2001).

RhoGTPases bind to GDP/GTP with a common biochemical mechanism. The G-domain of Rho GTPases folds into a conserved α/β structure forming a shallow surface pocket that accommodates guanine nucleotide (Scheffzek and Ahmadian, 2005). The binding to guanine nucleotide involves three regions in the G domain, including Switch I region, Switch II region and P-loop. Switch I and II regions contact γ-phosphate directly in the GTP-bound state, which results in considerable conformational difference of the G-domain compared to the GDP-bound state. Such conformational difference in the active state of Rho GTPases can be recognized by down-stream effectors, which only bind to and are activated by the active Rho GTPases. The G domain also has intrinsic GTPase ability to hydrolyze the bound GTP into GDP. But this intrinsic reaction is very slow. After the GTP hydrolysis, Rho GTPases return to the inactive state and terminate

downstream signaling. To turn back into activited status, the tightly-bound GDP on Rho GTPses then has to be released for the exchange of the next GTP (Scheffzek and Ahmadian, 2005).

1.1.1.2 Regulators in the RhoGTPase cycle

The transitions between the two states of Rho GTPases are regulated by three types of molecules inside the cell: guanine nucleotide exchange factors (GEFs), GTPase activating proteins (GAPs) and guanine nucleotide dissociation inhibitors (GDIs). When Rho proteins are in active state, they can interact with downstream effectors and lead to cellular effects (Figure 1.2).
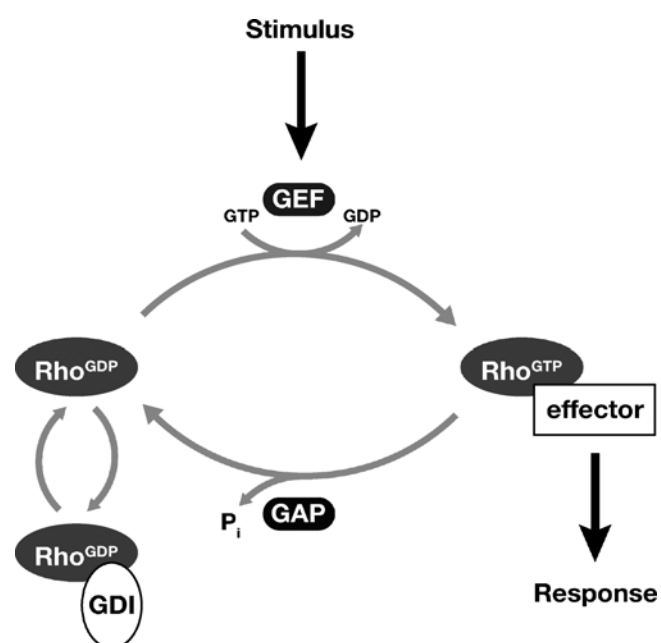
Figure 1.2 The Rho GTPase cycle mediates cellular response downstream of extracellular stimuli. The cycle is regulated by GEFs, GAPs and GDIs. When Rho

GTPases are in active state, they can interact with effectors and lead to cellular response. (Adapted from Jaffe and Hall, 2005.)

GEFs are activators of Rho GTPases. In the Rho GTPase cycle, the GDP-GTP exchange reaction is the rate limiting step. GEFs catalyze the exchange of GDP for GTP by increasing the rate of GDP dissociation from Rho proteins (Erickson and Cerione, 2004). GEFs activate Rho GTPases upon the stimulation of growth factors and some extracellular agents. There are 85 GEFs found in human genome. Since the upregulation of many Rho GTPases contributes to oncogenesis, there is no wonder why many GEFs, as the activators of Rho proteins, were identified as oncogenes (Hall, 2005).

RhoGAPs are negative regulators of Rho GTPases. In the active state of Rho GTPases, the GTP-hydrolysis by the intrinsic activity of its G-domain is very slow. The inactivation of Rho GTPases by RhoGAPs is achieved by stimulating the GTPase activity of Rho GTPases and promoting the hydrolysis of bound GTP to GDP.

GDIs form in complexes with Rho GTPases to regulate their intracellular localizations and block their downstream cellular effects (Olofsson, 1999). GDIs conduct three kinds of biochemical activities on Rho GTPases to downregulate the biological effects of Rho proteins. First, they keep Rho GTPases in inactive states, by inhibiting the dissociation of GDP from Rho GTPases and blocking the activation by GEFs. Second, GDIs interact with GTP-bound Rho proteins, inhibiting GTP hydrolysis and blocking their interaction with downstream effectors. Third, GDIs can regulate the cycling of Rho

4

GTPases between cytosol and membranes where such effectors are located (DerMardirossian and Bokoch, 2005).

1.1.2 Cellular functions of Rho GTPases

Rho GTPases are key regulators down-stream of extracellular-stimuli that regulate a diverse set of biological activities, including cytoskeleton organization, vesicle transport, cell polarity, cell cycle progression, gene expression, enzymatic activation, differentiation and oncogenesis (Etienne-Manneville and Hall, 2002).

1.1.2.1 Rho GTPases are key regulators of actin cytoskeleton

The first characterized function of Rho GTPases is their regulation on cytoskeleton reorganization. Rho GTPases are key regulators of actin cytoskeleton that link extracellular signals and cell surface receptors to the dynamic organization of actin cytoskeleton. It is well known that Rho regulates the formation of contractile actin-myosin filaments to form stress fibers and the assembly of focal adhesion complexes in response to lysophosphatidic acid (LPA) or integrin engagement. Rac induces actin polymerization that lead to the assembly of a meshwork of actin filaments at the cell periphery to form sheet-like lamellipodia and membrane ruffles in response to platelet-derived growth factor (PDGF), epidermal growth factor (EGF) or insulin. Cdc42 triggers actin filament assembly and bundling at the cell periphery to form actin-rich

protrusions on the cell surface called filopodia or shorter protrusions call microspikes in response to bradykinin and interleukin 1 (IL-1) (Figure 1.3) (Alberts *et al.,* 2002; Hall, 1998; Nobes and Hall, 1995; Hall, 2005).
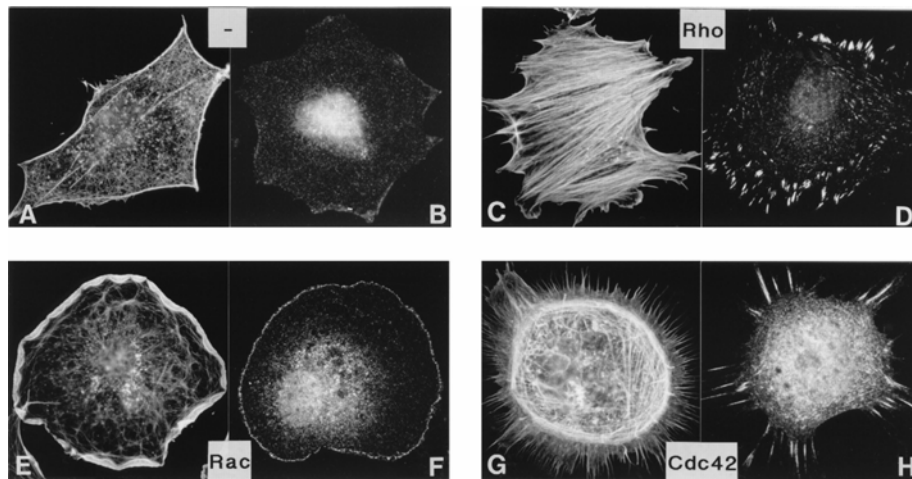
Figure 1.3 Roles of Rho, Rac, and Cdc42 in actin cytoskeleton organization. Compared with quiescent cells (-), active Rho induces the formation of stress fiber and focal adhesion while active Rac and active Cdc42 induce the formation of lamellipodia and filopodia respectively. Actin filaments were shown in A, C, E and G and adhesion complexes were shown in B, D, F, and H. (Adapted from Hall, 1998.)

1.1.2.2 Rho GTPases in cell adhesion and cell migration control

Cytoskeleton makes up the framework for eukaryotic cells. Dynamic reorganization of cytoskeleton is the basis of many other cellular activities, such as vesicle trafficking, cell adhesion, endocytosis, cell migration and morphological changes during the process of apoptosis. The key roles of Rho GTPases on cytoskeleton

reorganization are closely related to their ability in the regulation of other cellular activities coordinate with actin dynamics, including cell adhesion and cell migration. For cell adhesion, Rho activity is required in the assembly of integrin-based focal complexes in cell attachment to extracellular matrix. Besides, Rho GTPases regulate the formation and maintenance of cadherin-based cell-cell adhesion complexes (Hall, 1998; Malliri and Collard, 2003). For cell migration, dynamic rearrangement of cytoskeleton provides the driving force for migration in animal cells. In this process, actin polymerization and filament elongation at the front and actin:myosin filament contraction at the rear are required for directed cell migration *in vivo*, which are controlled by the coordinate regulation of Rac, Rho and Cdc42. Active Rac accumulates at the front of migrating cells to form lamellipodia and membrane ruffles to push forward the leading edge membrane. Rho induces stress fibers and generates contractile forces at the rear of the cells to move cell body forward. Cdc42 senses the extracellular cues and establishes the cell polarity, which determines the localization of active Rac and makes the cell movement directional (Jaffe and Hall, 2005). In addition to actin dynamics, Rho GTPases also regulate microtubule dynamics involved in cell migration (Malliri and Collard, 2003).

1.1.2.3 Rho GTPases in cell cycle control

Rho GTPases also play important roles in cell cycle progression. First, they contribute to G1 phase progression. Second, Rho GTPases are crutial for the reorganization of the microtubule and actin cytoskeletons during M phase (Jaffe and Hall,

2005). The importance of Rho GTPases in cell cycle control is further supported by the evidence that their activities are essential for Ras-induced cell transformation (Hall, 1998). The roles of Rho GTPases in cell cycle control implicate that their deregulation will consequently contribute to malignant transformation and cancers (Villalonga and Ridley, 2006).

1.1.2.4 Rho GTPases in oncogenesis

Besides the role of Rho GTPases in cell cycle control, their functions in cytoskeleton reorganization, cell adhesion, migration and gene expression also contribute to oncogenesis. Deregulation of Rho GTPases contributes to the growth, survival and invasiveness of tumor cells. There have been many evidences showing aberrant Rho signaling or elevated Rho expression in the formation and progression of tumors. Early indications of the role of Rho GTPases in oncogenesis came from *in vitro* transformation studies of fibroblasts. Constitutively active Rac1 (V12Rac) and RhoA (V14RhoA) or overexpression of Rho proteins were able to transform normal cells (Prendergast *et al.*, 1995; van Leeuwen *et al.*, 1995). The transforming capacity of Rho GTPases is correlated with the fact that they mediate downstream effects of oncogenic Ras activity in tumors (Khosravi-Far *et al.*, 1995). It is now clear that Rac signaling is required for oncogenic Ras-induced tumorigenesis, in which Rac stimulates cell growth and enhances cell survival under cellular stress (Joneson and Bar-Sagi, 1999). More recently, *in vivo* studies using knockout and transgenic mice of various Rho GTPases demonstrated that the

deregulation of Rho GTPases contributes to various aspects of oncogenesis besides transformation. Rho GTPases affect the process of tumor invasion/metastasis through their pivotal roles in cytoskeleton organization, cell-cell adhesion and migration (Malliri *et al.*, 2002; Hakem *et al.*, 2005; Cleverley *et al.*, 2000). Furthermore, some Rho proteins, such as RhoC and Rac3, are shown to be upregulated in more metastatic cancers (Kandpal, 2006). The role of Rho GTPases in oncogenesis has made them promising targets for anti-cancer drug research.

1.1.3 The downstream effectors of Rho GTPases

In the Rho GTPase cycle, binding of GTP induces conformational changes of Rho GTPases, after which they can interact with downstream effectors to mediate various cellular functions. To date, there are more than 50 effectors identified for Rho, Rac and Cdc42, including serine/threonine kinases, tyrosine kinases, lipid kinases, lipases, oxidases and scaffold proteins (Jaffe and Hall, 2005). According to their specificity towards Rho GTPases and the interaction region homology, they can be divided into two groups, effectors targeting RhoA and effectors targeting Cdc42 and Rac.

1.1.3.1 Effectors targeting Rho

Rho mediates their cellular functions via specific effectors, including

serine/threonine protein kinases and scaffold proteins (Dvorsky *et al.*, 2004). Rho effectors recognizes and binds to active Rho, i.e. Rho in GTP-bound state, through Rho binding domains (RBD) within their coiled-coil regions (Bishop and Hall, 2000; Wheeler and Ridley, 2004).

Many effectors of RhoA are implicated in actin reorganization and actin-related activities. Among them, mDia and ROCK are the key molecules that mediate RhoA-induced stress fiber formation. mDia promotes linear elongation of actin filaments at the barbed ends upon activation by RhoA-GTP, while ROCK mediates the cross-linking of myosin to actin and leads to the assembly of contractile actin:myosin filaments induced by RhoA (Riento and Ridley, 2003; Hall, 2005; Jaffe and Hall, 2005).

1.1.3.2 Effectors of Rac and Cdc42

Rac and Cdc42 have relatively high (around 70%) sequence identity and they have some common effectors. Correspondingly, their effectors contain a common 15-residue long binding motif to target Rac/Cdc42, which is called Cdc42/Rac-interactive binding (CRIB) motif (Hakoshima *et al.*, 2003). The CRIB motif was first identified as a consensus Cdc42-binding sequence for the serine/threonine kinase PAK-1 (p21-activated kinase 1) and the activated Cdc42-associated tyrosine kinase (ACK) (Bishop and Hall, 2000). Later study found that the CRIB motif is essential for the interaction of these effectors with Cdc42 or Rac and it only recognizes GTP-bound Rac/Cdc42. So through

the CRIB motifs, effectors are able to mediate downstream effects of activated Rac/Cdc42.

Currently, several CRIB-motif containing proteins have been identified. Among these effectors, PAKs and the Wiskott-Aldrich syndrome protein (WASP) are the best studied. PAK kinases can interact with Cdc42 and Rac, and mediate the activation of c-JUN kinase and p38 MAP kinase. PAKs also link Cdc42 and Rac to cytoskeletal components such as myosin light chain kinase, which are involved in Cdc42/Rac-induced cytoskeleton rearrangements and cell migration (Hoffman and Cerione, 2000). WASP directly interacts with actin-related protein 2/3 (Arp2/3) to promote the branched actin polymerization and leads to filopodia formation induced by Cdc42 (Millard *et al.*, 2004).

1.2 The RhoGAP family

1.2.1 Structural mechanism of the Rho GTPase-downregulation by RhoGAPs

The RhoGAP family is defined by the presence of a conserved RhoGAP domain in the primary sequence that consists of about 150 amino acids and shares at least 20% sequence identity with other family members (Moon and Zheng, 2003).

The RhoGAP domain consists of nine alpha helices. A highly conserved arginine residue is presented in a loop structure (Moon and Zheng, 2003). The conserved arginine residue is essential for the GAP activity and is generally called as "Arginine finger". In

RhoGAP-stimulating GTP hydrolysis, the long side chain of this arginine residue allows it to "dip" like a finger into the GTP-binding pocket of G-domain and to stabilize the negative-charged core during the transition state of GTP hydrolysis with its positively charged guanidinium group. The significance of this Arginine finger has been further confirmed by mutational approaches. Mutation of this arginine residue into alanine or lysine greatly decreases the GAP activity of most RhoGAPs though they maintain binding capacity towards their target Rho GTPases (Nassar *et al.*, 1998; Li *et al.*, 1997).

1.2.2 The complexity of RhoGAPs for the regulation towards Rho GTPases

Although RhoGAPs share a common structural mechanism to down-regulate Rho GTPases, the regulation process is very complex at the same time. There are more than 70 RhoGAPs identified in mammals and 59 to 70 RhoGAP-domain containing proteins predicted from human genome (Figure 1.4) (Tcherkezian and Lamarche-Vane, 2007), much more than the 22 isoforms of Rho GTPases. The excess of RhoGAPs indicates that the regulation of Rho GTPases by RhoGAPs is specific and complex. This is illustrated by the fact that every Rho GTPase is regulated by multiple GAPs and many members of RhoGAPs have GAP activity towards different Rho GTPases. The complexity of their regulation is further enhanced by the fact that all GAPs carry multiple protein modules, the functions of which remain largely unknown. These protein modules include catalytic domains such as protein kinase, Rho GEF and ArfGAP domains, protein-protein and protein-lipid adaptor modules such as SH2, SH3, PH and CR domains,

BCH domain as well as the conserved RhoGAP domains (Figure 1.4) (Moon and Zheng, 2003). The varying combination of modules could serve to regulate the dynamic disposition, activity as well as an anchorage of molecular assembly in different temporal and spatial manners. Thus, aside from being negative regulators of Rho GTPases, RhoGAPs play important roles in many aspects of cell dynamics control by integrating other signaling pathways with Rho GTPases pathways.
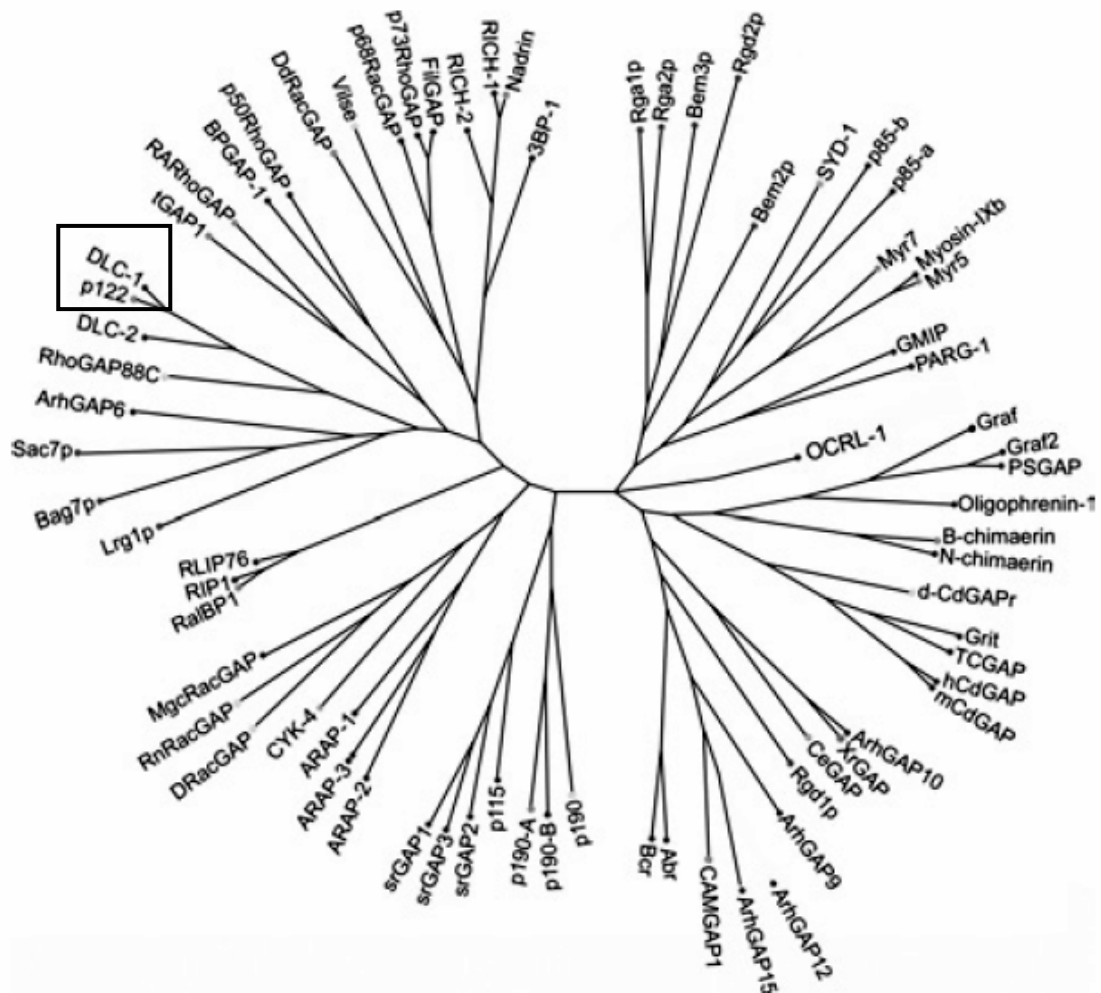
Figure 1.4 Phylogenic tree of the RhoGAP family. 73 RhoGAPs from yeast to human were aligned for their RhoGAP domains using the ClustalW program. The focus of this

study, human DLC1 protein and its rat homologue p122RhoGAP, are highlighted in a box. (Adapted from Tcherkezian and Lamarche-Vane, 2007.)

1.2.3 Cellular functions of RhoGAPs

1.2.3.1 RhoGAPs in cell migration

As Rho GTPases are key regulators of cytoskeletal dynamics, some RhoGAPs play important roles in cell migration. One mouse RhoGAP, ARAP3, was found to inhibit cell spreading and cell migration (Tcherkezian and Lamarche-Vane, 2007). The Cdc42 specific srGAP participates in a pathway of neuronal cell migration (Wong *et al.,* 2001). Recently, our group identified BPGAP1 as a novel RhoGAP that coordinately regulates pseudopodia and cell migration via the interplay of its BNIP-2 and Cdc42GAP Homology (BCH) domain, RhoGAP domain and proline-rich region. Furthermore, we showed that BPGAP1 interacts with a cortical actin binding protein, Cortactin, and facilitates its translocation to cell periphery to enhance cell migration (Shang *et al.,* 2003; Lua and Low, 2004).

1.2.3.2 RhoGAPs in endocytosis and molecule trafficking

Rho GTPases have emerged as important regulators of endocytosis and intracellular molecule trafficking, and RhoGAPs could play a role in such processes

(Moon and Zheng, 2003). The human RLIP76 interacts with a number of proteins involved in endocytosis and it was suggested to play a pivotal role in Ral-mediated protein trafficking by integrating Ral and Rho signaling (Awasthi *et al.*, 2003). TCGAP has been reported to be involved in insulin-mediated glucose-transport signaling (Chiang *et al.*, 2003). Recently, our group showed that BPGAP1 interacts with endocytic protein EEN/endophilin II and they together mediate EGFR (epidermal growth factor receptor) endocytosis and the activation of ERK signaling (Lua and Low, 2005).

1.2.3.3 RhoGAPs in cell growth, apoptosis and differentiation

Rho GTPases regulate cell growth and differentiation. RhoGAPs, as the regulators of Rho GTPases, are also suggested as regulators of cell growth and differentiation. Such activity has been reported for many RhoGAPs. The down-regulation on Cdc42 by MgcRacGAP has been implicated in cytokinesis regulation by affecting central spindle formation (Zhao and Fang 2005). Mice lacking the RhoGAP p190-B display smaller cell size and animal size, a severe reduction in thymus size and brain defects. These defects are associated with a failure in cell differentiation possibly as a result of upregulated Rho signaling (Sordella *et al.*, 2002).

Some RhoGAPs may affect cell growth and differentiation through the induction of apoptosis. tGAP1 (testicular GAP 1) is a rat protein found in male germ cells, which was shown to induce apoptosis of somatic cells. This implicates an important role during

spermatogenesis, since a significant number of male germ cells produced from mitosis and meiosis are eliminated through apoptosis (Modarressi *et al.*, 2004).

1.2.3.4 RhoGAPs in tumor suppression

Given the role of Rho GTPases in oncogenesis, the deregulation of RhoGAPs could be associated with tumor progression. In fact, many RhoGAPs were suggested as candidate tumor suppressors since deletion or downregulation of several RhoGAPs have been found in various tumors. For example, deletion, point mutation and insertion of GRAF, the focal adhesion kinase associated RhoGAP, were found in patient with leukemia (Borkhardt *et al.*, 2000). RhoGAPs Beta-chimaerin and p50RhoGAP are downregulated in breast cancer and drug-resistant ovarian cancer cells respectively (Kandpal, 2006). Consistently, the expression of some RhoGAPs could suppress transformation or metastasis. For example, p190RhoGAP can repress Ras-induced transformation in NIH3T3 fibroblast (Wang *et al.*, 1997). Another RhoGAP PI3-kinase p85-alpha subunit plays a role in metastasis suppression in ovarian cancer (Kobayashi *et al.*, 2004). At same time, some RhoGAPs were found to be upregulated in tumors, such as RacGAP1, srGAP1 and p115RhoGAP (Kandpal, 2006). The different effects of various RhoGAPs to tumors further implicate that the regulation of Rho GTPases by RhoGAPs is a specific and complex process.

1.2.3.5 RhoGAPs in neuronal morphogenesis

One of the established physiological roles of Rho GTPases is the regulation of the actin cytoskeleton during neuronal migration, axonal growth and guidance, and formation of synapses. Consequently, RhoGAPs play a role in neuronal morphogenesis. In fact, mutations or deletions of various RhoGAP genes have been linked to mental defects, such as Myosin-IXa, srGAP3, oligophtrnin-1 (Moon and Zheng, 2003). More research has been done to elucidate their function in neuronal morphogenesis. For example, α2-chimaerin, a brain specific GAP, was shown to induce neurite outgrowth in neuroblastoma cells and to be involved in growthcone collapse (Shi *et al.*, 2007B). Another RhoGAP, p190RhoGAP, was shown to be necessary for axon ourgrowth, guidance and fasciculation, and neuronal morphogenesis (Brouns *et al.*, 2001).

1.2.3.6 Crosstalks of Rho GTPase pathways and other signaling pathways mediated by RhoGAPs

The multifunctional features of many RhoGAPs make them signal convergent/ divergent points to mediate crosstalks between the Rho GTPase signaling and various signaling pathways. For example, BPGAP1 activate endocytosis by integrating Rho pathway with MAPK pathway (Lua and Low, 2005). RA-RhoGAP integrates Rap1 and Rho signaling during neurite ourgrowth (Yamada *et al.*, 2005). The crosstalks mediated by RhoGAPs in turn lead to a more precise and intricate regulation on Rho GTPase functions.

1.2.4 The regulation on RhoGAPs

The cellular functions of various RhoGAPs are very specific and different and this may attribute to the multiple-domain nature of many RhoGAPs. A RhoGAP protein may act as a signal convergent/divergent point by binding various molecules to its multiple domains/motifs. Such interactions could serve to regulate the dynamic disposition, activity as well as the anchorage of molecular assembly of RhoGAPs in different temporal and spatial manners. It has been found that RhoGAPs are regulated by various mechanisms, including phosphorylation, phospholipid-binding, protein-protein interaction and proteolytic degradation. First, phosphorylation could activate/inhibit the activity of many RhoGAPs or even change their specificity towards Rho GTPases (Moon and Zheng, 2003). For example, p190 RhoGAP could be phosphorylated on tyrosine residues by activated Src or be phosphorylated on serine/threonine by activated protein kinase C. The phosphorylation induces conformational change that leads to the translocation of p190 and/or activation of its GAP activity (Roof *et al.*, 1998; Hu and Settleman, 1997). Another example could be MgcRacGAP, whose GAP specificity is changed from Rac1 and Cdc42 to RhoA after serine phosphorylation by ROCK (Rho-associated kinase) during cytokinesis (Lee *et al.*, 2004). Second, phospholipid-binding were also found to regulate the function of some RhoGAPs. Phospholipids interact with non-catalytic motifs of RhoGAPs and could exert regulatory

effects on the subcellular localization or catalytic activity of RhoGAPs (Moon and Zheng, 2003). For example, the interaction of the RhoGAP ARAP3 and phosphatidylinositol 3,4,5-triphosphate (PIP$_3$) could cause conformational change of ARAP3 to translocate it to the plasma membrane and/or to regulate its GAP activity (Krugmann *et al.*, 2004). Since phospholipids are important mediators of signal transduction downstream of many growth factor receptors, regulation on RhoGAPs by phopholipid-binding could thus link RhoGAP function to growth factor stimulation (Bernards and Settleman, 2005). Third, protein-protein interaction is one major mechanism that regulates RhoGAP activity. The interaction of CdGAP with intersectin and the interaction of TCGAP with Fyn kinase present examples for the regulation of GAPs by protein-pretein interactions. Both these interactions inhibit the GAP activity of these two RhoGAPs, which is possibly due to conformational changes (Jenna *et al.*, 2002). Finally, proteolytic degradation could regulate the function of RhoGAPs in a temporal manner by affecting their cellular expression levels. It is known that the expression of p190-A RhoGAP is cell cycle regulated through ubiquitin-mediated degradation (Su *et al.*, 2003). The various regulatory mechanisms together contribute to the efficient and tight control on the GAP activity and substrate specificity of so many RhoGAPs (more than 70 in mammals) inside the cells.

1.3 DLC1 as a novel RhoGAP protein

The human gene frequently deleted in liver cancer (*DLC1*) encoding a novel

RhoGAP-domain containing protein was originally identified as a candidate tumor suppressor gene (Yuan *et al.,* 1998). It was mapped to chromosome 8p21.3-22. Allelic losses from chromosome 8p have been found in various cancers including liver, prostate, ovary, breast, lung and colorectal cancers, strongly suggesting the presence of a tumor suppressor gene in chromosome 8p (Yuan *et al.,* 1998; Ng *et al.,* 2000). Loss of heterozygosity of *DLC1* was first identified in primary hepetocellular carcinomas (HCCs). It was shown that *DLC1* gene is deleted in 7 of 16 primary HCCs and in 10 of 11 HCC cell lines (Yuan *et al.,* 1998). The chromosomal location of *DLC1* gene and its frequent downregulation in liver cancer first-time indicated DLC1 protein as a candidate tumor suppressor.

1.3.1 Homologues of human DLC1

There are three homologous proteins sharing the SAM-RhoGAP-START domain organization (which will be introduced later) in human, including DLC1, DLC2 and DLC3. Human DLC1 amino acid sequence is 58% and 44% identical to human DLC2α isoform and human DLC3α isoform respectively (Durkin *et al.*, 2007B). DLC2 and DLC3 were also identified as candidate tumor suppressors (Ching *et al.*, 2003; Durkin *et al.*, 2007A; Durkin *et al.*, 2007B). It remains to be investigated whether the three human homologues cooperate in their cellular functions such as tumor suppression.

Respective orthologues of the three DLC proteins have been identified in other

vertebrate, including mouse, rat, dog, chicken, frog and puffer fish (Durkin *et al.*, 2007B). Human DLC1 shares 93% identity and 92% identity in amino acid sequence with the rat and mouse orthologues (Durkin *et al.*, 2007B). Its rat orthologue is named as p122RhoGAP, which was initially identified as a novel regulator in the phospholipase C-delta 1 (PLC-δ1) signaling pathway in screening for PLC-delta 1-binding partners from rat brain expression library. It was shown that p122RhoGAP binds to PLC-delta 1 and activates its activity in hydrolyzing phosphatidylinositol 4,5-bisphosphate (PIP2) (Homma and Emori, 1995). It was also shown that p122RhoGAP has a RhoGAP domain located near its C-terminus, with GAP activity specific for RhoA, not Rac1. Later research found that overexpression of p122RhoGAP inhibits the formation of stress fiber and focal adhesions in adherent cells, and leads to cell rounding and detachment. However, such effects can be blocked by the constitute-active mutant of RhoA, RhoA-G14V. Furthermore, GAP negative mutants of p122RhoGAP, R668E, K706E and R710E, lost the function in altering actin cytoskeleton organization (Sekimata *et al.*, 1999). It was concluded that the cellular morphological changes induced by p122RhoGAP are dependent on its GAP activity. Previous work on p122RhoGAP further suggested that p122RhoGAP may integrate the downregulation of RhoA and the hydrolysis of PIP2 to induce actin cytoskeleton rearrangement. Whether DLC1 is similarly involved in PLC signaling has not been addressed yet. Most of the research of DLC1 is focused on its RhoGAP function and tumor suppressor function which will be introduced in the subsequent sections.

1.3.2 Essential function of DLC1 in embryonic development

DLC1 is widely expressed in all normal adult and fetal tissues in human (Seng *et al.*, 2007). Northern blot analysis of mouse DLC1 mRNA shows that mouse DLC1 is also widely expressed, with the highest levels in heart, liver and lung (Durkin *et al.*, 2002). Using mice as the animal model, homozygous DLC1 inactivation was shown to be lethal. The homozygous mutant embryos did not survive beyond 10.5 days post coitum with defects in the neural tube, brain, heart and placenta. Cultured fibroblasts from these DLC1-deficient embryos have fewer long stress fibers and a reduced number of focal-adhesion-like structures (Durkin *et al.*, 2005). These results indicate that DLC1 play specific and essential functions in actin cytoskeleton dynamic and embryonic development, which can not be compensate by other RhoGAPs or DLC1 homologues.

1.3.3 DLC1 as a tumor suppressor

Ever since the identification of DLC1 as a candidate tumor suppressor, there have been increasing evidence to support this notion. DLC1 was reported to be deleted or lowly-expressed in various tumors and cancer cell lines, showing that its downregulation contributes to tumorigenesis of such tumors and cancer cell lines. *DLC1* gene was initially found to be deleted in around 50% of primary HCCs and not expressed in 28% of HCC cell lines (Yuan *et al.,* 1998). Similarly, another group also showed that *DLC1* was not expressed in six of 30 (20%) human HCC samples and 2 of 5 (40%) HCC cell lines, and

was deleted in two of six HCC samples and the two HCC cell lines with no DLC1 expression (Ng *et al.,* 2000). It was further found that DLC1 mRNA was significantly underexpressed in the tumor tissue comparing the surrounding nontumorous liver tissue of the same patients with HCC (Wong *et al.,* 2003). Besides HCCs, DLC-1 was shown to be deleted in 40% of primary breast tumors (Yuan *et al.,* 2003). Low levels or absence of DLC1 mRNA were also observed in 57% of primary breast cancer and 62.5% of breast cancer cell lines (Plaumann *et al.,* 2003), 70% of breast, 70% of colon, and 50% of prostate tumor cell lines (Yuan *et al.,* 2003), 95% of primary non-small cell lung carcinoma (NSCLC) and 58% of NSCLC cell lines (Yuan *et al.,* 2004), seven of nine human gastric cancer cell lines (Kim *et al.,* 2003), 91% nasopharyngeal carcinoma, 40% esophageal, 63% cervical and 33% breast carcinoma cell lines (Seng *et al.,* 2007). Recently, microarray technique was used on breast cancers and ovarian cancers, and consistently shows similar expression profiles for DLC1 (Goodison *et al.,* 2005; Syed *et al.,* 2005).

Several findings have addressed the issue of how DLC1 is downregulated in tumors. In most cases, transcriptional silencing rather than genomic deletion is responsible for the downregulation of DLC1 in various tumor samples. It was shown that transcriptional silencing of DLC1 is caused by hypermethylation in the promoter region of DLC1 gene. Methylation in the DLC-1 promoter CpG island was abserved in HCCs and HCC cell lines, non-small cell lung carcinomas, supratentorial primitive neuroectodermal tumors, gastric cancer cell lines, nasopharyngeal carcinoma, esophageal, cervical and breast carcinomas and Non-Hodgkin's lymphoma (Yuan *et al.,* 2003B; Kim *et al.,* 2003;

Wang *et al.,* 2003; Yuan *et al.,* 2004; Pang *et al.,* 2005; Seng *et al.*, 2007; Shi *et al.*, 2007A).

Some other work focuses on the suppressive role of DLC1 in tumorigenesis mostly using *in vitro* models. It was shown that DLC1 could inhibit *in vitro* tumor cell growth. When the expression of DLC1 was restored in several cancer cell lines lacking endogenous DLC1-expression, their growth was significantly inhibited compared to the control cell lines. Such inhibitory effect was shown from less amount of cells proliferated, and reduced ability of tumor cells in anchorage-independent growth or in colony-formation, in cell lines of HCC, breast cancer, non-small cell lung carcinomas and ovarian cancer (Ng *et al.,* 2003; Yuan *et al.,* 2003; Plaumann *et al.,* 2003; Yuan *et al.,* 2004; Wong *et al.,* 2005; Syed *et al.,* 2005). Furthermore, DLC1 could induce caspase-3-mediated apoptosis when restoring its expression in two HCC cell lines and three ovarian cancer cell lines. The restoration of DLC1 expression activates caspase-3 and reduces the level of Bcl-2, an antiapoptotic protein (Zhou *et al.,* 2003; Syed *et al.,* 2005). The role of DLC1 was further shown in the inhibition of *in vitro* tumor cell migration and invasiveness. These effects have been proved for several HCC cell lines, ovarian cancer cell lines and one metastatic breast cancer cell line (Zhou *et al.,* 2004; Goodison *et al.,* 2005; Syed *et al.,* 2005; Wong *et al.,* 2005), implicating the role of DLC1 as a metastasis suppressor. Recently, *in vivo* models were used to study the role of DLC1 for tumorigenisis under physiological conditions. When introducing DLC1 into some cancer cell lines lacking endogenous DLC1 expression, it abolished or significantly reduced the ability of these cells to form tumors in athymic nude mice. Consistent results

were achieved from several HCC cell lines, breast carcinoma cell lines and NSCLC cell lines (Yuan *et al.,* 2003; Zhou X *et al.,* 2004; Yuan *et al.,* 2004; Goodison *et al.,* 2005; Wong *et al.,* 2005).

Taken together, the above findings demonstrate the role of DLC1 as a tumor suppressor in tumor growth and metastasis. Meanwhile, the underlying molecular mechanism remains unknown. Only recently, progress has been made in elucidating the mechanistic functions of DLC1. Their findings will be introduced further in this chapter.

1.3.4 DLC1 as a mutidomain RhoGAP

Domains are structural units of a protein that can fold independently into compact and stable structures (Alberts *et al.,* 2002). Domains are also functional units of a protein. They play important roles in regulating many cellular events by their enzymatic activities, or by interaction with other moleculars. Some domains possess catalytic functions such as phosphorylation activities, protein kinase activities or lipid kinase activities. Others can mediate interactions between proteins, or between proteins and lipids or nucleic acids (Pawson *et al.,* 2002). The domains mediating interaction can target proteins to a specific subcellular location, detect posttranslational modifications or molecule-binding on proteins, affect signaling kinetics, nucleate the formation of multiprotein signaling complexes, and regulate the conformation, activity, and substrate specificity of enzymes (Pawson and Nash, 2003). According to amino acid sequence

similarity, domains are divided into various conserved domain families. The same-family domains in different proteins not only have consensus amino acid sequences, but usually they also have similar tertiary structures and binding properties (Pawson and Nash, 2003). The property of a newly identified domain can be predicted from the known structures and/or known properties of other domains within the same domain family. Hence, the biological functions of a protein can be predicted according to its domain composition (Pawson and Nash, 2003).

Like most RhoGAPs, DLC1 carries multiple protein domains. Two more domains as well as the GAP domain were identified in DLC1, when analyzing the amino acid sequence of DLC1 (GenBank accession number gi:33188437) with the Conserved domain Architecture Retrived Tool (CDART) (http://www.ncbi.nlm.nih.gov/Structure/cdd/wrpsb.cgi). One is a Sterile-Alpha Motif (SAM) domain flanking the extreme N-terminus of DLC1 followed by a long stretch of sequence. The other is a steroidogenic acute regulatory protein (StAR)-related lipid-transfer (START) domain flanking the C-terminus of DLC1 (Figure 1.5). For the functions of DLC1, functional significance of other regions except the catalytic GAP domain had long been unclear. Through studying the conserved properties of the domain families within these regions, it may help to predict the molecular mechanism of DLC1 in cell dynamic control.
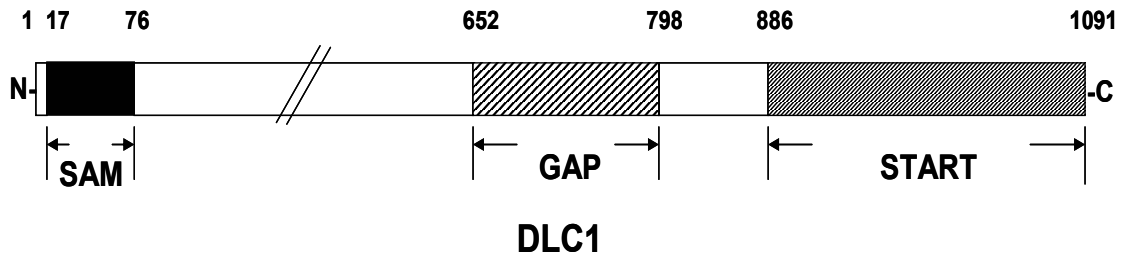
Figure 1.5 Schematic diagram showing the composition of protein domains for human DLC1. Human DLC1 GenBank accession number gi:33188437. SAM, Sterile-Alpha Motif; GAP, GTPase-activating protein; START, StAR-related lipid-transfer domains.

1.3.4.1 The RhoGAP domain of DLC1

The RhoGAP domain of DLC1 possesses *in vitro* GAP activity specific towards RhoA, RhoB, RhoC and Cdc42, but not Rac1 (Wong *et al.,* 2003; Healy et al., 2007). Consistently, the *in vitro* GAP activity of DLC1 rat homolog p122RhoGAP is specific towards RhoA, not Rac1, while the activity towards Cdc42 was not examined (Sekimata *et al.*, 1999). Since the *in vivo* activity and *in vitro* activity of many GAPs are different (Moon and Zheng, 2003; Tcherkezian and Lamarche-Vane, 2007), the GAP specificity of DLC1 under physiological conditions can not be concluded from the *in vitro* data. While there is no published work showing its *in vivo* GAP activity towards Cdc42, some data indirectly or directly implicate the *in vivo* RhoA specificity of DLC1. Ectopic expression of DLC1/p122RhoGAP could lead to the dissociation of stress fibers (Sekimata *et al.*, 1999; Wong *et al.*, 2005), showing the downregulating effect on RhoA. The observation

that active RhoA could rescue the effects of p122RhoGAP overexpression on actin cytoskeleton and cell morphology further demonstrates RhoA as a target of DLC1 *in vivo* (Sekimata *et al.*, 1999). Indeed, DLC1 dramatically reduced RhoA activity at the leading edge of cellular protrusions (Healy *et al.*, 2007).

The GAP activity of DLC1 had long been viewed essential for the anti-tumor function. Previous work showed that the RhoGAP activity is essential for the effect of DLC1 and p122RhoGAP on cytoskeleton and cell morphology (Sekimata *et al.*, 1999; Wong *et al.*, 2005). For both DLC1 and p122, full-length GAP-negative mutants or various truncation mutants lacking GAP domain lost the ability in causing the dissociation of stress fibers and focal adhesions, cell rounding and detachment (Sekimata *et al.*, 1999; Wong *et al.*, 2005). It was further shown that the GAP activity of DLC1 is necessary for its tumor suppressor function. The GAP-negative mutant of DLC1 (K714E) lost the suppressive effect on colony formation of HCC cells. However, it was also shown that the DLC1 GAP domain alone is not sufficient to inhibit the formation of stress fibers and the growth of HCC cells, suggesting that the N-terminal region and the C-terminal region flanking the RhoGAP domain in DLC1 are also necessary for the tumor suppressor function of DLC1, though the exact cellular functions and molecular mechanisms of these regions are still unknown (Wong *et al.*, 2005).Subsequently, this notion was further supported by the finding that the anti-tumor activity of DLC1 was mediated by both RhoGAP-dependant and -independent manners (Healy *et al.*, 2007). Previous work together show that GAP function is essential but not enough for the function of DLC1, implying that other domains/motifs in DLC1 could play important

functional roles which remain to be faithfully elucidated.

1.3.4.2 The SAM domain of DLC1

SAM domains are found in a wide range of signaling and nuclear proteins. SAM domain was originally identified as a novel motif in four proteins essential for the yeast sexual differentiation, *i.e.* byr2, STE11, ste4 and STE50 (Ponting 1995). As such, it is named as the sterile alpha motif. Up till now, around 200 SAM-domain-containing proteins have been identified in the human genome (Qiao and Bowie, 2005).

SAM domains from different proteins adopt similar tertiary folds. Each SAM domain contains 70-100 amino acids encoding mainly 5 alpha helixes, that fold into a conserved globular tertiary structure with a hydrophobic core.

Although SAM domains have similar structures, they have versatile binding properties and diverse functions. This is shown by the fact that SAM-domain-containing proteins exist in all subcellular locations, and they participate in various cellular process ranging from signal transduction to transcriptional and translational regulation (Kim and Bowie, 2003; Qiao and Bowie, 2005). SAM domains have long been considered as protein-protein interaction modules. Many of them can mediate homotypic or heterotypic SAM-SAM interactions to form dimmers, oligomers or polymers. For example, the SAM domains of several transcriptional repressors, such as TEL (translocation Ets leukemia), Polyhomeotic and Sex-comb-on-midleg, can form similar head-to-tail helical homotypic

polymer strucutures (Kim and Bowie, 2003). The SAM domains Byr2 and Ste4 mediate the formation of oligomers of these two proteins (Kim and Bowie, 2003). Some other SAM domains can interact with non-SAM domain containing proteins. For example, BAR (Bifunctional Apoptosis Regualtor), a protein involved in apoptotic pathways, can bind to Bcl-2 and Bcl-XL via its SAM domain and suppress BAX-induced apoptosis through a SAM domain-dependent mechanism (Qiao and Bowie, 2005). Recently, several papers reported novel binding properties of some SAM domains, showing that roles of SAM domains are not restricted in mediating protein-protein interactions. One surprising finding is that the SAM domains of translational repressor Smaug and its homologues could bind to stem-loop RNA structures (Green *et al.*, 2003; Aviv *et al.*, 2003). Although the function of these SAM domains are completely different from previously studied SAM domains, the crystal structure of Smaug-SAM still adopts the conserved globular fold and is extremely similar to the SAM domain of EphB2, which has the canonical protein binding property. Careful comparison of their structures and sequences shows that Smaug SAM has a unique electropositive surface, through which it binds to RNA (Green *et al.*, 2003). Such findings may define a novel subfamily of SAM domains with nucleic-acid-binding function. Another novel function reported for the SAM family was the *in vitro* lipid-binding property of the SAM domain of p73, a homologue of tumor suppressor p53 (Barrera *et al.*, 2003).

The function of the SAM domain of DLC1 was however barely studied. One recent paper suggests that SAM domain is not necessary for the RhoGAP and tumor suppressor function of DLC1. It is shown that only SAM domain alone could not cause

cell morphological changes or inhibit colony formation, nor could SAM-deletion mutant affect these functions of DLC1 to HCC cells (Wang *et al.*, 2005). Meanwhile, DLC1-SAM domain could still play a role for the functions of DLC1. Given the fact that the regulation of many RhoGAPs is an intricate process inside the cells, DLC1-SAM might play its role under physiological conditions. Furthermore, SAM domain could participate in other cellular functions of DLC1 in normal cell growth, cell migration and embryonic development.

1.3.4.3 The START domain of DLC1

START domain is defined as a putative lipid-binding module with 200-210 amino acids. It was first identified as a conserved region at the C-termini of two cholesterol-binding proteins, steroidogenic acute regulatory protein (STAR) and metastatic lymph node 64 (MLN64). Now 15 START-domain-containing proteins have been found in humans (Alpy and Tomasetto, 2005).

Crystal structures of the START domains of MLN64, STARD4, and phophatidylcholine transfer protein (PCTP) have been solved. Their structures share a conserved 'helix-grip' fold, with α-helixes at the N and C termini and nine β-strands forming a β-sheet in the middle. The most striking feature is that, with the C-terminal α-helix acting like a lid, the β-sheet forms an internal hydrophobic tunnel, which is big enough to accommodate a lipophilic molecule, such as cholesterol and

phophatidylcholine (Soccio and Breslow, 2003). With such conserved 'helix-grip' fold structures, START domains are able to bind lipids. But their target lipids are different. For all the known lipid-binding capacity of different START domains, each START domain has only one or two specific lipid targets. The identified lipid ligands for STARD1/MLN64/STARD5, STARD5, PCTP/STARD10, STARD10 and STARD11 are cholesterol, 25-hydroxycholesterol, phosphatidylcholine, phosphatidylethanolamine and ceramides respectively (Alpy and Tomasetto, 2005). Their binding specificity may indicate that the functions of different START domain-containing proteins are specific and not compensable.

In fact, START domain-containing proteins are involved in various lipid-related cellular processes, including lipid trafficking, lipid metabolism, lipid-modulated signal transduction and transcriptional regulation. In such processes, the START domain serves as a versatile lipid-binding interface that functions as a lipid-transfer and/or lipid-sensing domain (Alpy and Tomasetto, 2005). Many START proteins are well known for their roles in lipid trafficking and lipid metabolism through their transferring capacity of lipids. For example, MLN64 is a transporter of endosomal cholesterol and may play a role in cholesterol homeostasis (Alpy and Tomasetto, 2006). STARD10 is concentrated in the sperm flagellum and may function in energy metabolism of sperms by transferring phophatidycholine PC (Yamanaka *et al.*, 2000). Some other START proteins may regulate signal transduction and/or transcriptional machinery by sensing the binding of lipids. For example, the START domain of STARD11 was suggested in the regulation of signal transduction in the Goodpasture disease by regulating the kinase activity of STARD11

towards Goodpasture antigen (Raya *et al.*, 2000). The START domain of STARD6 was implicated in transcriptional regulation during spermatogenesis through lipid-interaction (Gomes *et al.*, 2004). Taken together, START domain-containing proteins make use of the lipid-binding capacity to exert different lipid-related cellular functions.

The function of the START domain of DLC1 remains obscure. Multiple-sequence alignment of various START domains shows that DLC1-START has the well conserved residues flanking the phosphatidylcholine (PC) binding site of PC-transfer protein (Ponting and Aravind, 1999), indicating the potency of DLC1-START in binding to lipids like PC. Earlier work on p122RhoGAP revealed that it could interact with phospholipase C delta 1 (PLC-δ1) through its C-terminus (including the GAP domain and the START domain), suggesting the involvement of p122RhoGAP in phospholipase pathway and the potential interaction between its START domain and phospholipase or phospholipid(s) (Homma and Emori, 1995; Sekimata *et al.*, 1999). Later research showed that the START domain play an auxilliary role in localizing p122RhoGAP in caveolin-coated lipid-raft, caveolae, which could be due to the lipid-binding capacity of the START domain (Yamaga *et al.*, 2004). But till now there is still no direct evidence to show its lipid-binding activity. Recently, one paper showed that START-deletion mutant of DLC1 lost the effect in changing cell morphology and the inhibition on colony formation of tumors cells by this mutant is less potent than full length, demonstrating the functional significance of START domain to the RhoGAP and tumor suppressor function of DLC1 (Wong *et al.*, 2005). Despite all these findings, the actual role of START domain to the functions of DLC1 remains elusive.

1.3.5 Molecular mechanism of DLC1 in cell dynamics

Recently, several pieces of work started to unravel the possible molecular mechanism of DLC1/p122RhoGAP's functions in cellular signaling. Earlier work showed that p122RhoGAP could specifically bind to PLC-δ1 and activate it but not PLC-β1 or PLC-γ1, and the C-terminal half of p122RhoGAP is responsible for such interaction (Homma and Emori, 1995; Sekimata *et al.*, 1999). One later work shows that p122RhoGAP interacts with caveolin and it can localize at caveolin-enriched membrane, caveolae, while the functional significance of their interaction is not clear yet (Yamaga *et al.*, 2004). Another work identified serine 322 of rat p122RhoGAP (corresponding to serine 329 in human DLC1) as the phosphorylation site by protein kinase B (PKB) and ribosomal S6 kinase (RSK) upon insulin stimulation and it showed the involvement of the PI3K/Akt pathway and MEK/ERK/RSK pathway for the phosphorylation, but the downstream effect remains elusive (Hers *et al.*, 2006). One recent work suggested that the activity of DLC1 RhoGAP domain is essential but not enough for its function and the region between 292- to 648-amino acid and the START domain are also necessary for the tumor suppressor function of DLC1 (Wong *et al.*, 2005), implicating the importance of other domains/regions of DLC1. Most recently, it is clear that DLC1 can interact with the tensin family members tensin1, tensin2 and cten, through amino acids 440-445 of DLC1. Mutation of tyrosine 442 abolished the focal adhesion localisation of DLC1 targeted by tensins and impaired the tumor suppressor function of DLC1 (Yam *et al.*, 2006; Qian *et al.*, 2007; Liao *et al.*, 2007). The molecular mechanism of how DLC1 plays its function in cell dynamics requires more investigation. It is therefore necessary to study the

roles of other regions besides the GAP domain of DLC1 and search for its additional interaction partners to further elucidate the mechanistic function of DLC1 in normal cell growth, migration, morphogenesis as well as in tumor suppression.

1.4 Hypothesis and objectives of this study

The fact that GAP domain alone is not sufficient for the function of DLC1 (Wong *et al.*, 2005) raises the possibility that other regions of DLC1 may interact with certain molecules and lead to the crosstalk of RhoA/GAP pathways with other signaling arms. It might help us to address this point to identify the binding partner(s) of these regions of DLC1 and the interplay of its/their functions with the GAP function of DLC1 in cell dynamic control. Protein-protein interaction assays and appropriate cell dynamic assays would be required to elucidate potential mechanisms underlying the observed cellular effects.

This study may lead to a better understanding on the mechanistic function of DLC1 in the complicated signaling network. It may also enhance our understanding on the specificity and redundancy of different GAP proteins and different Rho GTPases in cell dynamic control. As a tumor suppressor of various kinds of tumors, DLC1 is a potential molecule in clinical research for the treatment of cancers. Understanding the mechanism of how DLC1 exerts its function in cellular events may contribute to the development of cancer-suppressing drugs.

In summary, we hypothesize that SAM domain, START domain or some unidentified motifs in DLC1 could regulate its cellular function *in vivo* via some unidentified interacting partners.

To test this main hypothesis, the major aims of this thesis work are to:

- clone human DLC1 cDNA and construct various truncation mutants of DLC1 for protein interaction assays and cellular studies;

- identify potential interacting partner(s) for different regions of DLC1 protein;

- study the properties of the interactions by identifying their binding motifs between DLC1 and its interacting partner(s); and

- identify the functional significance for the interaction between DLC1 and its interacting partner(s).

Chapter 2

Materials and methods

2.1 RT-PCR cloning and plasmid construction

2.1.1 RNA isolation and RT-PCR

To acquire the full length cDNA of human DLC1 and human EF1A1, total RNAs from human kidney 293T cells were isolated using the RNeasy (Qiagen) according to the manufacturer's instructions. 5 μg of RNA was subjected to the first strand cDNA synthesis with Reverse Transcriptase (Roche) using oligo-dT (Operon) as primer for 60 min at 42°C in a total volume of 20 μl. For PCR reaction, 1 μl of 293T cDNA was amplified using specific primers corresponding to the cDNA sequences of NM_006094 (for human DLC1), NM_178006 (for human DLC2) and NM_001402 (for human EF1A1) by the DyNAzyme EXT DNA polymerase (Finnzymes). To facilitate subsequent cloning, the PCR primers contain restriction enzyme sites and their sequences were listed at Table 2.1, 2.2 and 2.3. The following PCR conditions were used: initial denaturation 94°C for 2 min; subsequent cycling (35 cycles) at 94°C for 45 sec, annealing at 55°C for 30 sec, and extension at 72°C for 3 min 40 sec (for DLC1) or for 2 min (for EF1A1); final extension at 72°C for 10 min.

Primer name	Primer sequence
DLC1-F	5' CGG<u>GGATCC</u>ATGTGCAGAAAGAAGCCGG 3'
DLC1-R	5' CGG<u>CCCGGG</u>TCACCTAGATTTGGTGTCTTTGG 3'
SAM-R	5' CGG<u>CCCGGG</u>TCAACTTCGTTTCCGATGAGG 3'
P-F	5' CGG<u>GGATCC</u>ATGCTAGAAATTAGTCCTCATCGG 3'

P-R	5' CGG <u>CCCGGG</u>TCATGTGCGCTGCACGTTGACCG 3'
GAP-F	5'CGG<u>GGATCC</u>CAACCGTTGCCTCAGAGCATCC 3'
GAP-R	5' CGG<u>AAGCTT</u>TCAATGGAAGAGGGAAGGCGC 3'
R-F	5' CGG<u>GGATCC</u>ATGACCCTGAAGAGAGAG AATTCC 3'
R-R	5' CGG<u>CCCGGG</u>TCAAGCTGAGTCATCATTACCC 3'
START-F	5' CGG<u>GGATCC</u>ATGGATGACTCAGCTGACTACC 3'
P1-R	5' CGG<u>CCCGGG</u>TCACGCACTGAGGCTCCGGGTCC 3'
P2-F	5' CGG<u>GGATCC</u>ATGTGCAACAAGCGGGTGGGC 3'
P2-R	5' CGG<u>CCCGGG</u>TCACTGATTGACTATCCGCTGC 3'
P3-F	5' CGG<u>GGATCC</u>ATGTGGTCGGAGAAGTTTTCTGA 3'

Table 2.1 Primers used for the cloning of DLC1 full length and domains. Underlined are restriction site used for cloning.

Primer name	Primer sequence
DLC2SAM-F	5' CGG<u>GGATCC</u>ATGAAAGAAGCATGTGACTGGCT 3'
DLC2SAM-R	5' CGG<u>CCCGGG</u>TGATTTCATTGAGGCACACTTGT 3'

Table 2.2 Primers used for the cloning of DLC2 SAM domain. Underlined are restriction site used for cloning.

Primer name	Primer sequence
EF1A1-F	5' GGATCCATGGGAAAGGAAAAGACTC 3'
EF1A1-R	5' CTCGAGTCATTTAGCCTTCTGAGC 3'
DOMAIN1-R	5' CGGCTCGAGTCAACGAGTTGGTGGTAGGATGC 3'
DOMAIN2-F	5' CGGGGATCCATGCCAACTGACAAGCCCTTGC 3'
DOMAIN2-R	5' CGGCTCGAGTCAGTCATTTTTGCTGTCACC 3'
DOMAIN3-F	5' CGGGGATCCATGCCACCAATGGAAGCAGC 3'

Table 2.3 Primers used for the cloning of EF1A1 full length and domains. Underlined are restriction site used for cloning.

2.1.2 Cloning of the DLC1 and EF1A1 constructs

The full length PCR products were gel-purified (Qiagen) and cloned into Flag-tagged, HA-tagged, GFP-tagged or GST-tagged Pxj40 vector (Dr. E. Manser, Institute of Molecular and Cell Biology, Singapore), GST-tagged pGEX-4T-1 vector (Pharmacia Biotech) or myc-His-tagged pcDNA3.1 vector (Invitrogen) respectively. The resulting bacteria colonies were screened by double restriction digestion and positive clones were sequenced using ABI PRISM Bigdye Terminator Cycle Sequencing kit (Applied Biosystem) in both directions to confirm their identity.

Various cDNA fragments encoding the various domains of DLC1 or EF1A1 or the SAM domain of DLC2 were generated from the full-length template using the specific

primers in a standard PCR and then gel purified for cloning. The primers used for the domain PCR were listed in Table 2.1 and 2.2. (Cloning of BNIP-Sa full length and various domain constructs is courtesy of Dr. Zhou Yiting.)

2.1.3 Cloning of deletion mutants and point-mutation mutants of DLC1

Deletion mutants and point-mutation mutants of DLC1 were generated by polymerase chain reaction using specific primers (Table 2.3) with Pfu Turbo DNA polymerase (Stratagene). For deletion mutants, the following PCR conditions were used: initial denaturation 95 ^{o}C for 2 min; subsequent cycling (10 cycles) at 95 ^{o}C for 30 sec, annealing at 50 ^{o}C for 1 min, and extension at 68 ^{o}C for 7 min 40 sec; another subsequent cycling (15 cycles) at 95 ^{o}C for 30 sec, annealing at 50 ^{o}C for 1 min, and extension at 64 ^{o}C for 12 min; final extension at 64 ^{o}C for 10 min. For point-mutation mutants, the following PCR conditions were used: initial denaturation 95 ^{o}C for 30 sec; and subsequent cycling (16 cycles) at 95 ^{o}C for 30 sec, annealing at 55 ^{o}C for 1 min, and extension at 68 ^{o}C for 7 min 40 sec. 10 μl of PCR products were digested with 10 unit Dpn I enzyme (New England Biolabs) for 2 hour at 37 ^{o}C. PCR products for point-mutation mutants were subjected to transformation directly. PCR products for deletion mutants were subjected to PCR purification (Qiagen), single restriction enzyme digestion, ligation and transformation. Several clones from each plate wee selected and sequenced. (Cloning of DLC1-SAM-FLF, DLC1-SAM-F38, DLC1-SAM-L39 and DLC1-SAM-F40 is courtesy of Dr. Zhang Jingfeng.)

Primer Name	Primer Sequence
ΔP1-R	5'-CGG<u>GCGGCCGC</u>ACTTCGTTTCCGATGAGG-3'
ΔP1-F	5' CGG<u>GCGGCCGCC</u>TGCAACAAGCGGGTGGGC 3'
ΔP 3-R	5' CGG<u>GCGGCCGC</u>CTGATTGACTATCCGCTGC 3'
ΔP 3-F	5'CGG<u>GCGGCCGCC</u>CAACCGTTGCCTCAGAGC 3'
K48AR49A-F	5'GATATTTCCTTGGTC**GCGGCA**GAGCATGATTTTTG
K48AR49A-R	5' CAAAAAATCATGCTC**TGCCGC**GACCAAGGAAATATC 3'
R64AR65A-F	5'GAGGCTCTATGC**GCGGCT**CTAAATACTTTA 3'
R64AR65A-R	5' TAAAGTATTTAG**AGCCGC**GCATAGAGCCTC 3'
R677E-F	5'GGATCAGGTTGGGCTCTTC**GAA**AAATCGGGGGTCAAGTCC
R677E-R	5'GGACTTGACCCCCGATTT**TTC**GAAGAGCCCAACCTGATCC

Table 2.3 Primers used for DLC1 deletion mutants and point mutation mutants preparation. Underlined are restriction site used for deletion cloning. Mutation sites are shown by bold letters.

2.2 Identification of DLC1-interacting partners

Livers from adult female rats were homogenized in buffer (50 mM HEPES pH 7.4, 100 mM NaCl, 10 mM $MgCl_2$, 5 mM EDTA, 10% glycerol, 1% Triton X-100, 5 mM sodium-orthovanadate, 5 mM glycerol 2-phosphate and a mixture of protease inhibitors) using a dounce tissue grinder (Wheaton) with Pestle A and B. The homogenate was

centrifugated and the supernatant was carefully collected. Glutathione-sepharose beads (Amersham Biosciences) coated with 100 μg GST or GST-SAM were mixed with the lysate or just the lysis buffer (as control) and incubated overnight at 4°C with gentle shaking. After extensive washing, the bound proteins were eluted with lysis buffer containing 4 M urea, resolved by SDS-PAGE and visualized by sliver staining (Bio-Rad). Protein bands excised from SDS-polyacrylamide gels were reduced, alkylated, and then in-gel digested with trypsin. Their mass spectra were acquired with a matrix-assisted laser desorption ionization-time of flight (MALDI-TOF) mass spectrometer and identified as previously described (Lua *et al.,* 2004).

2.3 Cell culture and transfection

293T cells were grown in RPMI 1640 medium supplemented with 10% (vol/vol) fetal bovine serum, 2mM L-glutamine, 100U/ml penicillin, and 100μg/ml streptomycin and maintained at 37°C in a 5% CO_2 atmosphere, whereas NIH3T3 cells and MCF7 cells were grown in DMEM (high glucose) with 10% calf serum or 10% fetal bovine serum respectively (all from Hyclone Laboratories, Logan, UT). NIH3T3 were starved for 18-24 h in medium with 0.5% serum before treatment with 10ng/ml fibroblast growth factor (FGF) (Promega) for 20 min. The 293T cells were tranfected using Fugene 6 (Roche Diagnostics) according to the manufacturer's instructions. The NIH3T3 cells and MCF7 cells were tranfected using PolyMAG Magnetofection reagent (Chemcell) according to the manufacturer's instructions.

2.4 Precipitation/pull-down and co-immunoprecipitation studies

2.4.1 Mammalian cell lysate preparation

Mamamlian cells were lysed in RIPA buffer containing 150 mM sodium chloride, 50 mM Tris, pH 7.3, 0.25 mM EDTA, 1% (w/v) sodium deoxycholate, 1% (v/v) Trition X-100, 50 mM sodium fluoride, 5 mM sodium orthovanadate and a mixture of protease inhibitors (Roche Applied Science). Lysates were directly analyzed, either as whole-cell lysates (25 μg) or aliquots (250 μg) used in affinity precipitation/"Pulldown" assays, co-immunoprecipitation assays or direct binding studies.

2.4.2 Preparation of GST-fusion proteins for pull-down experiments

GST-tagged plasmids in pGEX-4T-1 vector were transfomed into *E.coli.* DH5α or BL21 strains. When bacterial culture growing at 37 $^{\circ}$C reached 0.3-0.6 at OD$_{600}$, 0.1 mM IPTG was added in it to induce the expression of GST-tagged proteins with over-night shaking at room temperature. The next day, the cell pellets were collected by centrifugation at 4 $^{\circ}$C, followed by freezing in -80 $^{\circ}$C for 1 hour. The pellets were then thawed on ice, resuspended in chilled 1XPBS containing 1% Triton-X-100, 1.52% DTT (w/v) and a mixture of protease inhibitors (Roche Applied Science) and lysed by sonication The cell lysate were centrifuged at 5000 rpm for 1 hour at 4 $^{\circ}$C. The supernatant was incubated with Glutathione Sepharose 4b (Amersham Sciences) at 4 $^{\circ}$C over night. Beads with GST-tagged proteins were washed 3 times with chilled 1XPBS containing 1% Triton-X-100 followed by 2-times washing with chilled 1XPBS.

2.4.3 Precipitation/pull-down

Various GST fusion proteins purified on Glutathione Sepharose 4b (Amersham Sciences) were incubated with 200 μl mammalian cell lysate at 4°C for 3 hours. The beads were then washed 3 times with chilled RIPA buffer. All protein complexes on the beads were separated on SDS-PAGE, blotted and probed with indicated antibodies. Blot was stripped and stained with amido black to reveal loading of GST-RBD.

2.4.4 Co-immunoprecipitation

200 μl mammalian cell lysates expressing Flag-tagged and various epitode-tagged proteins were incubated with M2 anti-Flag agarose beads (Sigma-Aldrich) at 4°C for 3 hours. The beads were then washed 3 times with chilled RIPA buffer. All protein complexes were separated on SDS-PAGE, blotted and probed with indicated antibodies.

2.4.5 G-actin *in vitro* binding studies

For G-actin binding studies, 293T cells transfected with Flag-tagged pXJ40 plasmids were lysed in RIPA buffer as described above. M2 anti-FLAG agarose beads (Sigma-Aldrich) were incubated with cell lysis in 4°C for 2 hours and washed 3 times with RIPA buffer to purify mammalian expressed Flag-tagged proteins. All Flag-tagged proteins purified on beads were incubated with 3μg purified G-actin (Cytoskeleton Inc.) in 150 μL 1xPBS with 0.1% Triton X-100 at room temperature for 1.5 hour. Then the beads were washed 3 times with 1X PBS with 0.1% Triton X-100. All protein complexes were separated on SDS-PAGE, blotted and probed with indicated antibodies.

2.5 Direct binding studies

For *in vitro* direct binding studies using proteins expressed from mammalian cells, 293T cells overexpressing His-tagged SAM were lysed in lysis buffer (pH8.0) with 50mM NaH_2PO_4, 0.5 M NaCl, 10mM imidazole, 1% Triton-X-100, 5 mM sodium orthovanadate and a mixture of protease inhibitors (Roche Applied Science). Ni-NTA agarose (QIAGEN) were incubated with cell lysis in 4°C for 2 hours and washed 4 times using washing buffer with 50mM NaH_2PO_4, 0.5 M NaCl and 20mM imidazole (pH6.0). His-tagged SAM purified on beads was then eluted by elution buffer with 0.05% Tween-20, 250mM imidazole, 300mM NaCl, 50mM NaH_2PO_4 (pH8.0). Various GST fusion proteins immobilized on Glutathione Sepharose 4b (Amersham Sciences) were incubated with the eluted His-tagged proteins in 200μl of 1XPBS buffer with 0.1% Triton-X-100, 20 mM NaCl and 18 mM imidazole at 4°C for 1 hour, followed by 5-times washing with cold 1XPBS containing 0.1% Triton-X-100. All protein complexes were separated on SDS-PAGE, blotted and probed with indicated antibody. Blot was stripped and stained with amido black to reveal loading of GST-fusion proteins.

For *in vitro* direct binding studies using proteins produced from bacteria and TNT system, Flag-tagged or HA-tagged proteins were produced *in vitro* with TNT® T7 Quick Coupled transcription/translation system (Promega) according to the manufacturer's instructions. The Flag/HA-tagged proteins were then subjected to pull-down assays with GST-fusion proteins purified and immobilized on beads as described above. All protein complexes on the beads were separated on SDS-PAGE, blotted and probed with indicated

antibodies. Blot was stripped and stained with amido black to reveal loading of GST-fusion proteins.

2.6 RBD assay

The endogenous RhoA activity was examined with pull-down assays with GST-tagged RBD domain of rhotekin which can specifically bind to GTP-bound RhoA (Ren *et al.,* 1999; Wheeler and Ridley, 2004; Shang *et al.,* 2003). Briefly, cells expressing various Flag-tagged proteins were lysed with RIPA buffer. 200 μl of lysates were subjected to pull-down assay at $4^{\circ}C$ for 30 min with GST-tagged RBD purified on glutathione-sepharose beads. Proteins in the whole cell lysate and the protein complex on the beads were processed with SDS-PAGE and immunoblotting. Endogenous RhoA, over-expressed proteins in the whole cell lysate and the active RhoA pulled down by GST-RBD were immunoblotted with indicated antibodies. Blot was stripped and stained with amido black to reveal loading of GST-RBD.

2.7 SDS-PAGE gel eletrophoresis and western blot analysis

The proteins were analyzed on 8% or 15% SDS-polyacrylamide gels (SDS-PAGE) with a Mini Protean II electrophoresus apparatus (Bio-Rad Laboratories). The gels were cast with 1.5 mm spacers and ten-well combs (Bio-Rad Laboratories). The resolving gel

contained 8% or 15% (w/v) acrylamide, 0.48% (w/v) N-N'-methylbisacrylamide, 0.375

mM Tris-HCl pH 8.8, 0.1% (w/v) SDS, 0.0075% (w/v) AMPS and 0.05% (v/v) TEMED.

The stacking gels contain 4% (w/v) acrylamide, 0.133% (w/v) N-N'-methylbisacrylamide,

0.125 mM Tris-HCl pH 6.8, 0.1% (w/v) SDS, 0.0075% (w/v) AMPS and 0.08% (v/v)

TEMED. Protein samples, together with protein markers (Bio-Rad Laboratories) were

mixed with 1/5 volumn of 6X loading buffer [3% (w/v) SDS, 15% (v/v) glycerol, 7.5%

(v/v) b-mercaptoethanol, 0.1 M Tris-HCl pH 6.8, 0.005% (w/v) bromophenol blue] and

boiled for at $95^{o}C$ 5 min. Electrophoresis was performed at 50mA/gel for 1 hour at room

temperature in SDS-running buffer [25 mM Tris, 192 mM glycine and 0.75% (w/v) SDS].

After eletrophoresis, proteins separated on the gels were transferred onto PVDF

membrane (Bio-Rad Laboratories) in transfer buffer [33.7 mM Tris, 256 mM glycine,

20% (v/v) methanol and 0.01% (w/v) SDS] at 100 Volt for 1.5 hour at $4^{o}C$ with a Mini

Trans-Blot Electrophoretic Transfer Cell (Bio-Rad Laboratories).

The blots were incubated in Blocking buffer (1% BSA, 0.1% Tween 20 in PBS) at

room temperature for 1 hour and then incubated with primary antibody diluted in

Blocking buffer at $4^{o}C$ overnight, followed by 10-min washing using 0.1% Tween 20 in

PBS at room temperature for 3 times. After that, blots were incubated with secondary

antibody diluted in PBS with 0.1% Tween 20 for 60 min at room temperature followed by

10-min washing using 0.1% Tween 20 in PBS at room temperature for 3 times. Proteins

on the blots were detected with ECL kit (Pierce). Antibodies used were polyclonal rabbit

anti-HA (Zymed Laboratories Inc.), monoclonal anti-actin and monoclonal M2-anti-Flag

(Sigma Aldrich), monoclonal anti-DLC1 (BD Transduction Laboratories, Lexicon, KY), monoclonal anti-His (Qiagen), monoclonal anti-EF1A1 (Upstate Biotechnology) and polyclonal rabbit anti-GFP (Invitrogen).

2.8 Pyrene Actin polymerization assay

Pyrene Actin polymerization assays were carried out using Actin polymerization Biochem Kit (Cytoskeleton Inc.) according to the manufacturer's manual. The GST-fusion proteins for the test were expressed from 293T cells or *E.coli.* and purified on glutathione beads as described above. Then the beads were incubated with Elution buffer (10 mM reduced glutathion in 50 mM Tris-HCl, pH 8.0) at room temperature for 10 min to elute the bound GST-fusion proteins. The concentration of the eluted proteins in the supernatant was examined by Braford assays (Bio-Rad Laboratories) according to the manufacturer's manual. The quality of the eluted proteins was examined by SDS-PAGE gel electrophoresis followed by Commassie-blue staining (0.2% Commassie blue R-250, 40% methanol, 10% acetic acid). The purified Arp2/3 was purfied from Cytoskeleton Inc. 50µg monomer pyrene-labeled actin was mixed with 10µg test protein and the mixture was incubated at room temperature for 10 minutes. Then 1/10th volume actin-polymerization buffer in the mixture was added to initiate actin polymerization. Actin polymerization was monitored immediately by pyrene fluorescence (excitation 365nm, emission 407nm) using Germini spectrofluorometer (Molecular Devices Inc.) with time intervals of 30 seconds.

2.9 Immnofluorescence

NIH3T3 cells were seeded on sterilized glass cover slips precoated with poly-D-lysine. The next day, cells were transfected with various epitope-tagged expression plasmids for DLC1 and/or EF1A1. 4 hours after transfection, cells were starved or stimulated as described above. Then the cells on cover slips were fixed in 1X PBS cantaining 3% paraformaldehyde at 4°C for 30 min and permeabilized in 1X PBS with 0.2% Triton-X-100 at room temperature for 15 min. Then the cells were incubated with monoclonal anti-paxillin (BD Transduction Laboratories, Lexicon, KY), polyclonal rabbit anti-HA (Zymed Laboratories Inc.) and/or monoclonal M2-anti-Flag (Sigma Aldrich) diluted in 1X PBS with 0.1% Triton-X-100 at room temperature for 1 hour followed by washing with 1X PBS containing 0.1% Triton-X-100 for 3 times. Next, the cells were incubated with Alexa Fluor 594-conjugated donkey anti-rabbit IgG, Alexa Fluor 488-conjugated donkey anti-mouse IgG, Pacific Blue-conjugated goat anti-rabbit IgG (Molecular Probes, Eugene, OR) and TRITC-phalloidin (Sigma Aldrich) diluted in 1X PBS with 0.1% Triton-X-100 at room temperature for 1 hour followed by washing with 1X PBS containing 0.1% Triton-X-100 for 5 times. Cells on the cover slips were examined under a fluorescence microscope or a confocal fluorescence microscope (Olympus FV500). All images were captured with a ×100 objective lens or a ×60 objective lens and presented by Microsoft PowerPoint software (Microsoft 2002).

2.10 Cell migration assay

Migration assays were carried out with a modified Boyden chamber (24-well Transwell, Corning Costar; 8 μm pore size) as previously described (Shang et al., 2003). The lower surface of the filter was coated with 5 μg/ml fibronectin (Sigma) as a chemoattractant at 37°C for 1-2 hours. Transfected NIH3T3 or MCF7 cells were seeded in the Boyden chamber at a density of 1.5X10^5 in 100 μl of DMEM (high glucose) with 0.2% bovine serum albumin. The lower compartment was added with 600 μl DMEM (high glucose) containing 10% serum. Equal amount of cells were seeded in 6-well plates in DMEM with 10% serum to show the relative total amount of transfected cells. Cells were allowed to migrate for 4 h or 12 h as described in the results. Then the cells that did not penetrate the filters were completely wiped off with cotton swabs. The cells transfected with green fluorescence that has migrated to the lower surface and the total transfected cells in the 6-well plate were fixed with 1X PBS with 4% paraformaldehyde and counted in different fields under a fluorescence microscope. In certain experiments, GFP plasmid was used as marker because the fluorescence of GFP-tagged DLC1 is much fainter than the GFP control. In another set of migration assays, NIH3T3 cells were transiently transfected with cell marker pCMV-βGAL alone (Ctrl) or together with 4 times quantity of epitode-tagged plasmids. Cells expressing pCMV-βGAL were shown by their blue color after fixation with 1X PBS with 4% paraformaldehyde and over-night incubation with X-GAL buffer (1X PBS containing 4 mM potassium ferricyanide, 4 mM potassium ferrocyanide, 2 mM MgCl$_2$ and 1 mg/mL X-GAL) at 37°C. Migrated and total transfected cells were counted in different fields under a white-light microscope.

Chapter 3

Results

3.1 Cloning of DLC1

Full length cDNA for DLC1 was generated by reverse-transcription based polymerase chain reaction from total RNA isolated from human 293T (Figure 3.1) and verified by sequencing entirely in both directions. For further binding and functional studies, full length and different truncation mutants of DLC1 were made as epitope-tagged recombinants by suitable primers designed (see Materials and Methods) that would express fragments of DLC1 protein (Figure 3.2).
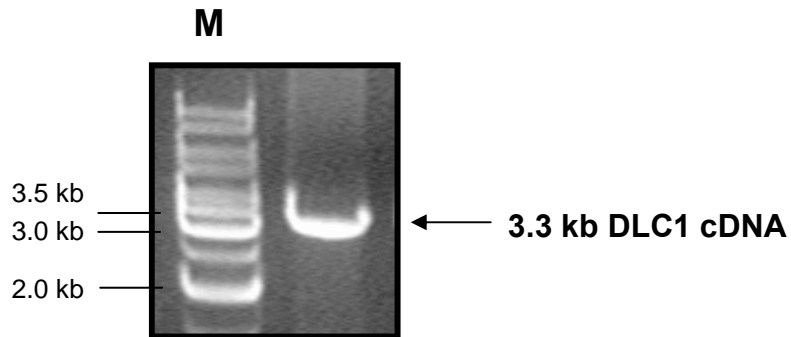
Figure 3.1 Molecular cloning of human DLC1 cDNA. RT-PCR was performed to amplify DLC1 cDNA from cDNA library of human 293T cells. M: DNA marker.
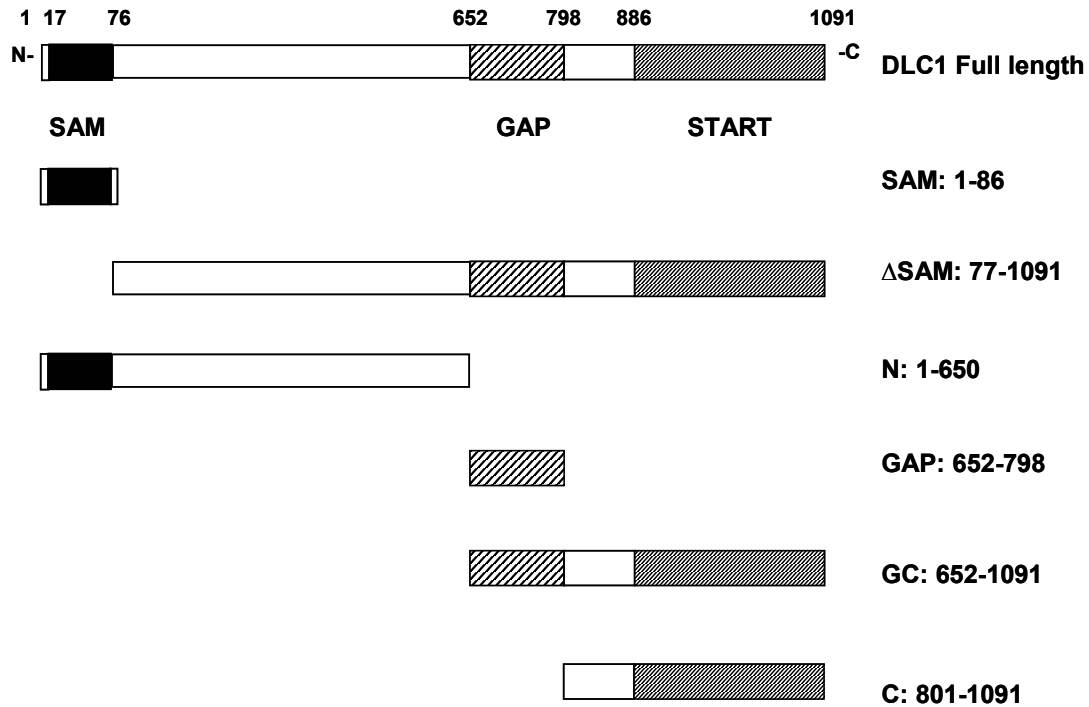
Figure 3.2 Schematic diagram showing the composition of protein domains of different truncation mutants of DLC1 protein.

3.2 Identifying EF1A1 as a novel interacting partner of DLC1-SAM domain

The GAP domain of DLC1 was known to be important for the effects of DLC1 in changing cell morphology and suppressing tumorigenesis (Wong *et.al.*, 2005). We hypothesized that other regions on DLC1 might modulate the function of DLC1 through the interplay with its GAP activity. Since a variety of SAM domains are widely used as regulatory modules in various cell activities through different mechanisms (see Chapter 1), the SAM domain of DLC1 (henceforth called DLC1-SAM) might as well has a regulatory function to the full length DLC1 protein. Therefore, we first sought to find out

whether the SAM domain might play a role in modulating the function of DLC1.

3.2.1 Multiple sequence alignment of various SAM domains

We hypothesized that the function of DLC1 might be regulated by the interaction of DLC1-SAM with some unknown molecule(s). However, it is uncertain whether such molecule(s) are proteins, nucleotides or lipids, since various binding properties have been found for different SAM domains, including protein-binding, DNA/RNA-binding and even lipid-binding property (Qiao and Bowie, 2005). In order to predict the putative binding property and putative binding partner(s) of DLC1-SAM, multiple sequence alignment of DLC1-SAM and several SAM domains with known structures and/or various known binding properties was carried out using the program CLUSTALW (http://www.ebi.ac.uk/clustalw) (Figure 3.3A). The alignment result shows that the amino acid sequence of DLC1-SAM is highly similar to DLC2-SAM and their sequences share 73% identity. However, the binding property and function of DLC2-SAM is also unknown yet. Except for DLC2-SAM, DLC1-SAM shares low degree of identity (<20%) with other SAM domain sequences, indicating the binding partner of DLC1-SAM could be different from other SAM domains. Here, the phylogenetic tree generated by the alignment shows that DLC1-SAM is more closely related to the SAM domains of BAR, FLI1, EphA4 and EphB2 and less close to the SAM domains of p73-SAM, VTS1-SAM and Smaug-SAM (Figure 3.3B). The SAM domains of BAR, FLI1, EphA4 and EphB2 are involved in protein-protein interaction, whereas p73-SAM has potential lipid-binding property, and VTS1-SAM and Smaug-SAM have nucleotide-binding

property (Qiao & Bowie, 2005; Green *et al.*, 2003; Aviv *et al.*, 2003; Stapleton *et al.*, 1999; Smalla *et al.*, 1999; Mackereth *et al.*, 2004). The alignment result shows that DLC1-SAM is likely to be involved in protein interaction though the target remains unknown.

A

```
                                                                   Residues
hsDLC1    LTQIEAKEACDWLR-ATG---FPQVAQLYEDFLFP-IDISLVKREHDFLDRDA-IEALCRRLNT----LNKCAVMK-  (11-76)
hsDLC2    QQEIEAKEACDWLR-AAG---FPQVAQLYEDSQFP-INIVAVKNDHDFLEKDL-VEPLCRRLNT----LNKCASM--  (55-119)
mmEPHA4   PEFSAVVSVGDWLQ-AIK---MDRYKDNFTAAGYTTLEAVVHMSQDDLARIG--ITAITHQNKI----LSSVQAMR-  (908-973)
hsEPHB2   PDYTSFNTVDEWLE-AIK---MGQYKESFANAGFTSFDVVSQMMMEDILRVG--VTLAGHQKKI----LNSIQVMR-  (869-961)
scSTE11   EKTNDLPFVQLFLE-EIG---CTQVLDSFIQCNLVTEEEIKYLDKDILIALG--VNKIGDRLKI----LRKSKSFQ-  (38-103)
hsARAP2   SVSEVNVDIKDFLM-SIN---LEQVLLHFHESGFTTVKDCAAINDSLLQKIG--ISPTGHRRRI----LKQLQIIL-  (3-68)
mmSAMSN1  RRRENHQTIQEFLE-RIH---LQEYTSTLLLNGYETLDDLKDIKESHLIELN--IADPEDRARL----LSAAESLL-  (230-295)
scVTS1    TDPKLLKNIPMWLK-SLR---LHKVSDALSGTPWI---ELIYLDDETLEKKG--VLALGARRKL----LKAFGIVI-  (26-88)
dmSMAUG   TRNVGMSGIGLWLK-SLR---LHKYIELFKNMTYE---EMLLITEDFLQSVGV-TKGASHKLALCIDKLKERANIL-  (593-660)
hsP73     PPYHADPSLVSFLT-GLG---CPNCIEYFTSQGLQ---SIYHLQNLTIEDLG--ALKIPEQYRMT--IWRGLQDLKQ  (485-550)
mmBAR     VDKWTTEEVVLWLE-QLGPW-ASLVRDRFLSERVN-GRLLLTLTEEEFSRAPYTIENSSHRRVI----LTELERVR-  (173-247)
hsFLI1    PTLWTQEHVRQWLEWAIKEYSLMEIDTSFFQ-NMD-GKELCKMNKEDFLRATTLYNTEVLLSHLS--YLRESSLLA-  (124-201)
```

B
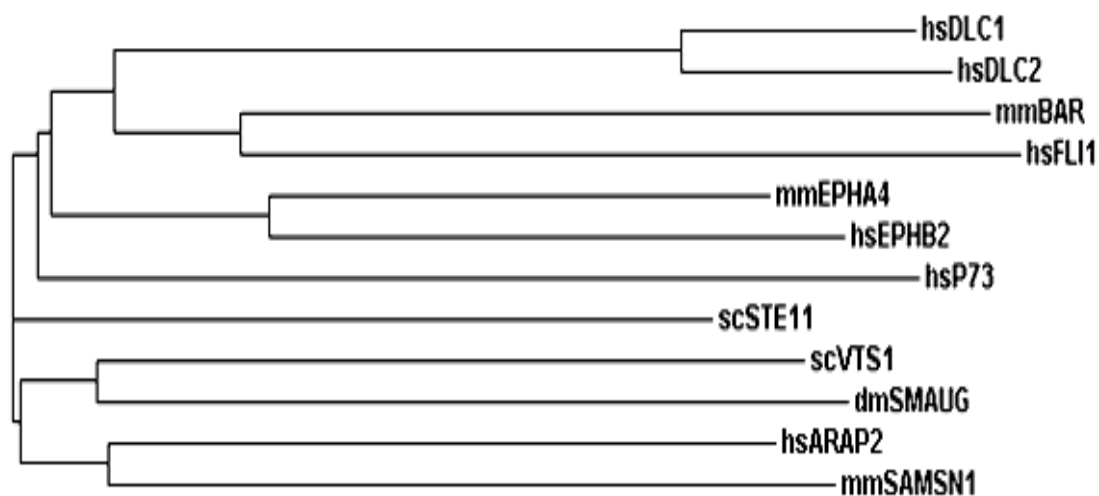
Figure 3.3 Homology of DLC1-SAM with other SAM domains of known structures/binding properties. (A) Multiple sequence alignment was generated using the program CLUSTALW (http://www.ebi.ac.uk/clustalw) with default settings. Residues totally conserved in all sequences are shaded *black*, those conserved in most of the sequences are in *dark grey*, while the significant but least conserved ones are in *light grey*. Species abbreviations: hs, *Homo sapiens*, mm, *Mus musculus*; sc, *Saccharomyces cerevisiae*. GenBank accession number gi: hsDLC1, 33188437; hsDLC2, 28976169; mmEPHA4, 30705030; hsEPHB2, 119615430; hsFLI1, 14603316; scSTE11, 609414; mmBAR, 21313130; scVTS1, 74583753; hsARAP2, 16118245; mmSAMSN1, 10800126. (B) Phylogenetic tree generated by the alignment shows the evolutionary relationship for the SAM domains of various proteins.

3.2.2 DLC1-SAM does not mediate homophilic interaction

Based on the alignment result that DLC1-SAM is more closely related to the SAM domains with canonical protein-binding property, we set out to investigate the protein-binding activity of DLC1-SAM. Since many SAM domains can lead to homophilic interaction to form dimers, trimers or even oligomers (Qiao & Bowie, 2005), we wondered whether DLC1-SAM can bind to itself. To investigate whether DLC1-SAM has homophilic binding property, protein-precipitation was carried out using bacterial-expressed GST-tagged SAM and the lysate of human 293T embryonic kidney epithelial cells expressing Flag-tagged SAM (Figure 3.4A). 293T cells were used because 293T cell line is good for protein expression. The result shows that GST-SAM could not

pull down Flag-tagged SAM from whole cell lysate. To further confirm that DLC1-SAM could not mediate homophilic interaction, immunoprecipitation assay was carried out using Flag-tagged SAM co-expressed with HA-tagged DLC1 full length in 293T cells (Figure 3.4B). The immunoprecipitation result shows that DLC1-SAM could not mediate interation with DLC1 full length either. Our conclusion was further supported by our collaborators' results showing that DLC1-SAM exists in a monomeric form even at a protein concentration of ~1 mM as demonstrated from dynamic light scattering, gel filtration and NMR relaxation experiments (courtesy of Dr. Yang Daiwen, Yang Shuai and Dr. Zhang Jingfeng).

A   **B**

WCL PD   WCL   IP

Anti-Flag ── 15kDa Flag-SAM   Anti-HA ── 150kDa ← HA-DLC1
          ── 10kDa   ── 100kDa

          ── 37kDa GST-SAM   Anti-Flag ── 15kDa ← Flag-SAM
          ── 25kDa   ── 10kDa
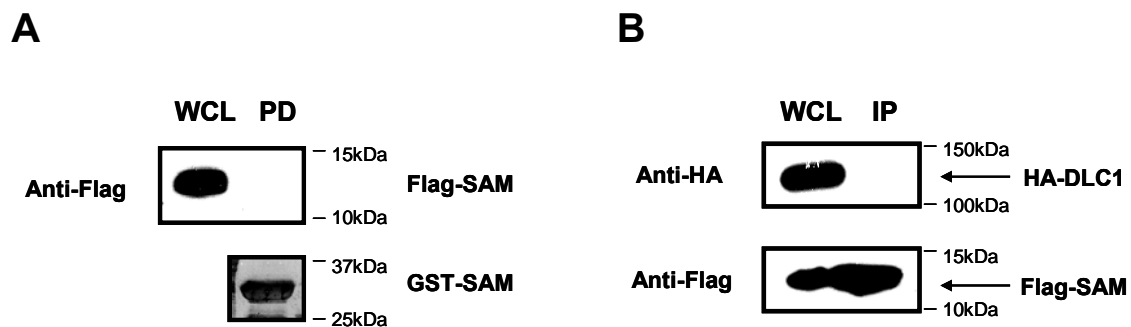
Figure 3.4 The SAM domain of DLC1 does not mediate homophilic interaction. (A) GST- SAM purified on glutathione-sepharose beads were used for pull-down (PD) assay with 293T whole cell lysates (WCL) expressing Flag-tagged SAM. (B) Whole cell lysates of 293T cells transfected with Flag-tagged SAM and HA-tagged DLC1 were incubated with M2-anti-Flag beads and Flag-constructs were immunoprecipitated (IP) on the beads. (A, B) The associated proteins were then separated on SDS-PAGE, blotted and probed with indicated antibodies. Blot in (A) was stripped and stained with amido black to reveal loading of GST recombinants (bottom panel).

3.2.3 EF1A1 is a novel DLC1-interacting partner

Although DLC1-SAM can not bind to itself, it might interact with other proteins. So we continued to identify its putative protein target(s) by using protein precipitations and MALDI-TOF mass spectrometry analyses. Purified GST and GST-tagged DLC1-SAM on glutathione beads were incubated with the rat liver homogenates or lysis buffer. One unique band of 48 kDa was consistently observed (Figure 3.5A; *arrow*). Further tryptic digests and analyses by matrix-assisted laser desorption/ionization-time of flight (MALDI-TOF) mass spectrometry revealed various peptides that formed different parts of eukaryotic translation Elongation Factor 1 alpha 1 (EF1A1, previously known as EF-1α) (with 23% coverage of total sequence; Figure 3.5B), showing EF1A1 as the putative novel interacting partner of DLC1.

A
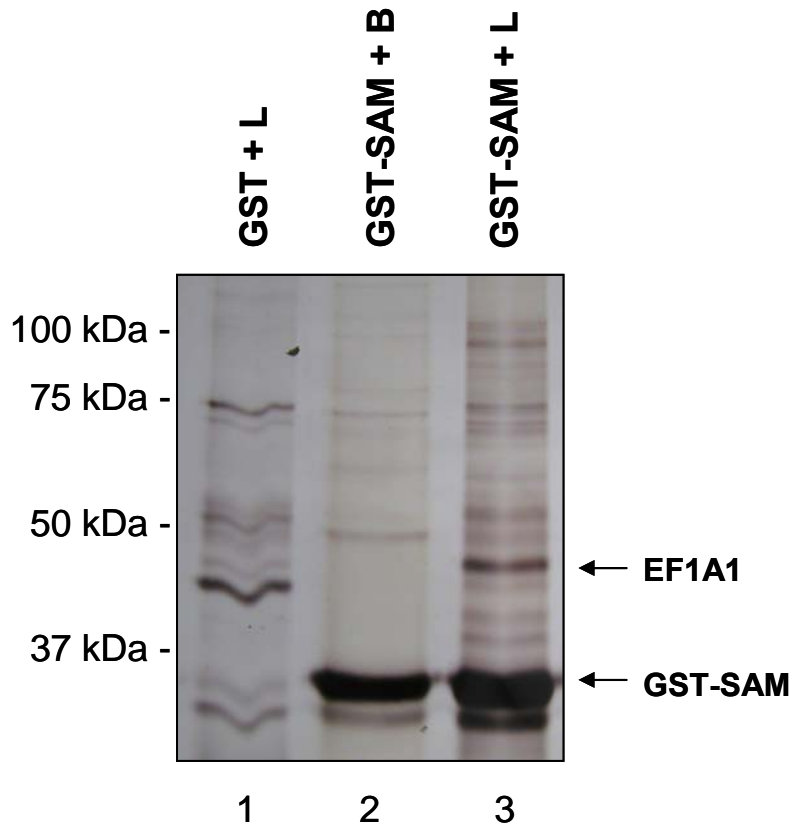
B

```
  1 MGKEKTHINI VVIGHVDSGK STTTGHLIYK CGGIDKRTIE KFEKEAAEMG KGSFKYAWVL
 61 DKLKAERERG ITIDISLWKF ETSKYYVTII DAPGHRDFIK NMITGTSQAD CAVLIVAAGV
121 GEFEAGISKN GQTREHALLA YTLGVKQLIV GVNKMDSTEP PYSQKRYEEI VKEVSTYIKK
181 IGYNPDTVAF VPISGWNGDN MLEPSANMPW FKGWKVTRKD GSASGTTLLE ALDCILPPTR
241 PTDKPLRLPL QDVYKIGGIG TVPVGRVETG VLKPGMVVTF APVNVTTEVK SVEMHHEALS
301 EALPGDNVGF NVKNVSVKDV RRGNVAGDSK NDPPMEAAGF TAQVIILNHP GQISAGYAPV
361 LDCHTAHIAC KFAELKEKID RRSGKKLEDG PKFLKSGDAA IVDMVPGKPM CVESFSDYPP
421 LGRFAVRDMR QTVAVGVIKA VDKKAAGAGK VTKSAQKAQK AK
```

Figure 3.5 Identification of Elongation Factor 1A1 as a novel partner of DLC1. (A) GST-SAM expressed and purified from *E. coli* was immobilized on glutathione-sepharose beads and incubated either with lysis buffer (B) or rat liver lysate (L). As controls, GST beads were mixed with the lysate or the GST-SAM incubated with the lysis buffer and processed the same way. After elution, bound proteins were resolved by SDS-PAGE and visualized by silver staining. A unique band around 48 kDa bound to the SAM domain of DLC1 (lane 3, labelled by arrow). (B) The band was subjected to trypsin-digestion followed by MALDI-TOF analysis (see Methods) and identified as elongation factor 1A1 (EF1A1). Peptide sequences representing 23% coverage of EF1A1 are underlined.

EF1A1 is very abundant in cells. To confirm that EF1A1 was indeed a *bona fide* partner of DLC1 *in vivo* and *in vitro*, coimmunoprecipitation and GST-pulldown experiments were conducted. First, the interaction between full-length DLC1 and EF1A1 was examined. 293T cells were transfected with Flag-tagged DLC1 full length. Whole cell lysate of untransfected cells was used as negative control. Figure 3.6A shows that endogenous EF1A1 could be co-immunoprecipitated with Flag-tagged DLC1 but not in the untransfected negative control, confirming their existence as a physiological complex *in vivo*. Next, 293T cells were transfected with Flag-tagged EF1A1 and were kept under quiescent state (Q) in medium without serum or were stimulated (S) with 10% serum after starvation before collection for IP. Consistently, immunoprecipitation of Flag-tagged EF1A1 also detected the endogenous DLC1 where their interaction appeared to increase moderately by treatment with serum (Figure 3.6B).

Second, the interaction between DLC1-SAM and EF1A1 was examined. Since the amino acid sequences of DLC1-SAM and DLC2-SAM are very similar with 73% identity (Figure 3.3A), we wondered whether EF1A1 has affinity only towards DLC1-SAM or towards both DLC1- and DLC2-SAM. Pulldown experiments were carried out using GST, GST-tagged DLC1-SAM or DLC2-SAM expressed in *E.coli.* and purified on glutathione beads with whole cell lysate of 293T cells. Figure 3.6C shows pulldown using GST-DLC1-SAM readily detected endogenous EF1A1, but neither the GST control nor the GST-DLC2-SAM could pull down EF1A1, showing the interaction specificity of DLC1-SAM and EF1A1. It is not clear why the amount of EF1A1 pulled down by GST-DLC1-SAM

is so little compared to the amount of EF1A1 in the lysate. This may be explained by the fact that a large portion of EF1A1 already forms complexes of the protein synthesis machinery or interacts with other binding partners inside the cells. Thus only a small portion of EF1A1 from the cell is free to bind to GST-DLC1-SAM. An alternative explanation would be that the binding between EF1A1 and SAM might be transient, *i.e.* the complex formed by EF1A1 and SAM may associate and disassociate quickly. Therefore only a part of EF1A1 that has ever bound to GST-DLC1-SAM can be shown by the pull-down result. It is also possible that the binding buffer may not have the optimum ionic condition for their binding and it may affect their binding affinity.

Next, coimmunoprecipitation assays were carried out using 293T cells overexpressing GFP-tagged EF1A1 together with Flag-tagged DLC1-SAM or a Flag-tagged control protein. Here, EF1A1 was fused with GFP tag to raise its molecular weight to avoid overlapping in the SDS-PAGE with the heavy chains of the M2-anti Flag antibody from the immunoprecipitation. Likewise, Figure 3.6D shows that immunoprecipitation of Flag-tagged SAM domain but not the unrelated protein control, detected GFP-tagged EF1A1. Altogether, our results confirm that EF1A1 is a novel *bona fide* binding partner of DLC1.
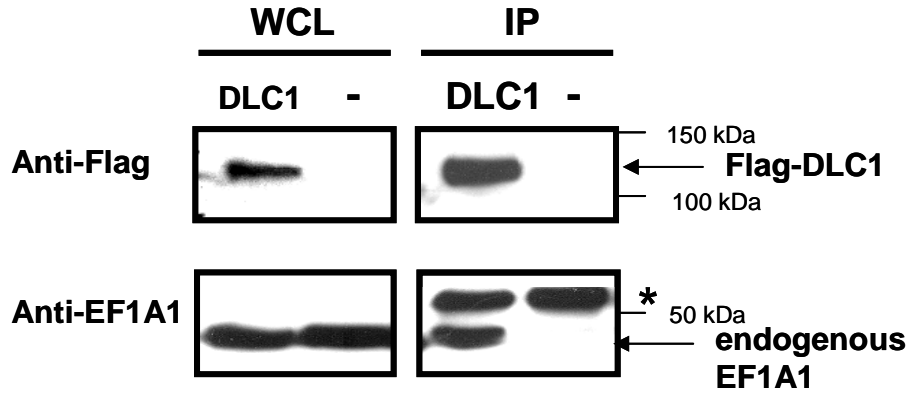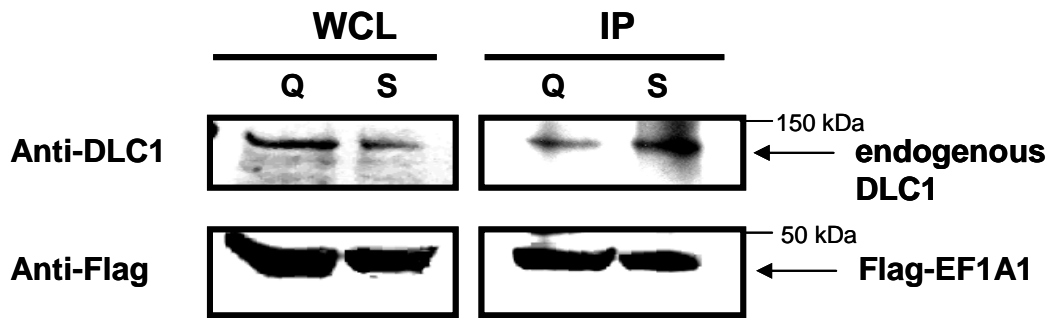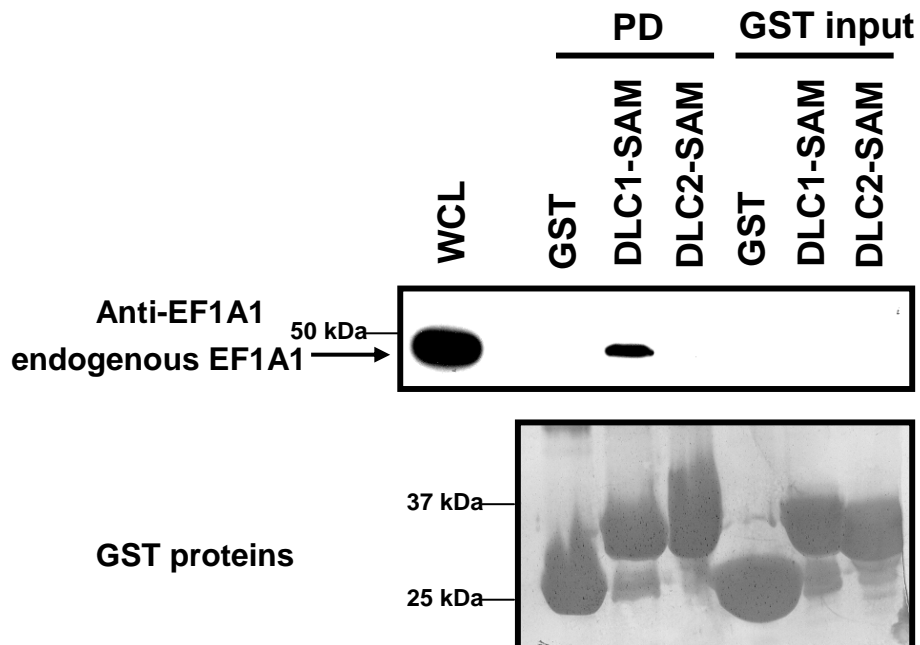
D
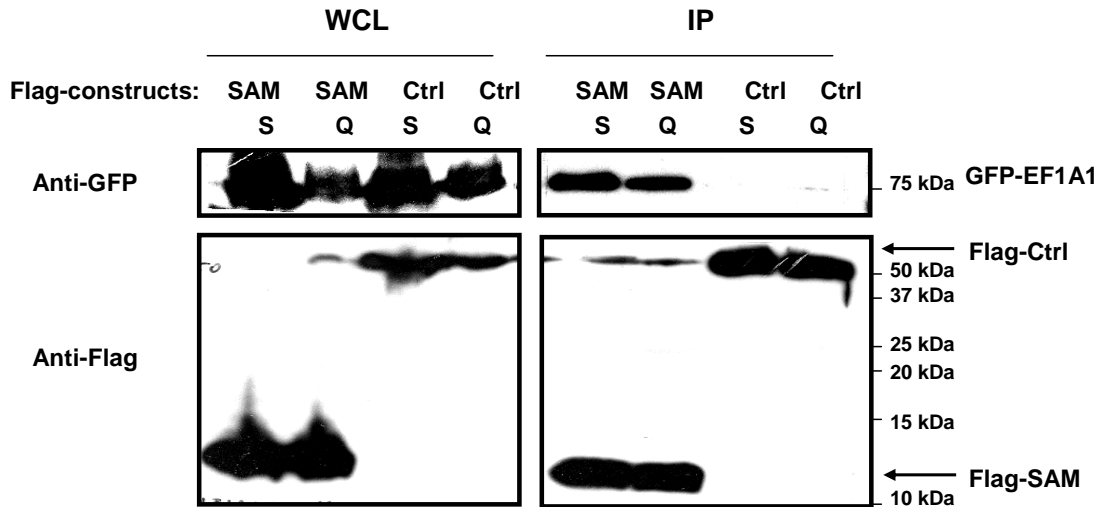
Figure 3.6 EF1A1 binds to full length DLC1 and DLC1-SAM *in vitro* and *in vivo*. (A) Whole cell lysates (WCL) of untranfected 293T cells or cells transfected with Flag-tagged DLC1 were incubated with M2-anti-Flag beads and Flag-constructs were immunoprecipitated (IP) on the beads. Bound proteins were separated on SDS-PAGE, blotted and probed with indicated antibodies to reveal the bound endogenous EF1A1. *Asterisk* indicates heavy chains of the anti-Flag antibody on the M2-beads. (B) IP, SDS-PAGE and immuno-blotting as in (A) were used with cell lysate expressing Flag-tagged EF1A1 to reveal the bound endogenous DLC1. Cells were kept under quiescent state (Q) or were stimulated (S) with 10% serum after starvation before collection for IP. (C) GST, GST-DLC1-SAM or GST-DLC2-SAM purified on glutathione-sepharose beads were incubated with 293T cell lysates. The associated proteins were separated on SDS-PAGE, blotted and probed with EF1A1 antibodies (upper panel). Blot was stripped and stained

with amido black to reveal loading of GST recombinants (bottom panel). (D) 293T cells co-expressing GFP-EF1A1 with either Flag-tagged SAM or an unrelated control (Ctrl) were made quiescent or stimulated with 10% serum after starvation and lysates immunoprecipitated with M2-anti Flag beads. Bound proteins on the beads were processed to reveal Flag-tagged constructs and the bound GFP-EF1A1.

However, SAM and EF1A1 did not interact with one another when both of them were produced as bacterial fusion proteins as shown from dynamic light scattering and gel filtration experiments by our collaborator (courtesy of Dr. Yang Daiwen, Yang Shuai and Dr. Zhang Jingfeng), suggesting that their interaction could either involve additional modifications or extra partner(s). To examine this, direct binding studies were carried out. His-tagged SAM was overexpressed and purified from human 293T cells instead of the bacterial host, through which DLC1-SAM was produced with post-translational modification and suitable folding in eukaryote cells, and at the same time in a more pure state for the binding assay. Then the purified His-SAM was subjected to protein pulldown assay (Figure 3.7A). His-SAM was strongly enriched by GST-EF1A1 and not by the GST control. Interestingly, there are two close bands at 15 kDa in the purified His-tagged SAM sample and only the upper band was enriched by GST-EF1A1. We wondered whether these two bands were really DLC1-SAM or just non-specific proteins from 293T cells. To confirm the identity of the two bands, purified His-SAM sample prepared as above was analyzed on SDS-PAGE and stained by PAGE-BLUE (Figure 3.7B). These two bands were then cut out separately and sent for analyses by MALDI-TOF mass

spectrometry after tryptic digests. MALDI-TOF results confirmed that both of the two bands are His-tagged DLC1-SAM. However, due to the low amount of proteins and their small molecular weight, the differences of the SAM in the two bands could not be identified from the MALDI-TOF results. Possible explanation for the result that purified His-SAM from 293T cells existed as two bands in the SDS-PAGE and only the upper band could bind to EF1A1, could be that additional post-translational modification(s) or different folding of the SAM domain in eukaryotic system for the upper band is necessary for the binding between DLC1 and EF1A1. To further substantiate their direct interaction, Flag-tagged DLC1 was transcribed and translated *in vitro* and then subjected to pulldown assays by GST-EF1A1. Rabbit reticulocyte *in vitro* translation system was used here to express Flag-tagged DLC1 because proteins produced in this system is more pure than proteins expressed from mammalian cells while proteins could have proper folding and posttranslational modifications from eukaryote translation system (Glass and Pollard, 1990). The result consistently shows that Flag-tagged DLC1 interacted with GST-EF1A1 but not the GST control (Figure 3.7C). Altogether, these results show that the interaction between SAM and EF1A1 is direct.
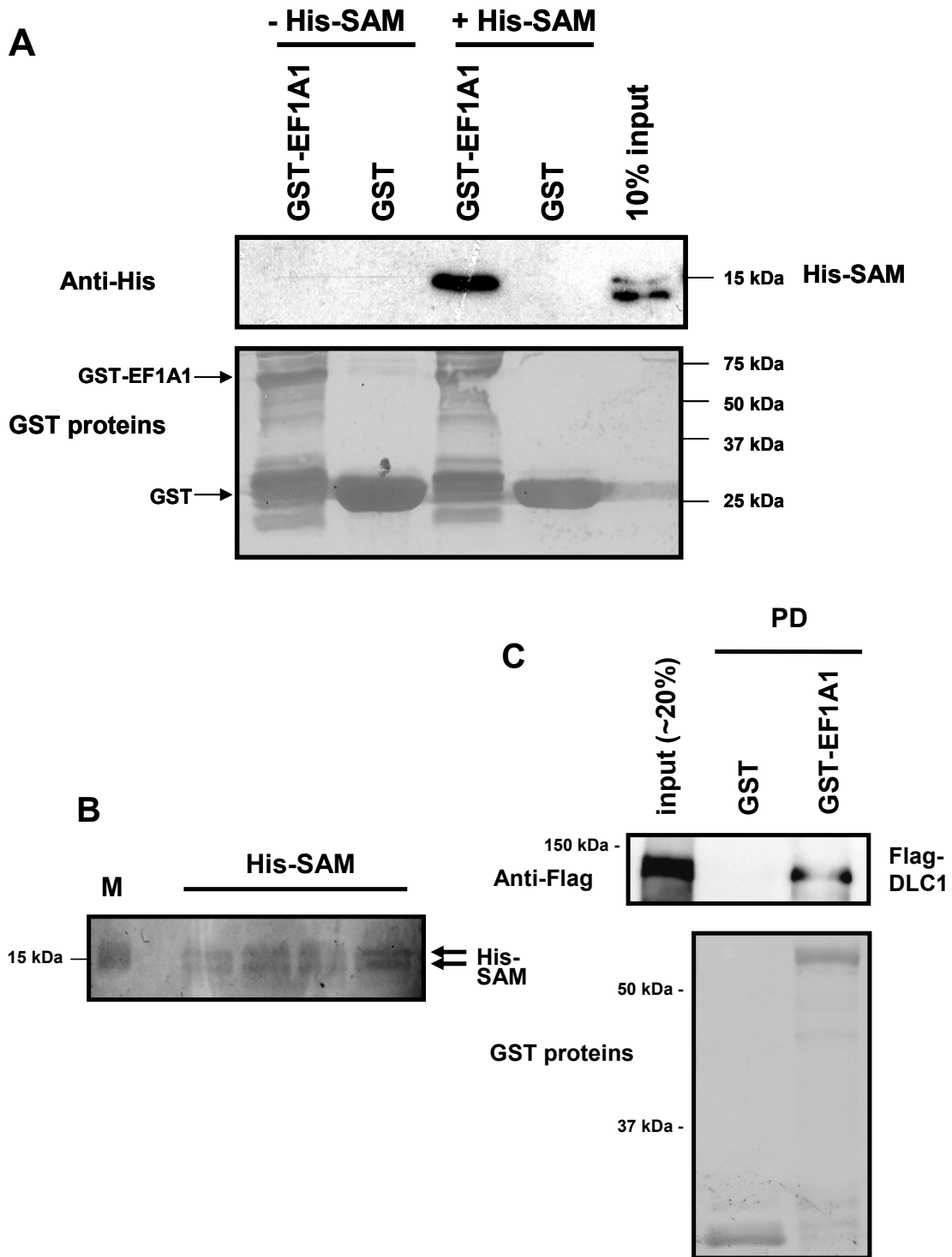
Figure 3.7 EF1A1 directly binds to full length DLC1 and DLC1-SAM. (A) GST or

GST-EF1A1 purified on glutathione-sepharose beads were incubated with or without His-

tagged SAM overexpressed and purified from 293T cells (see Materials and Methods). GST proteins and the bound His-SAM were separated on SDS-PAGE, blotted and probed with anti-Histidine antibodies (upper panel). Blot was stripped and stained with amido black to reveal loading of GST recombinants (bottom panel). (B) His-SAM expressed and purified from 293T cells was analyzed on SDS-PAGE and the protein gel was stained by PAGE-BLUE. Bands in the four wells at the same size were then cut out and sent for analyses by MALDI-TOF mass spectrometry after tryptic digests. (C) Flag-tagged DLC1 was transcribed and translated *in vitro* and incubated with either GST or GST-EF1A1 beads. GST proteins and the bound Flag-DLC1 were separated on SDS-PAGE, blotted and probed with Flag antibodies (upper panel). Blot was stripped and stained with amido black to reveal loading of GST recombinants (bottom panel). PD: pull down.

3.2.4 Two distinct motifs of EF1A1 are involved in binding to DLC1-SAM

EF1A1 comprises 3 distinct structural domains: Domain I at the N-terminus, the middle Domain II and Domain III at the C-terminus (Figure 3.8A). Domain I consists of a GDP/GTP-binding domain which binds to GTP in the active state of EF1A1, while Domains II and III are involved in the binding to aminoacyl-tRNA. Domains I and III have also been shown to be involved in binding globular-actin (G-actin) and bundling filamentous-actin (F-actin) (Murray *et al.,* 1996; Liu *et al.,* 2002; Gross *et al.,* 2005). We next set out to examine which part(s) of EF1A1 was involved in mediating its interaction with the DLC1-SAM domain so as to explore their binding mechanism. First, pulldown using GST-fusion of these three domains was carried out with His-SAM purified from

293T cells to detect the binding affinity of SAM to the three domains. The pulldown result shows that Domain III interacted most strongly with SAM. Binding to Domain I and Domain II was very weak or negligible under this condition (Figure 3.8A). To investigate whether their *in vivo* binding affinity was similar, immunoprecipitation assays were carried out using the HA-tagged full-length EF1A1 or its 3 domains co-expressed with either Flag-tagged DLC1 full-length or Flag-tagged SAM in 293T cells. Interestingly, both of the results show that binding by HA-Domain I alone is stronger than full length. By comparison, full-length EF1A1 or its Domain III interacted with either the full-length DLC1 or its SAM domain with similar affinity (Figure 3.8B & 3.8C). These results support the notion that binding of DLC1-SAM with EF1A1 are likely to be complex and could involve certain modulation on either one or both proteins *in vivo*. Taken together, these results confirm the specific interaction between the SAM domain of DLC1 and EF1A1 *in vitro* and *in vivo*. The molecular basis and the cellular and physiological significance of such interaction are further addressed in the discussion chapter.

A

B

C
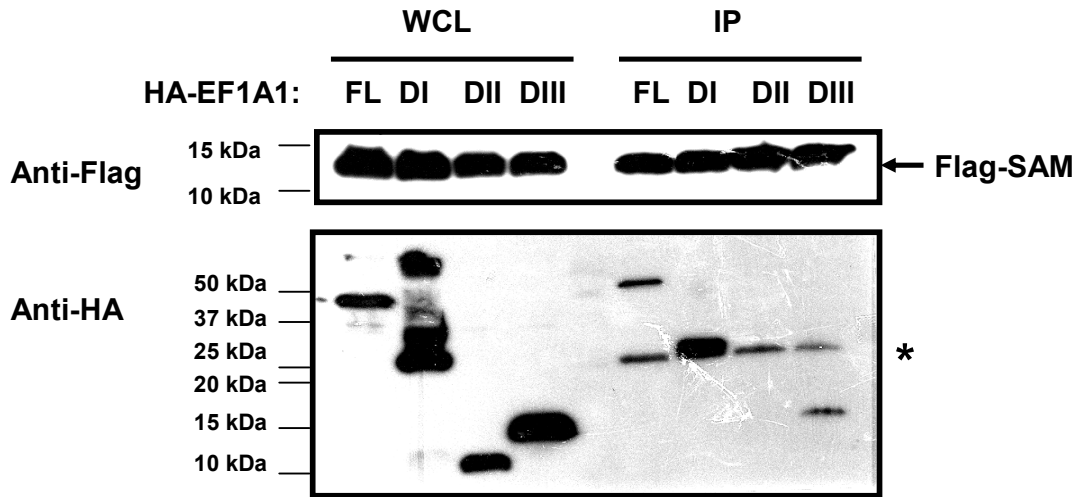
Figure 3.8 DLC1-SAM binds to distinct domains of EF1A1 *in vitro* and *in vivo*. (A) GST fusion of domain I (DI), domain II (DII)., and domain III (DIII) of EF1A1 were constructed based on the structure previously determined and indicated by the schematic diagram (upper panel). They were expressed in *E. coli* and purified on glutathione-sepharose beads. They were incubated with purified His-tagged SAM expressed in 293T cells and bound proteins were processed as described in Figure 2E. As negative controls, beads were incubated with buffer without His-SAM. (B, C) Whole cell lysates (WCL) from cells co-expressing HA-tagged EF1A1 full length (FL)., DI, DII or DIII and Flag-tagged DLC1 full length (B), or SAM (C) were used for immunoprecipitation (IP) with M2-anti Flag beads. WCL and IP samples were immunoblotted with indicated antibodies. Signal detected for DI is just above the light chain of Flag antibody (marked by an *asterisk*).

3.2.5 Identifying key EF1A1-binding motif in DLC1-SAM

3.2.5.1 Prediction of putative EF1A1-binding motif in DLC1-SAM

Given the pleotropic roles of various members of the SAM superfamily (Qiao and Bowie, 2005), it is important to examine the structure-function relationship of DLC1-SAM and how it interacts with EF1A1. So we continued to identify key EF1A1-binding motif in DLC1-SAM domain.

The NMR solution structure of DLC1-SAM (PDB ID: 2GYT) had been solved by our collaborator. The structure of DLC1-SAM shows that the SAM domain of DLC1 consists of four α-helices connected by well-defined loops (courtesy of Dr. Yang Daiwen, Yang Shuai and Dr. Zhang Jingfeng), which is different from the five-α-helice structure of most SAM domains (Qiao and Bowie, 2005). Based on the structure of DLC1-SAM, we tried to predict putative key EF1A1-binding residues. Protein-protein association can result from both hydrophobic and electrostatic/hydrogen bonding interactions between interfaces that comprise complementary nonpolar and charged/polar residues. A common type of interactive surface contains a hydrophobic patch surrounded by polar groups (Larsen *et al.,* 1998). There are three such regions on the DLC1-SAM surface (shown by *circle* in Figure 3.9B). In order to map out the binding site(s) of DLC1-SAM to EF1A1, we designed several SAM mutants with mutated residues in or close to the three potential binding interfaces and also some charged residues that could mediate binding by electrostatic interaction (shown by *dotted circle* in Figure 3.9B). They are: one double-mutant, K48A/R49A, one triple-mutant, F38G/L39G/F40G, and two quartet-mutants, K48A/R49A/R64A/R65A and F28G/F53G/L54G/A58G. The mutations were chosen on

the basis of the structure and van der Waals surface so that the mutants can retain the 3D structure of the wild type protein. Except for A58, all mutated hydrophobic residues were located in loop regions or the end of regular secondary structure elements. These mutants of DLC1-SAM were used for the following binding studies to investigate key-EF1A1 binding motif.

Figure 3.9 Putative EF1A1-binding motifs in DLC1-SAM. (A) Ribbon drawing of the 10 lowest-energy conformers of the solution structure of DLC1-SAM. The four helices are indicated in red/yellow. (B) Views of the van der Waals surface of DLC1-SAM, illustrating potential EF1A1-binding interfaces. The side chains are colored as green = hydrophobic, blue = basic, red = acidic and gray = polar (and main chain). Potential

EF1A1-binding hydrophobic patch surrounded by polar groups are shown by *circle*. Potential EF1A1-binding charged residues are shown by *dotted circle*. (The solution structure and the van der Waals surface courtesy of Dr. Yang Daiwen, Yang Shuai and Dr. Zhang Jingfeng.)

3.2.5.2 Residues F38 and L39 constitute key EF1A1-binding motif on DLC1-SAM

Next, we used mutants designed above for the immunoprecipitation assays to examine whether such mutations could decrease the binding affinity between DLC1-SAM and EF1A1. Flag-tagged wild type SAM, its mutants or an unrelated Flag-tagged control were co-expressed with HA-tagged EF1A1 in 293T cells and coimmunoprecipitations were carried out. The double-mutant K48A/R49A and the quartet-mutant K48A/R49A/R64A/R65A retained the binding to EF1A1 (Figure 3.10A), suggesting that the positively charged residues alone are not responsible for the binding. By comparison, the quartet-mutant F28G/F53G/L54G/A58G also retained the binding, yet the triple mutant F38G/L39G/F40G (abbreviated as FLF mutant hereafter) had significantly reduced binding. In order to confirm that the loss of binding between SAM-FLF and EF1A1 is not the result of spoiled secondary structure, CD spectra was carried out by our collaborator. CD spectra showed that this triple-mutant maintained the structure of the wild type (Figure 3.10B) (courtesy of Dr. Yang Daiwen, Yang Shuai and Dr. Zhang Jingfeng). Therefore, DLC1-SAM interacts with EF1A1 *via* either one or both of the two hydrophobic regions which are centered by or close to F40.

It is worth noting that the homologous DLC2-SAM did not show binding activity with EF1A1 (Figure 3.6C), though its structure is very similar to DLC1-SAM due to their high similarity on amini acid sequence (Li *et al.*, 2007; Kwan and Donalson, 2007). Although both of DLC1 and DLC2 SAM domains contain four α-helices, there are a number of significant differences, including their hydrophobic surfaces. Our result shows that triple mutation on residues F38G, L39G and F40G on DLC1-SAM had significantly reduced its binding to EF1A1 (Figure 3.10A). We wondered whether these residues could attribute to the EF1A1-binding selectivity towards DLC1-/DLC2-SAM (Figure 3.6C). So we first examined whether F38G, L39G and F40G of DLC1-SAM are conserved in DLC2-SAM. The alignment of their SAM domain sequences shows that F40 is conserved while F38 and L39 are substituted to S82 and Q83 in DLC2-SAM (Figure 3.10C). Further comparison of their structures shows that DLC2-SAM lacks the hydrophobic surface containing F38 and L39 in DLC1-SAM due to these residues being substituted to S82 and Q83 respectively (Figure 3.10D) (structure comparison courtesy of Dr. Yang Daiwen, Yang Shuai and Dr. Zhang Jingfeng). It is possible that it is F38 and/or L39 but not F40 that contribute to the binding selectivity of EF1A1. To examine this, we further designed mutants with single-point mutation at the three FLF residues, F38G, L39G and F40G, and carried out immunoprecipitation assays. 293T cells were used to coexpress HA-tagged EF1A1 with Flag-tagged DLC1 wild type SAM, FLF triple mutant, the three single-point mutants or DLC2-SAM. Figure 3.10E shows that single-point mutations F38G and L39G reduced the binding to EF1A1 as significantly as triple mutant FLF, yet the F40G mutant still retained the full binding ability to EF1A1. Consistent with the previous pulldown assay result (Figure 3.6C), DLC2-SAM did not bind to EF1A1 in the

coimmunoprecipitation assay (Figure 3.10E). These results suggest that the hydrophobic region containing F38 and L39 constitute a key binding motif that mediates the interaction between DLC1-SAM and EF1A1 and it contributes to the binding selectivity of EF1A1 towards DLC1-/DLC2-SAM.

Taken together, through structural and binding studies, we had identified residues F38 and L39 residues constitutes key EF1A1-binding motif on DLC1-SAM domain. This finding is important as comparing the cellular effects of EF1A1 with the wildtype and the non-interactive FLF mutant of DLC1 will allow immediate assessment of the functional consequence of their interactions.

A
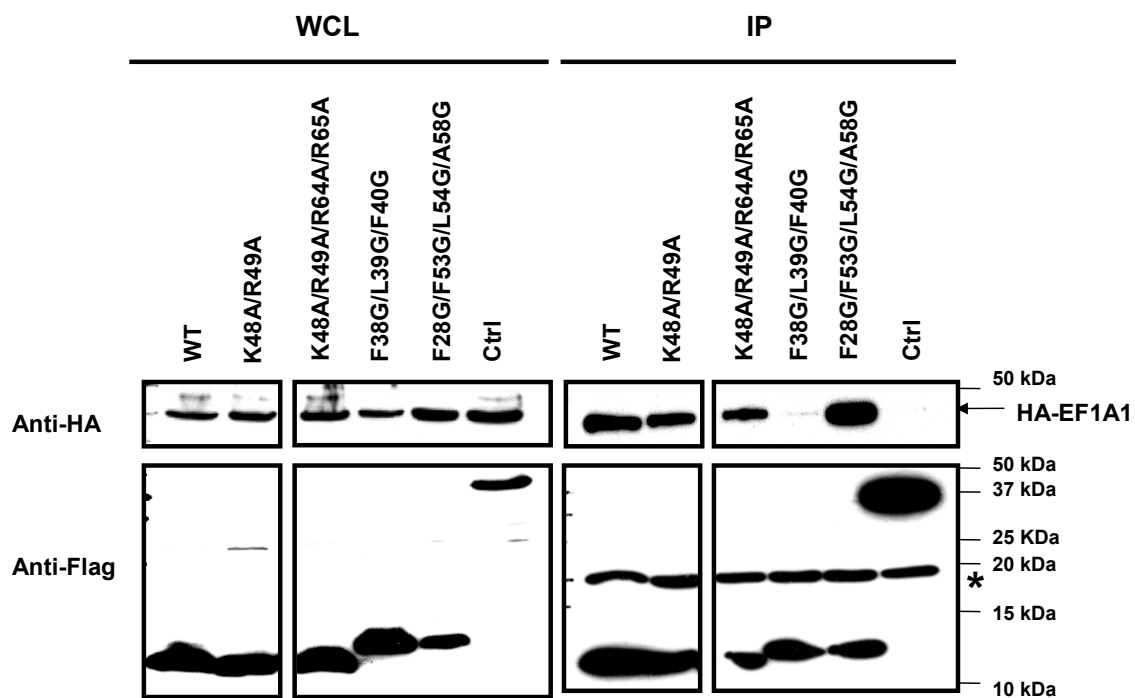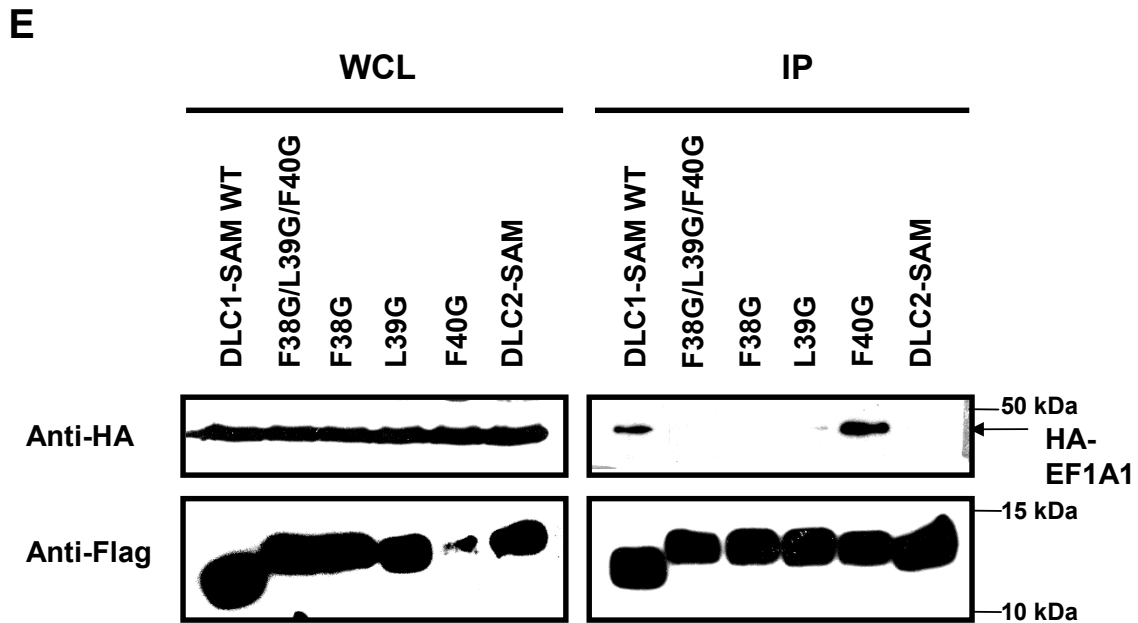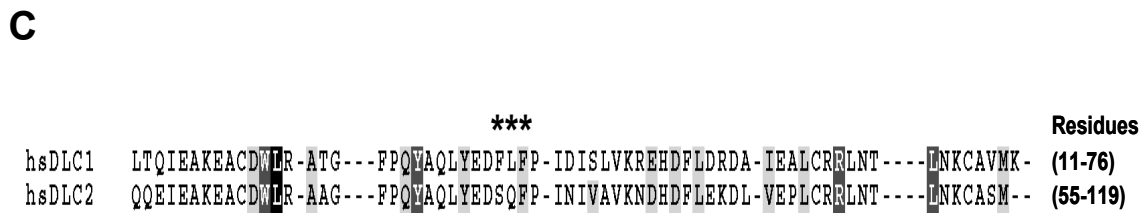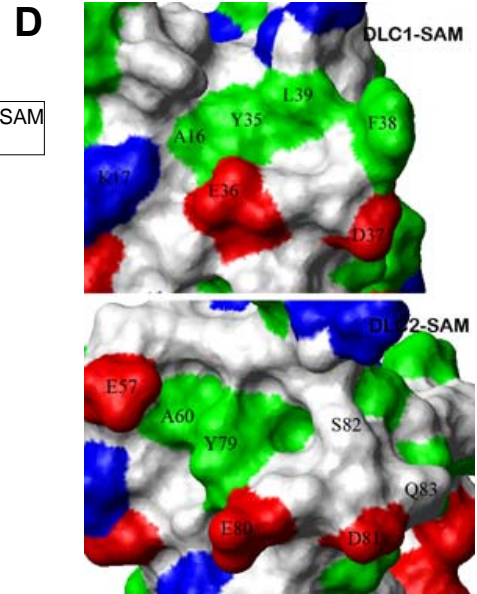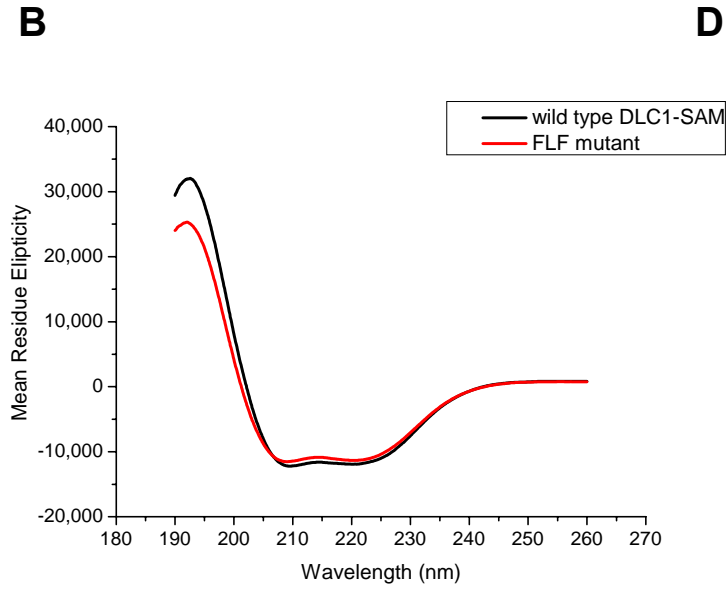
Figure 3.10 Identifying EF1A1-binding motif in DLC1-SAM. (A) 293T cells were co-transfected with plasmids encoding HA-EF1A1 and Flag-tagged SAM wild-type (WT), one double mutant, K48A/R49A, one triple mutant, F38G/L39G/F40G, or two quartet mutants, K48A/R49A/R64A/R65A, F28G/F53G/L54G/A58G or a Flag-tagged control encoding an unrelated protein (Ctrl). Whole cell lysates (WCL) were used for immunoprecipitation (IP) and incubated with M2-anti-Flag beads. WCL and IP samples were immunoblotted with indicated antibodies. *Asterisk* indicates the light chain of Flag antibodies. (B) CD spectra of the wild type and FLF mutant. The unit of mean residue ellipticity is deg $\cdot$ cm^2 $\cdot$ dmol^{-1} $\cdot$ residue^{-1}. The protein concentration was 20 μM. The spectra were acquired in 0.1-cm-pathlength cells. The conditions were 50 mM sodium phosphate, pH 7 at 25 °C. (C) Sequence alignment of DLC1-SAM (residues 11-76) and DLC2-SAM (residues 55-119) was generated as described in Fig. 3.3A. Residues totally conserved in all sequences are shaded *black*, those conserved in most of the sequences are in *dark grey*, while the significant but least conserved ones are in *light grey*. *Asterisks* indicate the corresponding residues of F38, L39 and F40 in DLC1-SAM. (D) Views of the van der Waals surface showing four hydrophobic residues A16, Y35, F38 and L39 on the EF1A1-binding motif of DLC1-SAM and four corresponding residues of DLC2-SAM (i.e. A21, Y40, S43 and Q44). (E) 293T cells were co-transfected with plasmids encoding HA-EF1A1 and Flag-tagged DLC1-SAM wild-type, one triple mutant, F38G/L39G/F40G, three single-point mutants, F38G, L39G, F40G or DLC2-SAM. Whole cell lysates were used for immunoprecipitation and processed as in (A). (CD spectra and views of the van der Waals surface courtesy of Dr. Yang Daiwen, Yang Shuai and Dr. Zhang Jingfeng).

3.2.6 DLC1-SAM facilitates dynamic disposition of EF1A1 to cell periphery

3.2.6.1 Effects of DLC1-SAM on actin-binding and polymerization

EF1A1 is a multi-functional protein that regulates general protein synthesis and also actin and microtubule network (Thornton *et al.,* 2003; Liu *et al.,* 2002; Gross & Kinzy, 2007; Moore *et al.,* 1998). EF1A1 regulates the actin network through its G-actin binding and F-actin bundling activity (Liu *et al.,* 2002; Gross & Kinzy, 2005; Murray *et al.,* 1996). Since DLC1 is a RhoGAP that acts on RhoA, which is a key regulatory switch for actin network, we hypothesized that DLC1's interaction with EF1A1 could be linked to actin-based dynamics.

Since the G-actin binding and F-actin bundling activity of EF1A1 had been shown previously (Liu *et al.,* 2002; Gross & Kinzy, 2005; Murray *et al.,* 1996), we set out to determine whether DLC1-SAM domain alone or its interaction with EF1A1 has any effect on the actin-binding and actin-proliferaction activity. First, we examined the *in vitro* G-actin binding activity of DLC1-SAM. Pulldown assay using purified globular actin (G-actin) and Flag-tagged wild type DLC1-SAM, FLF-mutant, DLC2-SAM expressed in 293T cells was carried out. The result shows that the wild type DLC1-SAM could pull down G-actin, while DLC1-SAM-FLF and DLC2-SAM could not (Figure 3.11). The failure to pull down G-actin by the FLF mutant and DLC2-SAM indicated that the interaction between SAM and actin could be mediated by EF1A1.
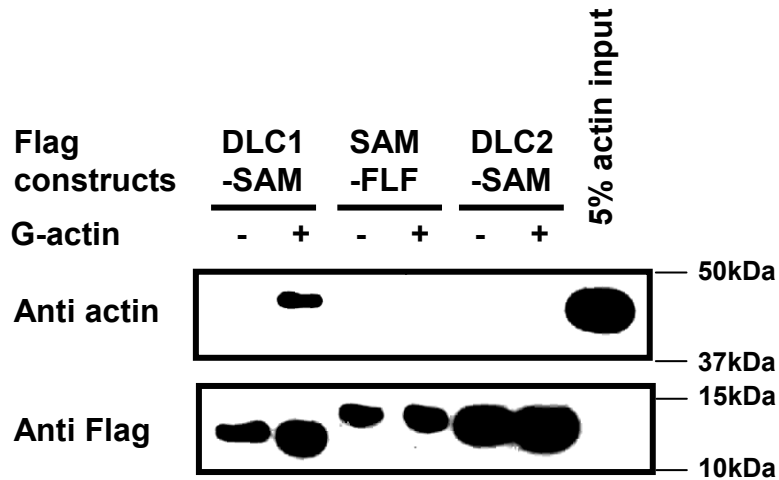
Figure 3.11 Interaction of DLC1-SAM with globular actin *in vitro*. SAM forms a complex with G-actin *in vitro*. Flag-tagged DLC1-SAM, DLC1-SAM-FLF and DLC2-SAM expressed in 293T cells and purified on M2-anti-FLag beads were incubated with purified globular actin at room temperature for 1.5 hour. Proteins bound on beads with incubation (+) or without incubation (-) were immunoblotted with indicated antibodies.

EF1A1 regulates actin dynamic and inhibits actin polymerization through binding and bundling actin filaments (Murray *et al.,* 1996). To assess whether DLC1-SAM binding to EF1A1 could have any direct effect on EF1A1 activity in actin dynamic, pyrene-labeled actin polymerization assays were performed in the presence of purified GST-EF1A1 with or without equimolar of GST-DLC1-SAM (Figure 3.12A). In this assay, fluorescence is enhanced when pyrene conjugated actin monomers associate into actin filaments and the steady state level of fluorecence correlates to the extent of polymerization. So the effects of certain compounds on actin polymerization can be indicated by the fluorescence level of the polymerization after adding the samples into the reaction. Samples

with EF1A1 all have a less steep gradient and a lower-valued plateau compared to the control, showing that EF1A1 could decrease actin polymerization speed and the final amount of polymerized actin. Such effects indicate an activity of EF1A1 in sequestering G-actin from actin polymerization. In comparison, SAM alone could not. Neither did SAM influence the activity of EF1A1 when both were present together (Figure 3.12B).

Some actin-regulating proteins affect actin polymerization only with the presence of the actin nucleator Actin-related protein 2/3 (Arp2/3) complex (Goley & Welch, 2006; Rohatgi *et al.,* 1999). To test whether SAM will affect actin polymerization under similar conditions, the assays with Arp2/3 were carried out. The result shows that SAM did not have any direct effect on the actin polymerization catalyzed by Arp2/3 complex (Figure 3.12A, 3.12C). These results therefore suggest that DLC1-SAM does not directly regulate EF1A1 activity towards actin binding and actin-polymerization. But it is still possible that the interaction between DLC1-SAM and EF1A1 might play a role in actin dynamic in intact cells instead.

A
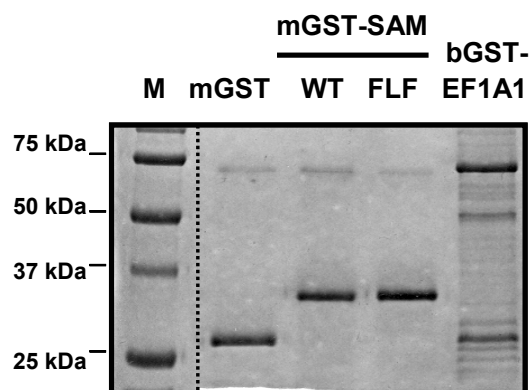
B
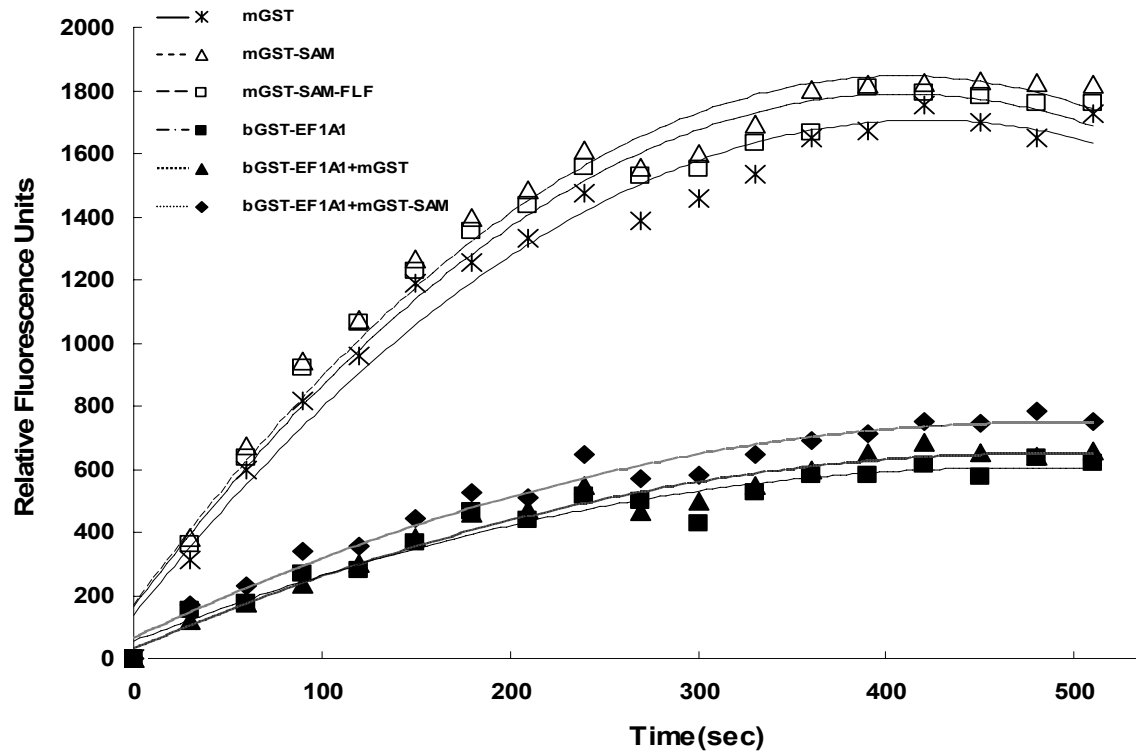
C
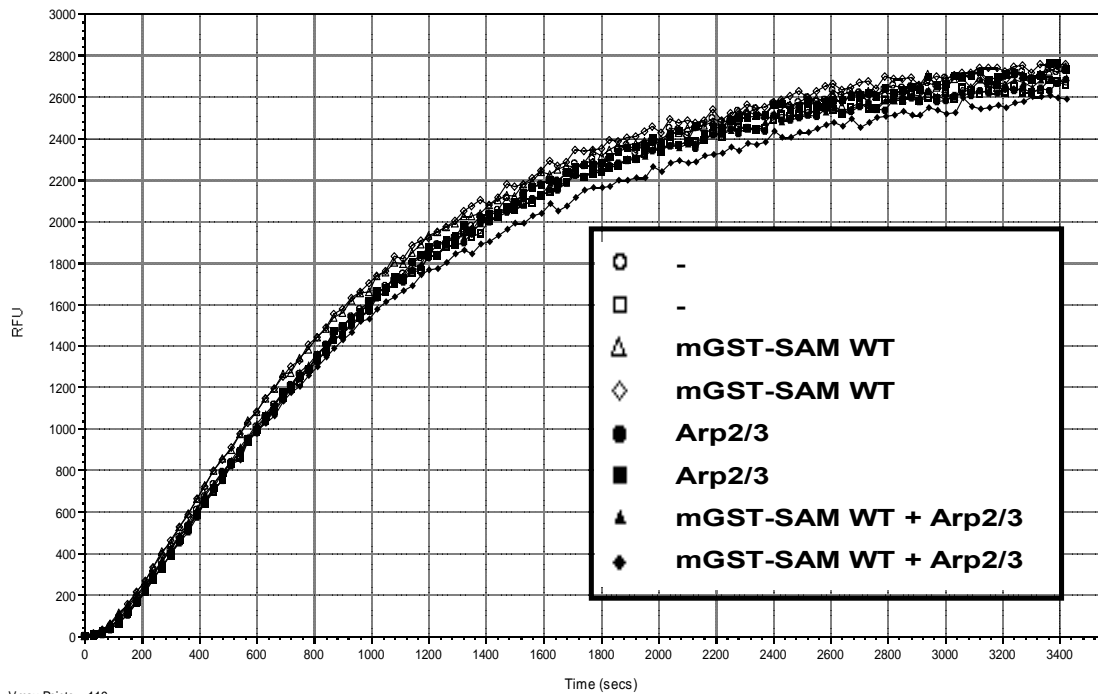
Figure 3.12 DLC1-SAM does not affect actin polymerization *in vitro*. (A) Purified mGST, mGST-DLC1-SAM wild type (WT), mGST-DLC1-SAM FLF mutant expressed in 293T cells and bGST-EF1A1 expressed in *E.coli.* were analyzed on SDS-PAGE and the protein gel was stained with Coomassie Blue to show the purity and equal amount of the peptides used in different samples. (B) Pyrene actin assay was performed to monitor the polymerization of 0.4 mg/ml pyrene-labeled G-actin in the presence of equimolar purified proteins as shown in (A). (C) DLC1-SAM does not affect actin polymerization in the presence of Arp2/3 complex. Pyrene actin polymerization was measured in the presence of purified mGST-DLC1-SAM wild type (WT) alone, purified Arp2/3 complex alone, both components added together, or no test proteins were added (-) as control. m: mammalian expressed; b: bacterial expressed; RFU: relative fluorescence units.

3.2.6.2 SAM domain mediates dynamic disposition of DLC1 with EF1A1 on cortical actin and membrane ruffles

Actin is assembled at major cellular structures such as focal adhesions, stress fibers, microspikes, membrane cortical and membrane ruffles (Rodriguez *et al.,* 2003). To better understand the functional relationship between DLC1-SAM and EF1A1 in actin-based cell dynamics, we used NIH3T3 cells treated with fibroblast growth factor (FGF) and confocal immunofluorescence microscopy to evaluate how DLC1 (wild type and mutants) and EF1A1 would regulate each other's disposition in some of these actin-rich structures. We first observed that expression of the full-length DLC1 in NIH3T3 fibroblasts led to drastic shrinkage of the cell body with resultant multiple protrusions.

These cells were also associated with major disruption at the focal adhesions. However, expression of DLC1-SAM or EF1A1 was never localized to the focal adhesions, as marked by paxillin staining in those cells, nor did it lead to drastic change of cell morphology, as compared with the non-transfected cell (*arrows*). Instead, they were diffused in the cytosol of the cells that still retained intact focal adhesions (Figure 3.13A). This result indicates that SAM domain is not required for DLC1's effect in dissolving focal adhesions.

Next, the disposition of DLC1 and EF1A1 at membrane cortical and membrane ruffles in quiescent and FGF-treated NIH3T3 cells were examined (Figure 3.13B). During quiescent state, DLC1 (wildtype or FLF) induced cell shrinkage indicative of an active RhoGAP. There, EF1A1 was mostly concentrated on cell periphery whereas DLC1 appeared to be partially colocalised with EF1A1 on cell periphery or being distributed in some punctate structures (labeled *P*). By comparison, overexpression of SAM domain and EF1A1 did not affect the cell morphology where SAM was seen colocalised strongly with EF1A1 in cytosol and at cortical actin (indicated by *box*). However, SAM-FLF that did not interact with EF1A1 failed to colocalise with EF1A1 (*dotted box*). To gain a better insight to the nature of the disposition of DLC1, the catalytic arginine-finger R677 within the GAP domain of DLC1 was mutated to glutamic acid. This mutant (DLC1-R677E) rendered cell spreading, thus allowing better studies of the intracellur distribution of these two proteins. There, the majority of DLC1-R677E was concentrated in large vesicular structures within the cytosol (labeled *P*), while EF1A1 now appeared more cytosolic-diffused than it was in the presence of a GAP-active DLC1. However, no colocalization of DLC1-R677E with EF1A1 was observed at cell periphery.

Comparing to the result by the DLC1-SAM domain alone, this result suggests that despite the presence of SAM domain, the inactivation of the GAP activity caused the retention of DLC1 in specific subcellular compartments, thus preventing its interaction with EF1A1 during the quiescent state. Consistently, DLC1-R677E carrying further mutations on FLF motif (DLC1-R677E-FLF) presented the same results as DLC1-R677E.

Interestingly, after FGF treatment, the DLC1 full-length, SAM and GAP-inactive DLC1-R677E all exhibited strong colocalization with EF1A1 in the cytosol, cortical region and also on the membrane ruffles (highlighted in *boxes*). However, introducing the FLF mutant to these constructs resulted in weaker if not complete loss of colocalisation of EF1A1 with DLC1 on these cellular structures. Indeed, EF1A1 appeared to be "retarded" or de-localised to the perinuclear and cytosolic region (dotted boxes). Consistently, DLC2-SAM that lacks the hydrophobic surface formed by FL residues in DLC1-SAM and does not bind EF1A1, did not colocalise with EF1A1 on these structures either.

Taken together, these results indicate that upon FGF stimulation, the SAM domain of DLC1 facilitated EF1A1 relocalisation from the cytosol and perinuclear regions to the site of actin-rich membrane ruffles via its specific interaction with EF1A1. There, they could help establish specific protein complexes needed for cell dynamics control.

A

B (Continued)

B (Continued)

quiescent   + FGF

SAM

SAM-FLF

DLC2-SAM
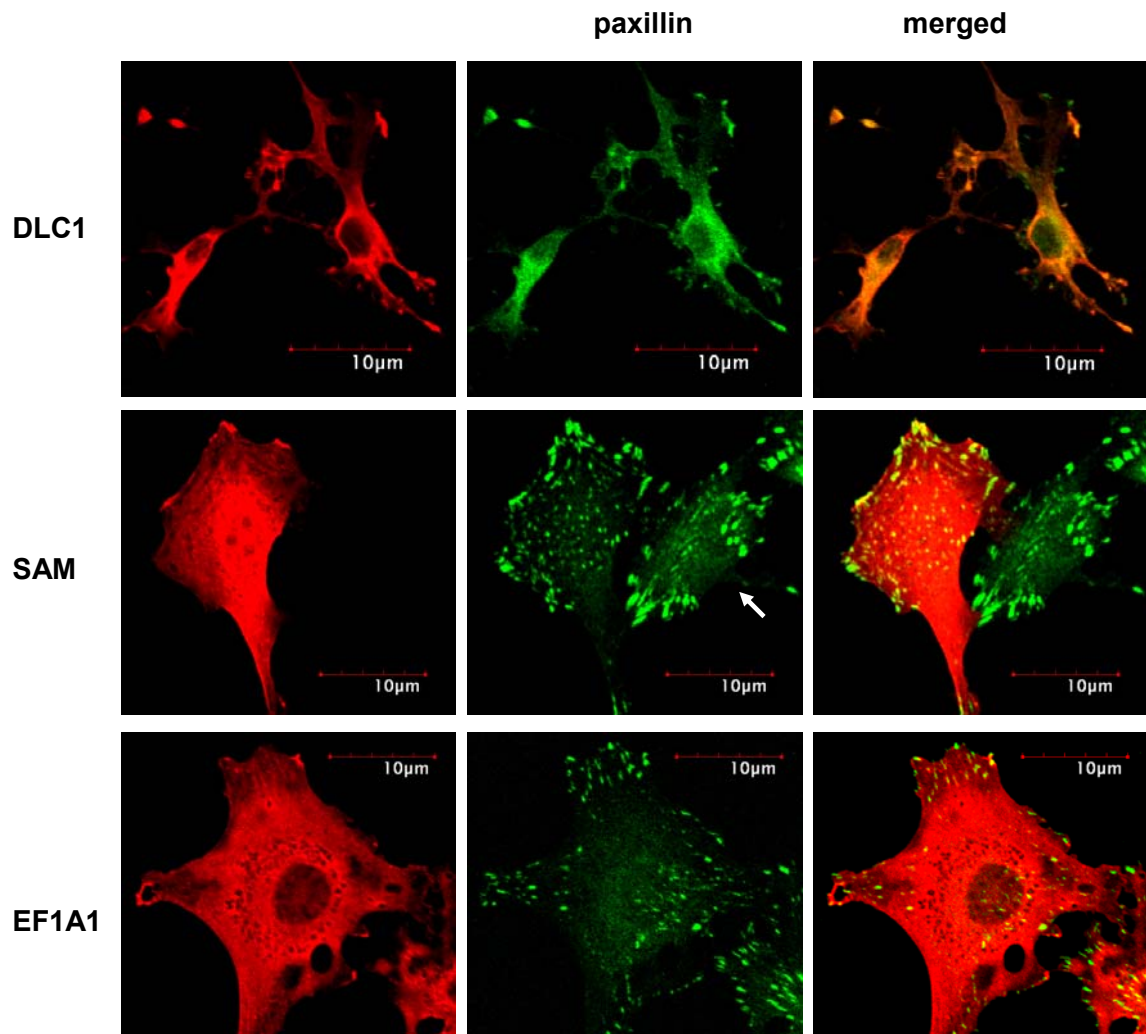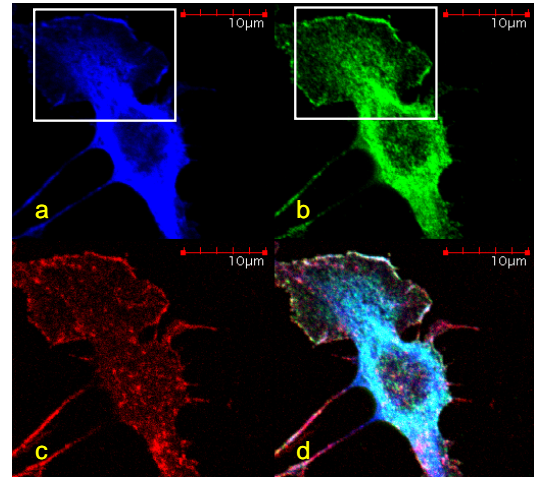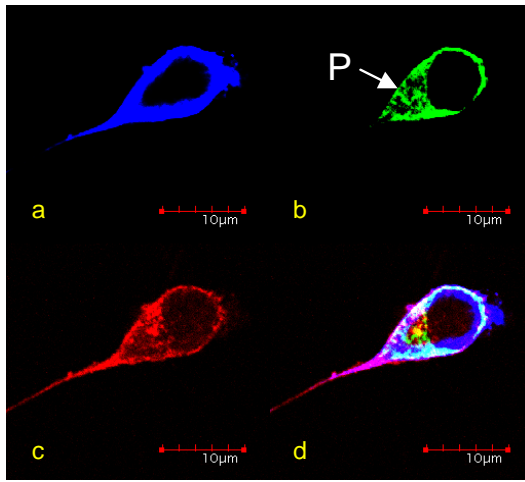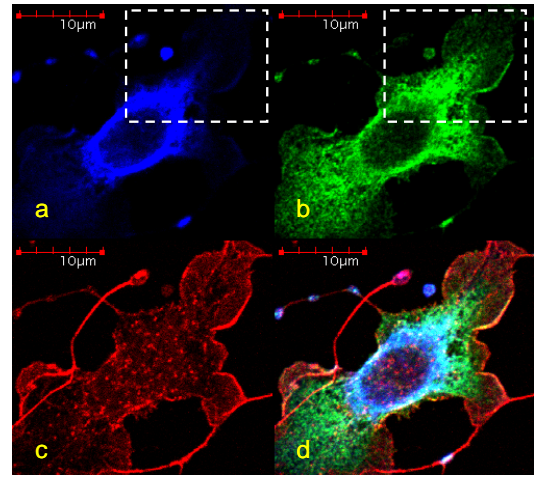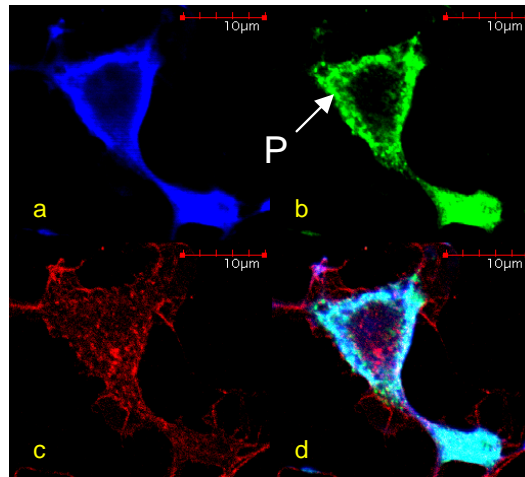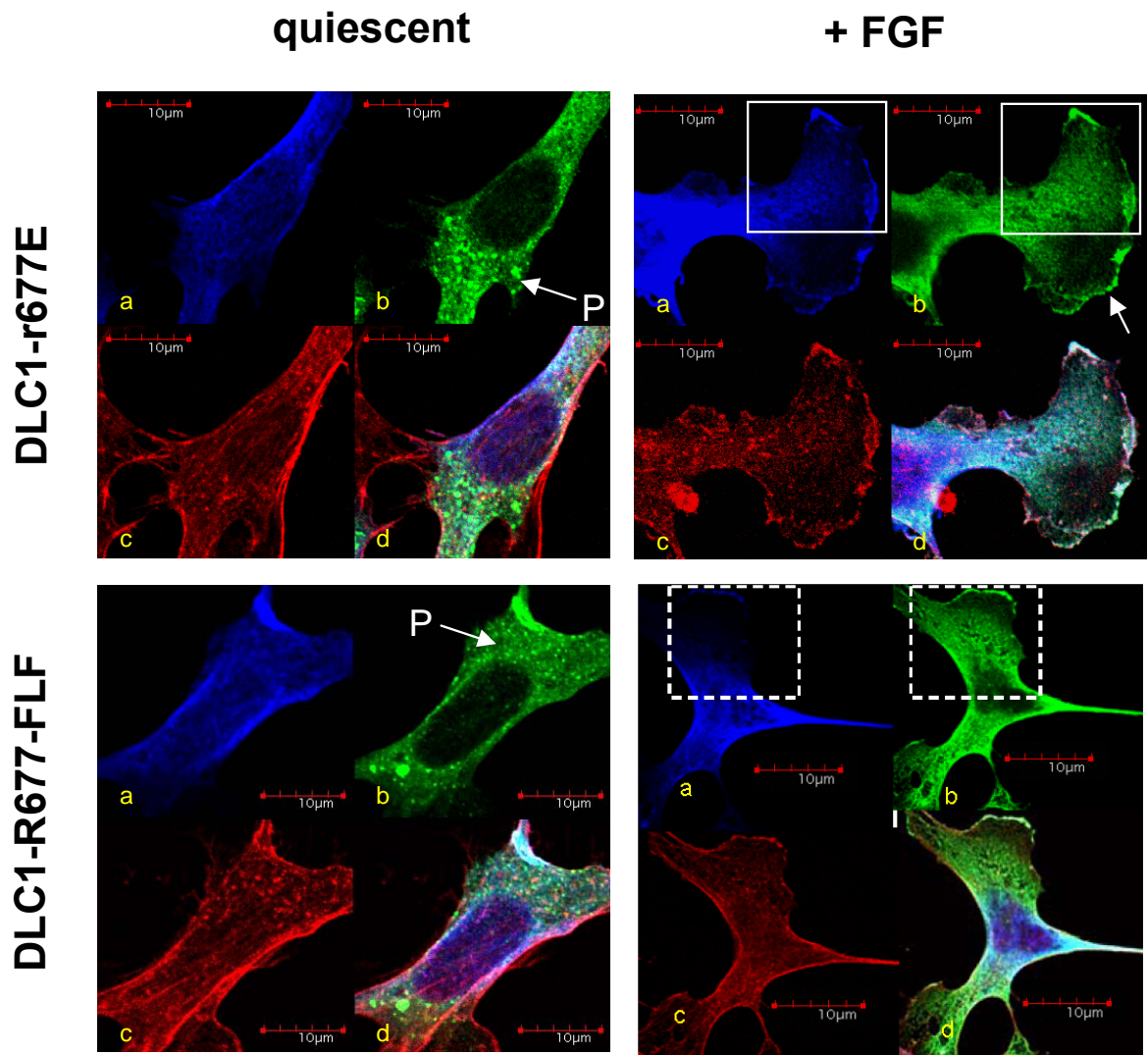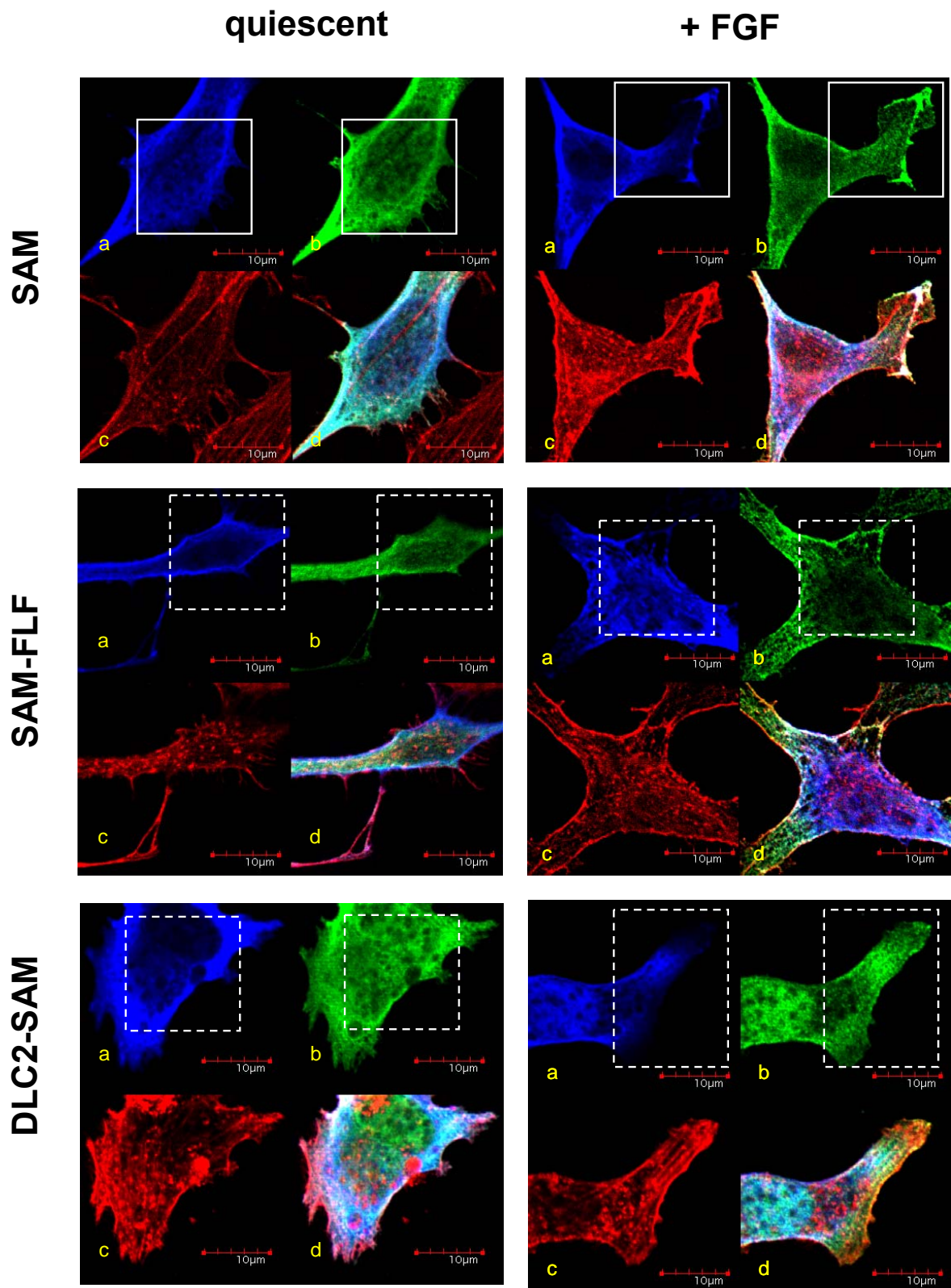
Figure 3.13 DLC1-SAM domain facilitates recruitment of EF1A1 to membrane periphery and membrane ruffles. (A and B) NIH3T3 cells were transfected with various constructs and made quiescent by maintaining in medium with 0.5% serum for 19 hours followed by treatment for 20 min with 10 ng/ml fibroblast growth factor (FGF). Cells were then fixed, permeabilized, stained and visualized under confocal immunofluorescent microcopy as described in "Materials and Methods". (A) DLC1-SAM and EF1A1 do not localize to paxillin at the focal adhesions. Cells were transfected with either Flag-DLC1, Flag-DLC1-SAM or HA-EF1A1 and treated with FGF before fixation. Ectopic expression of the proteins were detected by anti-Flag or anti-HA (red), and the focal adhesions are shown by anti-paxillin (green), followed by appropriate fluorophore-conjugated secondary antibodies. Merged signals are presented as overlaid staining (yellow). *Arrow* indicates untransfected control cell. (B) Cells were cotransfected with HA-EF1A1 and Flag-constructs of either DLC1 wild type (DLC1), DLC1 full length mutant F38G/L39G/F40G (DLC1-FLF), DLC1 full length mutant R677E (DLC1-R677E), DLC1 full length with combo-mutant of R677E and F38G/L39G/F40G (DLC1-R677E-FLF), DLC1-SAM domain wild type (SAM), SAM domain mutant F38G/L39G/F40G (SAM-FLF), or DLC2-SAM domain. Co-expressed HA-EF1A1 (a; blue), and different Flag-DLC1 constructs (b; green) were detected by appropriate anti-Flag and anti-HA followed by fluorophore-conjugated secondary antibodies. Cells were labeled with TRITC-phalloidin (c; red) to mark cell border, the cortical actin on cell periphery or membrane ruffles. Merged signals are presented as overlaid staining (d; cyan for A overlaid with B; purple for A overlaid with C; yellow for B overlaid with C; "bright white" for A overlaid with both B and C). The intensities of images were enhanced to

capture changes in the cell peripheries and cell protrusions. *Red bars* indicate 10 μm.

3.2.7 DLC1-SAM domain plays an auxiliary role in suppressing cell migration

It is known that DLC1 can suppress cell migration (Goodison *et al.*, 2005; Wong *et al.*, 2005). Here, we show that its SAM domain could recruit EF1A1 to cell periphery and membrane ruffles. Since formation of membrane ruffles is associated with cell migration, we sought to determine how DLC1-SAM could impact on this important biological process. Boyden chamber migration assays were used to examine the effects of wildtype and mutant constucts on cell migration. Motile NIH3T3 cells were transiently transfected with GFP plasmid together with greater excess of the Flag-tagged vector (Ctrl) or Flag-tagged wild-type/full length DLC1 (DLC1 WT), or with full length DLC1 with the specific triple FLF mutations (DLC1-FLF). After 4 hours, cells were allowed to migrate and the proportions of all transfected cells were then scored for their ability to exert migration as described in "Materials and Methods". Figure 3.14A shows that wildtype DLC1 greatly inhibited the rate of migration by more than 70%. However, the DLC1-FLF mutant displayed a significantly lower potency of inhibition compared to the wildtype (p=0.06). The result indicates that the interaction between EF1A1 and SAM domain could play a role in supporting the full suppression of cell migration by DLC1. In connection with this, it is predicted that introducing SAM domain could compete off the binding of endogenous EF1A1 with DLC1, thus affecting the intrinsic motility of these cells. To verify this, NIH3T3 cells were transiently transfected with GFP-tagged vector (Ctrl), DLC1-SAM wildtype (SAM) or SAM FLF-mutant (SAM-FLF) and allowed to

migrate for 4 hours. Figure 3.14B shows that cells expressing DLC1-SAM domain appeared to exert higher migration rate compared to the control and SAM-FLF. However, such stimulatory effect was only marginal probably because NIH3T3 cells already possessed high basal motility rate, making these cell lines best used for inhibition studies in cell migration as shown in Figure 3.14A. To further investigate the potentially stimulatory effect on cell migration by DLC1-SAM, we opted to use the epithelial MCF7 which was less motile at the basal level but confer high stimulatory capacity when compared to the NIH3T3. As a further control, effects of DLC2-SAM, which is highly homologous to DLC1-SAM but can not interact with EF1A1, was examined. Here, expression of the exogenous DLC1-SAM alone increased the rate of cell migration by more than two-folds ($p< 0.01$). However, this stimulatory effect was not observed at all when the corresponding DLC1-SAM-FLF mutant or DLC2-SAM was introduced (Figure3.14C). Since NIH3T3 and MCF7 cells have endogenous DLC1 expression (data not shown), it is conceivable that the exogenous SAM domain might act as a dominant negative mutant that interrupts the interaction between endogenous DLC1 and EF1A1, thus reversing the suppressive effect of the endogenous DLC1.

Taken together, our results strongly support the notion that DLC1 could mobilize EF1A1 to the membrane periphery and membrane ruffles via its SAM domain that could help establish actin-based dynamics necessary for the suppression of cell migration. Such auxiliary effect by SAM to the GAP-induced inhibition could serve to fine-tune the balance for cell motility that is essential for many aspects of bodily functions.
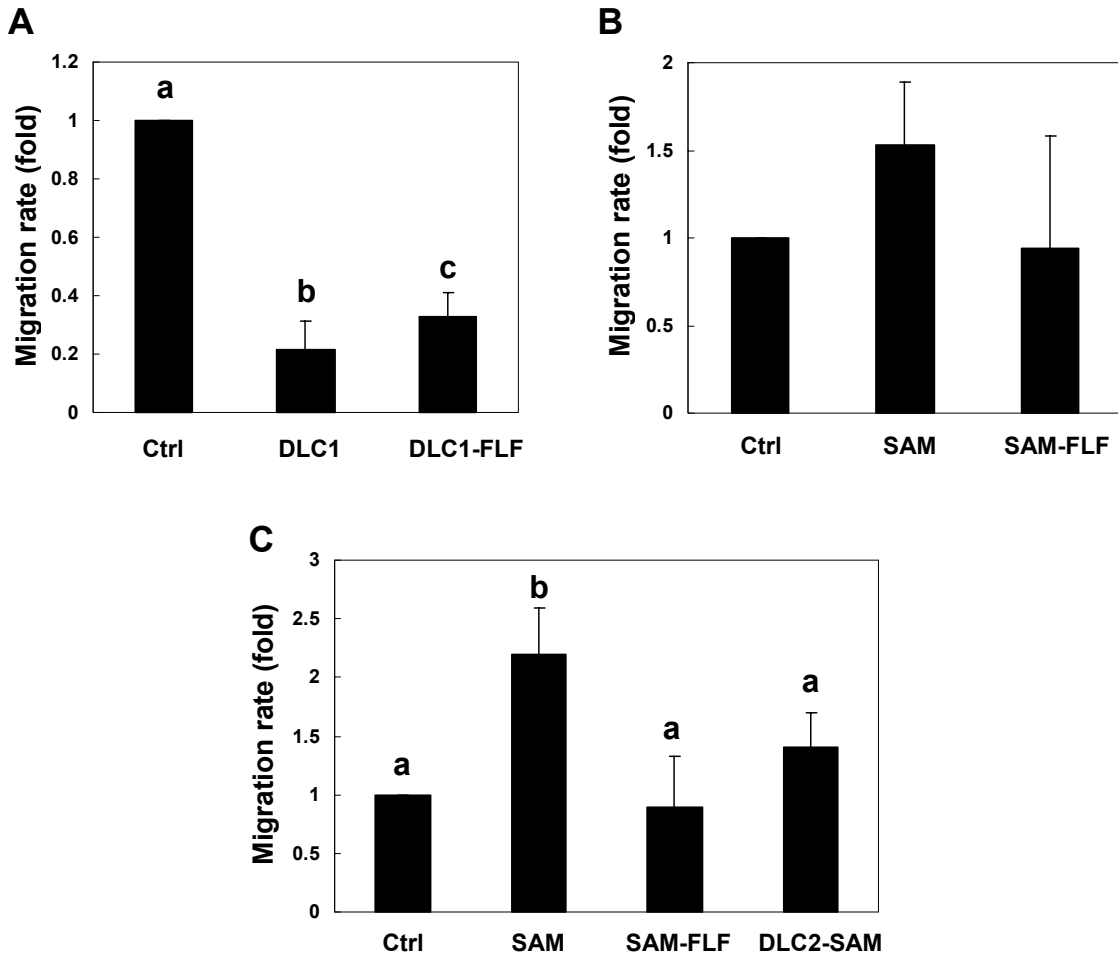
Figure 3.14 Effects of DLC1-SAM on cell migration. (A to C) The effects of different constructs on cell migration were assayed in Boyden chamber. Data were presented as the means +/- standard deviation (SD) compared with the control of 3 to 4 independent experiments. Statistical comparison was made using ANOVA and Newman-Keuls multiple comparisons. (A) NIH3T3 cells were transfected with GFP-tagged plasmid as cell marker together with 2 times quantity of Flag-tagged vector (Ctrl) or Flag-tagged DLC1 full-length wild-type (DLC1), FLF mutant of full length (DLC1-FLF). Data denoted by different letters indicate significant difference at p values of < 0.06. (B) NIH3T3 cells were transfected with GFP-tagged vector (Ctrl) or GFP-tagged DLC1-

SAM domain wild-type (SAM), FLF mutant (SAM-FLF). (C) MCF7 cells were transfected with GFP-tagged vector (Ctrl) or GFP-tagged DLC1-SAM domain wild-type (SAM), FLF mutant (SAM-FLF). Data denoted by different letters indicate significant difference at p values of < 0.02.

3.3 Identifying BNIP-Sα as a novel interacting partner of DLC1

3.3.1 Interaction of DLC1 with BCH domain-containing proteins

As a GAP with *in vitro* activity specific towards RhoA and Cdc42 but not Rac1 (Wong *et al.,* 2003), DLC1 was reported to promote apoptosis when restoring its expression in HCC cells (Zhou *et al.,* 2004). Another RhoA-interacting protein BNIP-2 Similar isoform alpha (BNIP-Sα) was identified as a proapoptotic protein by our group, for which the interaction with RhoA is essential for its proapoptotic function (Zhou *et al.,* 2002; Zhou *et al.,* 2006). It is worth noting that both DLC1 and BNIP-Sα are related to RhoA pathway and have apoptotic function. This raises an interesting issue whether both DLC1 and BNIP-Sα work in similar pathways. So we hypothesized that DLC1 might interact with BNIP-Sα. To test this hypothesis, binding studies were carried out for DLC1 and BNIP-Sα. Immunoprecipitation assay was carried out using 293T cells co-transfected with HA-tagged DLC1 and Flag-tagged BNIP-Sα. BNIP-Sα contains a BNIP-2 and CDC42 Homology (BCH) domain at its C-terminus (Figure 3.15A). Another two Flag-tagged proteins with similar domain organization, BNIP-2 and BNIP-2 Homology (BNIP-H), were also tested to compare their binding specificity towards DLC1 (Figure

3.15A). BNIP-2 can bind to Cdc42 through it BCH domain to induce cell elongation and membrane protrusions (Zhou *et al.*, 2005). BNIP-H can interact with glutaminase and regulate its enzyme activity (Buschdorf *et al.*, 2006). In the immunoprecipitation assay, an unrelated Flag-tagged control construct was used as negative control. The result shows that DLC1 was specifically co-immunoprecipitated by BNIP-Sα and BNIP-2, but not by BNIP-H or the control construct (Figure 3.15B). Since BNIP-H can bind to some of its interacting partners only under NGF stimulation condition in PC12 cells but not in 293T cells (unpublished data), binding assay of DLC1 and BNIP-H was further carried out under such condition by co-worker (courtesy of Chew Li Li). Consistently, the immunoprecipitation result shows no binding between DLC1 and BNIP-H. These results together show that DLC1 could specifically interact with two BCH domain-containing proteins, BNIP-Sα and BNIP-2.
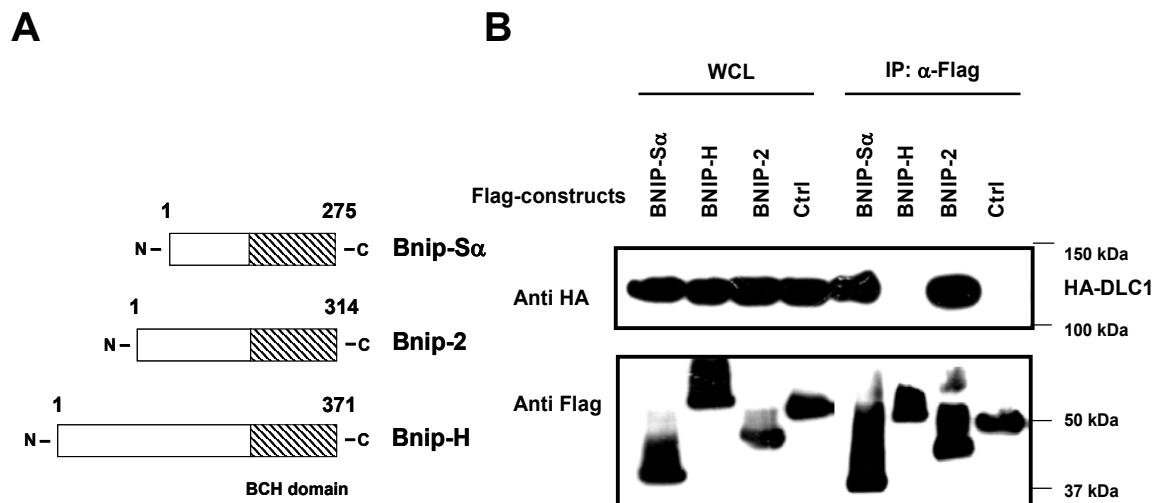
Figure 3.15 DLC1 could form complexes with BNIP-Sα and BNIP-2. (A) Schematic diagram showing the composition of protein domains of human BNIP-Sα, BNIP-2 and BNIP-H. (B) 293T cells were co-transfected with plasmids encoding HA-tagged DLC1 and Flag-tagged BNIP-Sα, BNIP-2, BNIP-H or a control encoding an unrelated protein

(Ctrl). Whole cell lysates (WCL) were used for immunoprecipitation (IP) and incubated with M2-anti-Flag beads. WCL and IP samples were immunoblotted with indicated antibodies.

3.3.2 Identifying key DLC1-interacting motif on BNIP-Sα

3.3.2.1 BCH domain of BNIP-Sα is important for the interaction with DLC1

Since both DLC1 and BNIP-Sα have proapototic function, we focused our following research on the binding between DLC1 and BNIP-Sα. We set out to look for important domain/motif of BNIP-Sα in the interaction with DLC1 in order to define the binding mechanism between BNIP-Sα and DLC1. BNIP-Sα contains one BCH domain in its C-terminus and no other domains or motifs are identified in its N-terminus. Our colleague found that BNIP-Sα interests with RhoA through its BCH domain which is essential for its proapoptotic function (Zhou *et al.,* 2002; Zhou *et al.,* 2006). We wondered whether BCH domain is also important for the interaction between DLC1 and BNIP-Sα. To address this issue, various truncation mutants of BNIP-Sα with or without BCH domain (Figure 3.16A) were used in the following binding studies to examine their affinity towards DLC1.

First, immunoprecipitation assay was carried out using 293T cells transfected with Flag-tagged BNIP-Sα full length (FL), NBCH construct or CBCH construct together with HA-tagged DLC1 full length (Figure 3.16B). The result shows that DLC1 interacts specifically with BNIP-Sα full length and CBCH construct, which both contain

BCH domain, but not with the NBCH construct without BCH domain, indicating that BCH domain is essential for the interaction. To confirm this, *in vitro* pulldown assay was carried out using whole cell lysate of 293T cells expressing Flag-tagged DLC1 and purified GST-tagged BNIP-Sα full length, N and CBCH construct expressed from bacteria (Figure 3.16C). Consistent with the immunoprecipitation result, the pulldown result shows that DLC1 can be pulled down by BNIP-Sα full length and CBCH construct, but not by N construct lacking BCH domain. The above results together show that the BCH domain of BNIP-Sα is important for the interaction with DLC1.

C

Figure 3.16 BNIP-Sα-BCH domain is important for the interaction with DLC1. (A) Schematic diagram showing the composition of protein domains of different BNIP-Sα truncation mutants. (B) 293T cells were co-transfected with plasmids encoding HA-tagged DLC1 and Flag-tagged BNIP-Sα full length (FL), NBCH or CBCH constructs. Whole cell lysates (WCL) were used for immunoprecipitation (IP) and incubated with M2-anti-Flag beads. WCL and IP samples were immunoblotted with indicated antibodies. (C) 293T whole cell lysates (WCL) expressing Flag-tagged DLC1 were used for pull-down assay (PD) with GST-tagged BNIP-Sα full length (FL), N and CBCH constructs purified on glutathione-sepharose beads. GST proteins and the bound Flag-DLC1 were separated on SDS-PAGE, blotted and probed with anti-Flag antibodies (upper panel). Blot was stripped and stained with amido black to reveal loading of GST recombinants (bottom panel).

3.3.2.2 GAP-binding motif in BNIP-Sα-BCH is important for its interaction with DLC1

Next, we tried to explore the possible molecular mechanism of the interaction between DLC1 and BNIP-Sα by examining functional motifs within the BCH domain of BNIP-Sα. It is known that BNIP-Sα has several binding partners, including BNIP-Sα itself, RhoA and p50-RhoGAP (Zhou *et al.,* 2002). Our group had defined the molecular mechanism of how BNIP-Sα mediates the interactions with several targets through its BCH domain. Previously, we identified that residues 215-221 is the homophilic interaction motif of BNIP-Sα (Zhou *et al.,* 2002). Recently, our group found out that there is a minimum RhoA binding region (amino acid 133-177) within the BCH domain of BNIP-Sα, and overlapping with this region there is a GAP-binding motif ("GBM") (amino acid 133-147) necessary for the interaction of BNIP-Sα and p50-RhoGAP (Zhou *et al.,* 2006). p50-RhoGAP is a RhoGAP targeting RhoA and Cdc42 (Barfod *et al.,* 1993; Lancaster *et al.,* 1994). Similarly, DLC1 has *in vitro* GAP activity towards RhoA and Cdc42 (Wong *et al.,* 2003). So we hypothesized that the GBM region of BNIP-Sα might also be essential for the interaction with DLC1. Alternatively, with RhoA being the cognate targets of BNIP-Sα and DLC1, RhoA could possibly mediate the interaction of BNIP-Sα and DLC1, leading the three proteins forming a complex. To shed light on these various possibilities, several deletion mutants of BNIP-Sα were used for the further binding studies (Figure 3.17A). ΔA mutant is deleted in the RhoA binding region and ΔA1 mutant is deleted in the GAP-binding motif within the RhoA binding region. Both of these two mutants lose the binding ability towards RhoA and p50-RhoGAP. ΔA2 mutant

is deleted in residues within the RhoA binding region but outside the GAP-binding motif, which can not bind to RhoA but still retains binding activity towards p50-RhoGAP. ΔB mutant is deleted in the homophilic interaction motif of BNIP-Sα and thus loses its self-interacting activity. Such Flag-tagged mutant and wildtype constructs of BNIP-Sα and HA-tagged DLC1 full length were co-transfected in 293T cells and the whole cell lysate was used for immunoprecipitation assays. Surprisingly, when the cells were transfected with ΔA, ΔA1 or ΔA2 together with DLC1, a lot of cells died and floated up in the medium within 24 hours after transfection, leading to low concentration of these proteins in the whole cell lysate. In our attempt to achieve similar expression level of all the constructs, we collected the whole cell lysate for immunoprecipitation at around 16 hours after transfection before a large portion of the cells would die. Figure 3.17B shows the immunoprecipitation result when most of the constructs were expressed on similar level except ΔA1 mutant. The result shows that only NBCH and ΔA mutants of BNIP-Sα lost the binding activity to DLC1. In contrast, binding of the wildtype BNIP-Sα, ΔA2 and ΔB mutants with DLC1 were still intact (Figure 3.17B). It shows that constructs devoid only the binding activity to RhoA or the homophilic interaction activity (ΔA2 and ΔB) still retain the interaction with DLC1, while constructs losing the p50-RhoGAP binding activity in addition to RhoA-binding activity (ΔA) lost the interaction with DLC1. Together the results suggest that the p50-RhoGAP-binding motif of BNIP-Sα is essential for the interaction with DLC1.

In order to confirm that the loss of binding between ΔA mutant and DLC1 was not due to the detrimental effect on cells caused by co-expressing these two proteins, an *in vitro* binding assay was performed using cell lysate of single transfected 293T cells,

under which condition most of the cells were not floating up. Cells were first transfected

with either HA-tagged DLC1, Flag-tagged wildtype BNIP-Sα or Flag-tagged ΔA mutant.

Then equal amount of cell lysate expressing HA-tagged DLC1 was mixed with cell lysate

expressing Flag-tagged BNIP-Sα wild type or ΔA mutant respectively. Later the HA-

DLC1 bound to BNIP-Sα was examined by anti-Flag immunoprecipitation and Western

Blotting. The result shows that BNIP-Sα wild type could still interact with DLC1, while

ΔA mutant did not show any interaction with DLC1 (Figure 3.17C). It shows that the loss

of binding is not a result of cell death or unhealthy growth condition, confirming that

deletion of the entire RhoA binding region in BCH domain results in the loss of

interaction between BNIP-Sα and DLC1. Binding assays of Figure 3.17B and 3.17C

together shows that the GAP-binding motif in BCH domain of BNIP-Sα is essential for

the interaction with DLC1.
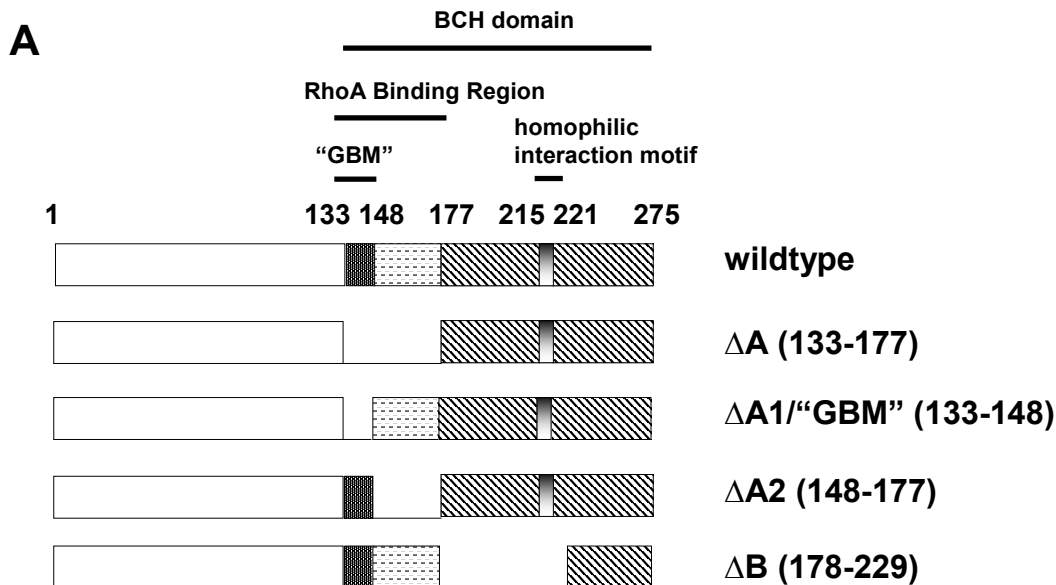
B
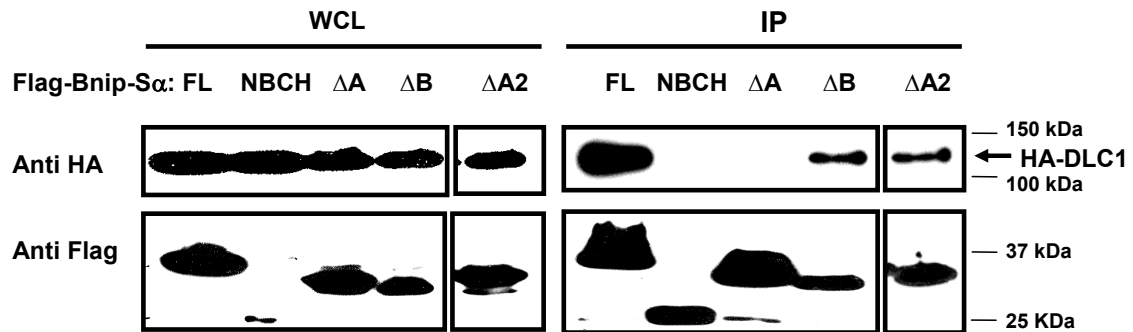
C

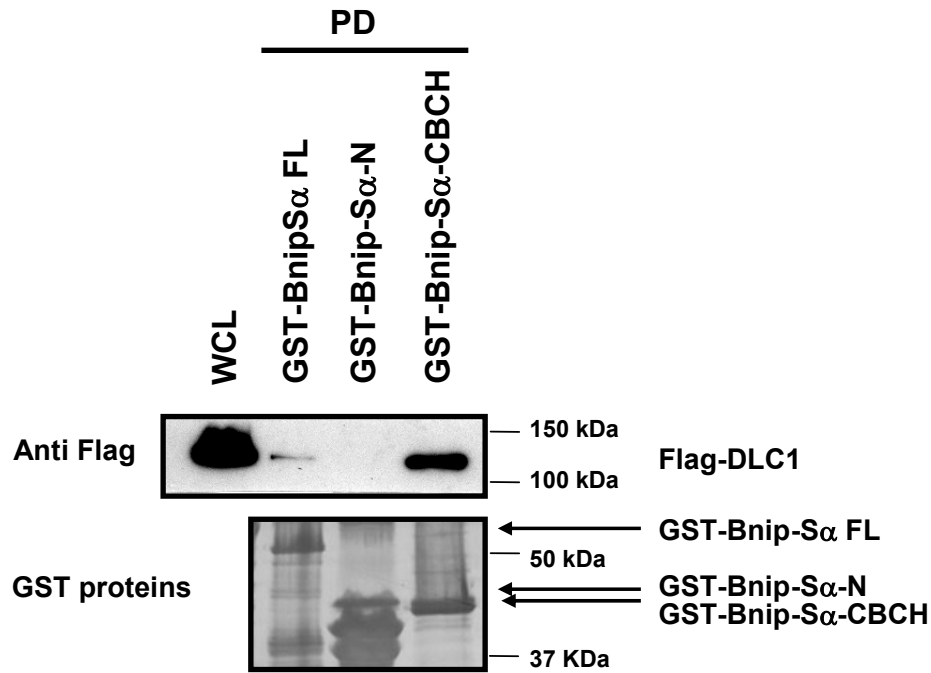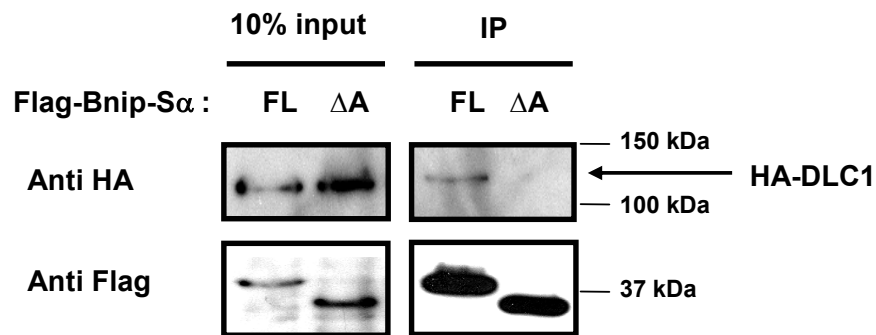**Figure 3.17 GAP-binding motif in BCH domain is important for the interaction with DLC1.** (A) Schematic diagram showing the composition of protein domains and functional motifs of different BNIP-Sα deletion mutants. Numbers in the brackets indicate the deleted amino acid sequences. (B) 293T cells were co-transfected with plasmids encoding HA-tagged DLC1 and Flag-tagged BNIP-Sα full length (FL), NBCH, ΔA, ΔB or ΔA2 constructs. Whole cell lysates (WCL) were used for immunoprecipitation (IP) and incubated with M2-anti-Flag beads. WCL and IP samples were immunoblotted with indicated antibodies. (C) 293T cell lysates expressing Flag-tagged BNIP-Sα full length (FL) or ΔA mutant were mixed with cell lysates expressing HA-DLC1 for 2 hours before incubation with M2-anti-Flag beads for another 2 hours for immunoprecipitation (IP). 10% lysate and IP samples were immunoblotted with indicated antibodies.

3.3.3 Identifying key BNIP-Sα-interacting motifs on DLC1

3.3.3.1 Multiple regions in DLC1 are involved in binding to BNIP-Sα

In our attempt in elucidating the interaction mechanism between DLC1 and BNIP-Sα, we continued to investigate key BNIP-Sα-interacting motifs on DLC1. DLC1 is a large protein with 1091 amino acid. So we made various truncation mutants containing different domains/regions of DLC1 for the following binding studies (Figure 3.18A). N mutant is the N-terminus fragment consisting of the SAM domain and the region between SAM domain and GAP domain of DLC1 (it is named as P region thereafter). GC mutant is the C-terminus fragment consisting of the GAP domain and the START domain. C mutant includes the START domain and the region between the GAP domain and the START domain (it is named as R region thereafter). Immunoprecipitation assays were carried out using whole cell lysate of 293T cells transfected with Flag-tagged BNIP-Sα full length together with various HA-tagged DLC1 truncation mutants (Figure 3.18B). N mutant, GC mutant and C mutant were co-immunoprecipitated by BNIP-Sα. Meanwhile, neither SAM domain nor GAP domain was co-immunoprecipitated by BNIP-Sα, even though their expression level is much higher than N, GC or C mutants. One interpretation of the result would be that there may be multiple interacting sites in DLC1 towards BNIP-Sα, at least one in the P region and one in R region or the START domain, either contributing to direct binding to BNIP-Sα or mediating the binding through an unknown third partner, possibly RhoA. An alternative explanation would be that the binding of either region is nonspecific. In order to confirm the binding specificity of N-terminus and C-terminus of DLC1 with BNIP-Sα, co-immunoprecipitation assays were

performed using HA-tagged N mutant or GC mutant of DLC1 co-expressed with Flag-tagged BNIP-Sα full length, NBCH mutant or CBCH mutant. Here NBCH construct was used as a negative control, since DLC1 full length did not bind to NBCH (as shown in Figure 3.16B). Figure 3.19A and Figure 3.19B show that neither N mutant nor GC mutant bound to NBCH mutant of BNIP-Sα, while both of them bound to BNIP-Sα full length and CBCH mutant, which is consistent with the binding specificity of DLC1 full length. The results confirm the specificity for the binding activity in the N terminus and C terminus in DLC1 towards BNIP-Sα.

A
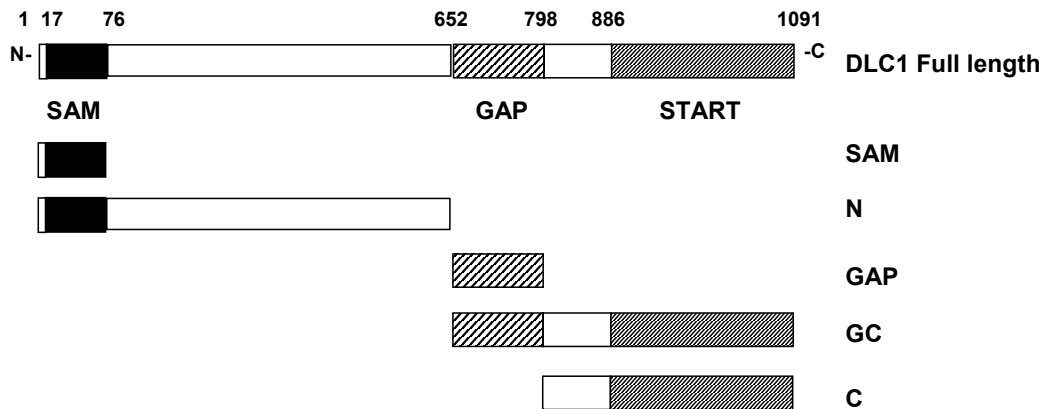
B
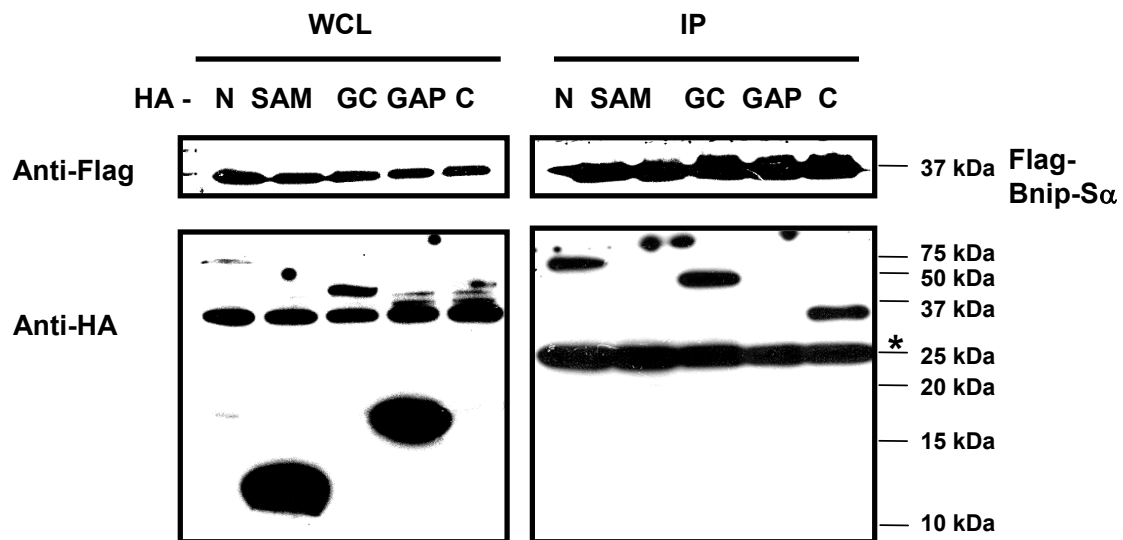
Figure 3.18 Multiple regions in DLC1 are involved in the binding to BNIP-Sα. (A) Schematic diagram showing the composition of protein domains of different DLC1 truncation mutants. (B) 293T cells were co-transfected with plasmids encoding Flag-tagged BNIP-Sα full length and HA-tagged DLC1-N, SAM, GC, GAP or C constructs. Whole cell lysates (WCL) were used for immunoprecipitation (IP) and incubated with M2-anti-Flag beads. WCL and IP samples were immunoblotted with indicated antibodies. *Asterisk* indicates heavy chains of the anti-Flag antibody on the M2-beads.

A

WCL   IP: α-Flag

Flag-Bnip-Sα: FL NBCH CBCH   FL NBCH CBCH

Anti-HA   — 50 kDa   **HA-DLC-GC**

Anti-Flag   — 37 kDa

                 — 25 KDa

B

WCL   IP: α-Flag

Flag-Bnip-Sα: FL NBCH CBCH   FL NBCH CBCH

Anti-HA   — 75 kDa   **HA-DLC-N**

Anti-Flag   — 37 kDa

                 — 25 KDa
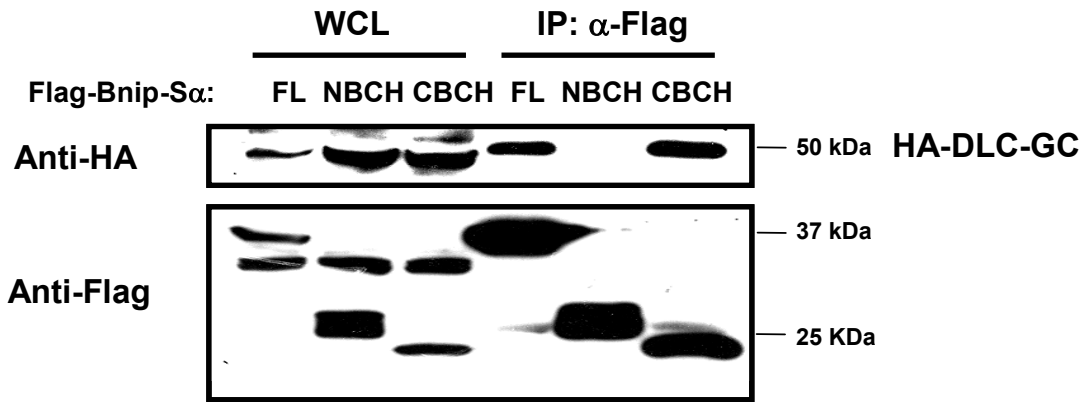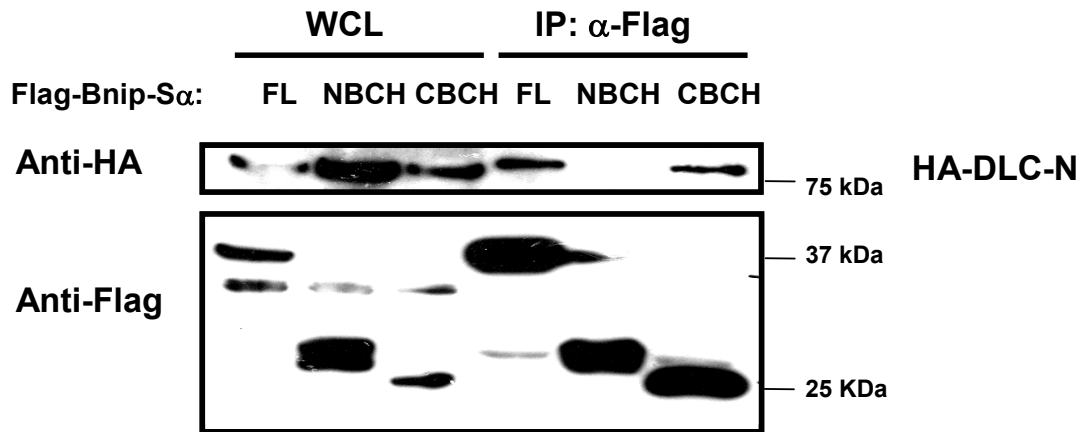
Figure 3.19 Both DLC1-N terminus and -C terminus specifically target BNIP-Sα-BCH domain. (A and B) 293T cells were co-transfected with plasmids encoding HA-tagged DLC1-N (A) or DLC1-GC (B) constructs and Flag-tagged BNIP-Sα full length (FL), NBCH mutant or CBCH mutant. Whole cell lysates (WCL) were used for immunoprecipitation (IP) and incubated with M2-anti-Flag beads. WCL and IP samples were immunoblotted with indicated antibodies.

3.3.3.2 DLC1-START domain has binding affinity towards BNIP-Sα

Our results show that the C-terminus of DLC1 has binding affinity towards the BCH domain of BNIP-Sα. BCH domain might have putative lipid-binding property since it share low degree of homology with the lipid-binding Sec14 domain (Low *et al.,* 2000A). Noticeably, there is a START domain located at the C-terminus of DLC1, which is also a putative lipid binding domain (as introduced in Chapter 1). DLC1- START domain could be involved in phospholipid pathways since the DLC1 mouse homologue, p122RhoGAP, could bind to PLCδ1, an enzyme for phospholipid PIP$_2$, and the C-terminus containing START domain is responsible for the activation of PLCδ1 by p122RhoGAP (Homma & Emori, 1995; Sekimata *et al.*, 1999). It is possible that lipid molecules might help bring the BNIP-Sα–BCH domain or DLC1-START domain into proximity. Thus, we raised our hypothesis that DLC1-START domain might be the binding site in the C-terminus for BNIP-Sα. To verify our hypothesis, we examined the binding activity of START domain towards BNIP-Sα. DLC1 truncation mutants containing different parts of the C-terminus were constructed and used for the following binding study (Figure 3.20A). Co-immunoprecipitation assay was carried out using 293T cells transfected with HA-tagged GR or START constructs of DLC1 together with Flag-tagged BNIP-Sα. The result shows that only START constructs not GR constructs was immunoprecipitated by BNIP-Sα, even though the expression level of GR was much higher than START (Figure 3.20B). Here, we show that the putative lipid-binding domain, START domain, is the C-terminal binding site of DLC1 towards BNIP-Sα. It is not clear whether their binding is direct or mediated by a third partner, possibly lipids. This will

need more detailed future investigation. Currently, the lipid-binding property of BNIPSa BCH domain is under investigation. The significance of such interaction will be discussed in chapter 4.

A
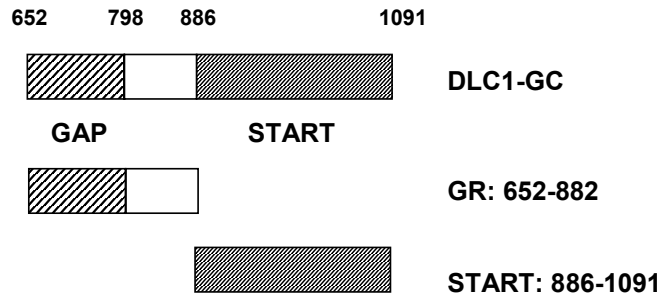
B
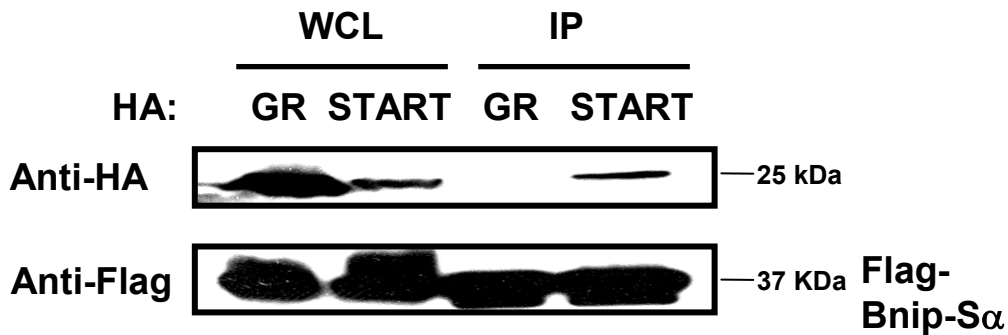
Figure 3.20 The START domain of DLC1 has affinity towards BNIP-Sα. (A) Schematic diagram showing the composition of protein domains of different DLC1-C terminus truncation mutants. (B) 293T cells were co-transfected with plasmids encoding HA-tagged DLC1-GR or DLC1-START constructs and Flag-tagged BNIP-Sα full length. Whole cell lysates (WCL) were used for immunoprecipitation (IP) and incubated with M2-anti-Flag beads. WCL and IP samples were immunoblotted with indicated antibodies.

3.3.3.3 DLC1-P1 and P3 sequences have binding affinity towards BNIP-Sα

We also show that the N-terminus of DLC1 has binding affinity towards the BCH domain of BNIP-Sα and the linker region between SAM domain and GAP domain (P region) on DLC1 could be the binding site since DLC1-SAM does not bind to BNIPSα. DLC1-P region contains around 570 amino acids in it. Although no conserved domain could be identified in such a long sequence, the corresponding sequences of DLC2 and DLC3 are quite conserved with 48% and 29% identity with DLC1-P region respectively (Durkin *et al.*, 2007B). It raises our hypothesis that P region might play a role in the function of DLC1. Our current data showing the binding capacity of DLC1-P region towards BNIP-Sα supports our hypothesis (Figure 3.18B). To explore the function of P region, we continued to investigate the binding mechanism of DLC1-P towards BNIPSα through identifying shorter binding region within the long sequence of DLC1-P. To do this, we first made smaller truncation mutants of P region for the following binding study. Three truncation mutants, P1, P2 and P3, were generated according to the predicted secondary structure of P region (Figure 3.21A). The truncation sites of the mutants were designed in the predicted random coiled region to avoid spoiling any helice or beta strand structure. We continued to examine the binding affinity of DLC1-P1, P2 and P3 towards BNIP-Sα with co-immunoprecipitation assays. HA-tagged P, P1, P2 or P3 construct was transfected together with Flag-tagged BNIP-Sα or an unrelated Flag-tagged control construct in 293T cells. Immunoprecipitation assays show that only DLC1-P, P1 and P3 could be co-immunoprecipitated by BNIP-Sα, but not DLC1-P2 (Figure 3.21B). None of the P region mutants was co-immunoprecipitated by the Flag-tagged control protein

(Figure 3.21C), showing the specificity of the binding results. The results indicate that there might be two more motifs in the N-terminus having binding affinity towards BNIP-Sα in addition to the START domain on DLC1.

A

```
                80        90       100       110       120       130       140
                |         |         |         |         |         |         |
DLC1-P     LEISPHRKRSDDSDEDEPCAISGKWTFQRDSKRWSRLEEFDVFSPKQDLVPGSPDDSHPKDGPS
Sec.Cons.      eeccccccccccccccccce?ccceeeccccccc??hhhccccccccccccccccccccccccc

               150       160       170       180       190       200       210
                |         |         |         |         |         |         |
DLC1-P     PGGTLMDLSERQEVSSVRSLSSTGSLPSHAPPSEDAATPRTNSVISVCSSSNLAGNDDSFGSLPSPKELS
Sec.Cons.  ccccehch?hhhh?eeeeeecccccccccccccccccccccccceeeeeecccccccccccccccccccccc

               220       230       240       250       260       270       280
                |         |         |         |         |         |         |
DLC1-P     SFSFSMKGHEKTAKSKTRSLLKRMESLKLKSSHHSKHKAPSKLGLIISGPILQEGMDEEKLKQLSCVEIS
Sec.Cons.  ceeeeccccccc?hhhhhhhhhhhhhhhhccccccccccccceeeeecccchh?cchhhhhhhhhheeee

               290       300       310       320       330       340       350
                |         |         |         |         |         |         |
DLC1-P     ALNGNRINVPMVRKRSVSNSTQTSSSSSQSETSSAVSTPSPVTRTRSLSACNKRVGMYLEGFDPFNQSTF
Sec.Cons.  hcccccccc??eece?cccccccccccccccccccccccccc???c?ccccccceeeecccccccccccc

               360       370       380       390       400       410       420
                |         |         |         |         |         |         |
DLC1-P     NNVVEQNFKNRESYPEDTVFYIPEDHKPGTFPKALTNGSFSPSGNNGSVNWRTGSFHGPGHISLRRENSS
Sec.Cons.  chhhhhccccccccccccccceeeeccccccccccccccccccccccccccccceeeeecccccccccceeecccccc

               430       440       450       460       470       480       490
                |         |         |         |         |         |         |
DLC1-P     DSPKELKRRNSSSSMSSRLSIYDNVPGSILYSSSGDLADLENEDIFPELDDILYHVKGMQRIVNQWSEKF
Sec.Cons.  ccc?hhh?cccccccccceeeeecccceeeeccccchhhhcccccchhhhhhhhhh?c?hhhhhhhh?c

               500       510       520       530       540       550       560
                |         |         |         |         |         |         |
DLC1-P     SDEGDSDSALDSVSPCPSSPKQIHLDVDNDRTTPSDLDSTGNSLNEPEEPSEIPERRDSGVGASLTRSNR
Sec.Cons.  ccccccccccccccccccccccccccccceeeeccccccccccccccccccccccccccccccccccccc?e?cccc

               570       580       590       600       610       620       630
                |         |         |         |         |         |         |
DLC1-P     HRLRWHSFQSSHRPSLNSVSLQINCQSVAQMNLLQKYSLLKLTALLEKYTPSNKHGFSWAVPKFMKRIKV
Sec.Cons.  c?eeeeccccccccccccceeeecccchhhhhhhhhhhhhhhhhhhhhhccccccccccc?hhhhhhe?c

               640       650
                |         |
DLC1-P     PDYKDRSVFGVPLTVNVQRTGQ
Sec.Cons.  cccccceee??eeeeeccccc
```

h: Alpha helix   e: Extended strand   c: Random coil   ?: Ambiguous states

```
          1   76          330    485       650
         [████|░░░░░░░░░░░|      |░░░░░░░░]  DLC1-N
          SAM

              [░░░░░░░░░░░|      |░░░░░░░░]  P: 77-652

              [░░░░░░░░░░░]                  P1: 77-330

                          [      ]           P2: 331-485

                                 [░░░░░░░░]  P3: 486-650
```

B

C

Figure 3.21 DLC1-P1 and DLC1–P3 region has affinity towards BNIP-Sα. (A) The

NPS@ (Network Protein Sequence @nalysis) consensus secondary structure prediction

(http://npsa-pbil.ibcp.fr) was used to predict the secondary structure of DLC1-P region

(a.a. 77-652). Only the secondary structure consensus prediction is shown here. Based on

the prediction result, three truncation mutants were made for DLC1-P region. Schematic

diagram shows the composition of protein domains and the corresponding amino acid sequences of different DLC1-P region truncation mutants. (B and C) 293T cells were co-transfected with plasmids encoding HA-tagged DLC1-P, P1, P2 or P3 constructs and Flag-tagged BNIP-Sα full length (B) or a control encoding an unrelated protein (Ctrl) (C). Whole cell lysates (WCL) were used for immunoprecipitation (IP) and incubated with M2-anti-Flag beads. WCL and IP samples were immunoblotted with indicated antibodies. *Asterisk* indicates heavy chains of the anti-Flag antibody on the M2-beads.

3.3.3.4 Deletion in DLC1-P3 lost the function in changing cell morphology

Our binding studies together show that 3 regions on DLC1 have binding affinity towards BNIP-Sα and the GAP-binding motif on the BCH domain of BNIP-Sα is essential for their interaction (Figure 3.22). Morphological changes are closely linked to cellular functions. Since full length DLC1 can cause drastic morphological changes of cells (rounding of cell bodies and protruding long and thin "beads-on-a-string structures" accompanied by disruption of stress fibers and dissociation of focal adhesions) (Figure 3.13A, 3.13B), we examined whether deletion of any BNIP-Sα-interacting region on DLC1 (Figure 3.23A) could impact on the function of DLC1 on cellular morphology in order to investigate the functional importance of such regions. NIH3T3 cells transfected with wildtype DLC1 or the deletion mutants were fixed, immunostained for the overexpressed proteins and observed under fluorescence microscope. Cells were also immunostained for focal adhesion protein Paxillin to show intact focal adhesion structures. NIH3T3 cells were used here because they have clear stress fiber and focal

adhesion structures. Figure 3.23B shows that both ΔP1 and NG constructs as well as full-length DLC1 could cause rounding of cell bodies and dissociation of focal adhesions when compared with the control untranfected cell. In contrast, cells tranfected with ΔP3 mutant retained normal cell morphology and intact focal adhesions (*short arrows*). Furthermore, the majority of ΔP3 protein was concentrated in large vesicular structures within the cytosol (labeled *P*), while DLC1 full length, ΔP1 and NG proteins were diffused in the cytosol. The results suggest that deletion of P3 region strongly affects the function of DLC1. While the functional significance of P1 region and START domain remained to be deciphered in future research, we focused on P3 region in our following study to further investigate its role in the function of DLC1.
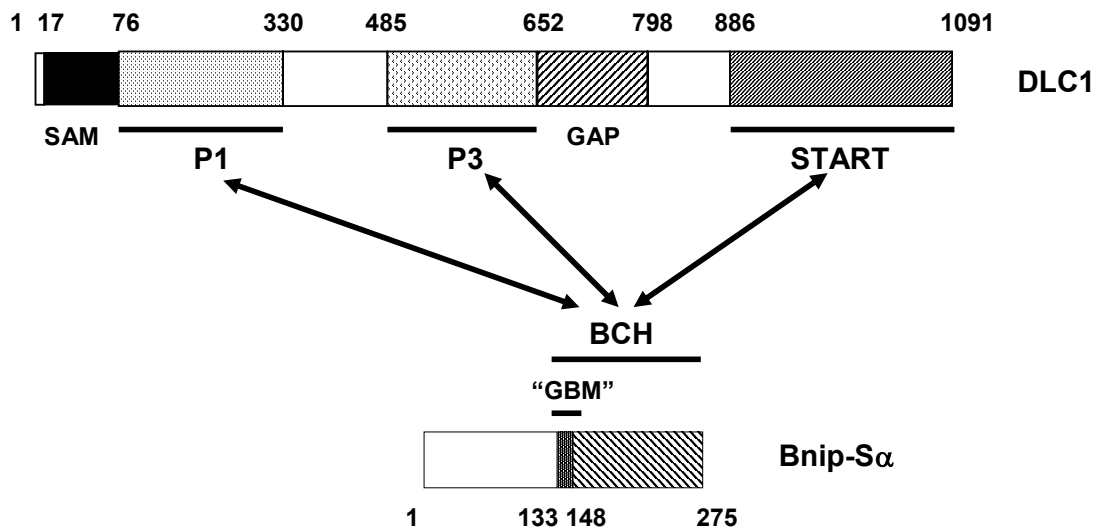
Figure 3.22 Schematic diagrams showing the regions on DLC1 and BNIP-Sα with binding affinity towards each other.
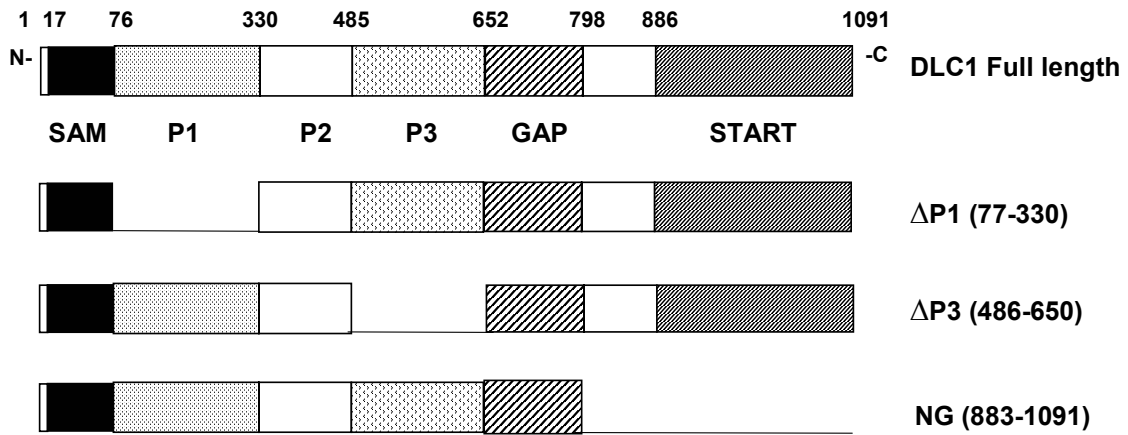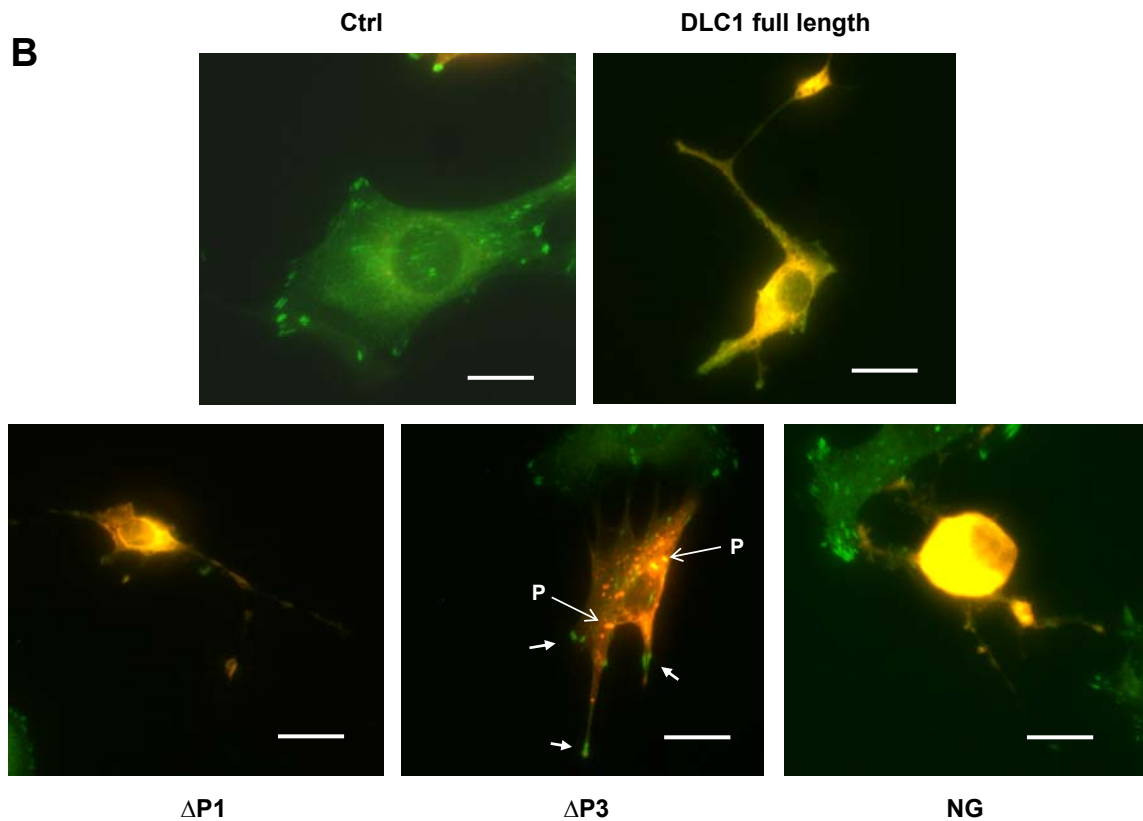
Figure 3.23 Effects on cell morphology of DLC1 mutants deleted in different BNIP-Sα-interactive regions. (A) Schematic diagram showing the composition of protein

domains of DLC1 mutants deleted in different BNIP-Sα regions. Numbers in the brackets indicate the deleted amino acid sequences. (B) DLC1-ΔP3 could not induce cellular morphology changes as full length DLC1. NIH3T3 untransfected cells (Ctrl) and cells transfected with either Flag-tagged DLC1 full length, ΔP1, ΔP3 or NG mutants were fixed, permeabilized, stained and visualized under fluorescent microcope. Ectopic expression of the proteins were detected by anti-Flag (red), and the focal adhesions are shown by anti-paxillin, followed by appropriate fluorophore-conjugated secondary antibodies (green). Merged signals are presented as overlaid staining (yellow). *Short arrows* indicate focal adhesions. *P labels indicate* large vesicular structures within the cytosol of DLC1-ΔP3. *White bars* indicate 10 μm.

3.3.3.5 DLC1-P3 was strongly enriched by BNIP-Sα in *in vitro* direct binding

We show that deletion in DLC1-P3 region leaded to the lost of function of DLC1 protein in changing cell morphology. We also show that DLC1-P3 had binding affinity towards BNIP-Sα in immunoprecipitation assay (Figure 3.21). It leads to our speculation whether such functional importance of P3 is due to its interacting activity with BNIP-Sα. Meanwhile, it was not clear whether such interacting activity is direct or indirect. To elucidate this, *in vitro* direct binding study for P3 and BNIP-Sα was carried out by coworker of our group (courtesy of Teo Ai Shi, Valerie). The TNT Quick Coupled Transcription/Translation system was used to produce DLC1-P3 peptide so that it could be soluble and functional with correct folding from the mammalian translation machinery, and be more pure for the direct binding study from this cell-free system. The DLC1-P3 peptide was then subject to GST-tagged BNIP-Sα expressed from bacteria and purified

on glutathione beads. Figure 3.24A shows that DLC1-P3 was specifically pulled down by GST-BNIP-Sα but not by GST control and it was greatly enriched by BNIP-Sα, indicating that the interaction between P3 and BNIP-Sα is direct and strong. To confirm the binding specificity, we continued to test the direct binding activity of DLC1-P3 with GST-tagged BNIP-Sα full length (FL), NBCH and CBCH (Figure 3.24B). The result shows that P3 was greatly enriched by CBCH as much as by BNIP-Sα full length. Meanwhile, a smaller amount of P3 was pulled down by NBCH, which is probably due to non-specific binding. The specificity in the *in vitro* direct binding between P3 and BNIP-Sα-CBCH is consistent with our previous *in vivo* immunoprecipitation result between DLC1-N and BNIP-Sα (Figure 3.24A). Altogether, the binding results prove that P3 region in the N-terminus of DLC1 protein mediates direct and strong interaction with the BCH domain of BNIP-Sα.
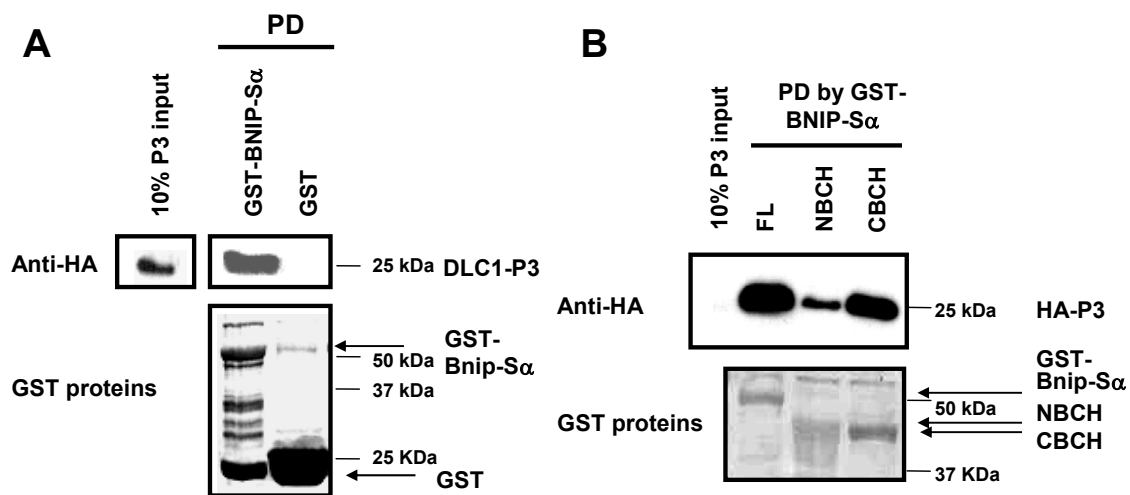
Figure 3.24 DLC1-P3 directly binds to BNIP-Sα-BCH *in vitro*. (A and B) HA-tagged P3 produced in TNT Quick Coupled Transcription/Translation system was used for pull-down assay (PD) with GST constructs purified on glutathione-sepharose beads: (A) GST or GST-tagged BNIP-Sα full length; (B) GST-tagged BNIP-Sα full length (FL), NBCH

and CBCH. GST proteins and the bound HA-P3 were separated on SDS-PAGE, blotted and probed with anti-HA antibodies (upper panel). Blot was stripped and stained with amido black to reveal loading of GST recombinants (bottom panel). (Results courtesy of Teo Ai Shi, Valerie)

3.4 DLC1-P3 is important for the function of DLC1

3.4.1 DLC1-ΔP3 and DLC1-R677E have similar effect in cell morphology

Our previous microscopy study shows that deletion in DLC1-P3 lost the function of full length DLC1 in causing cell body shrinkage and dissociation of focal adhesions. To confirm the strong impact to DLC1 caused by the deletion in P3 region, we continued to use confocal microscope to investigate the effect on stress fibers of DLC1-ΔP3. NIH3T3 cells were transfected with full-length DLC1 or DLC1-ΔP3, fixed, immunostained and observed under confocal microscope. Cells were also stained with TRITC-phalloidin to show actin structures. Consistent with Figure 3.22B, ΔP3 protein was concentrated in large vesicular structures within the cytosol (*label P*) in most of the cells expressing ΔP3, while the cells retain intact stress fibers (*Short arrows*) (Figure 3.25). Interestingly, such puntate distribution and lose of function of ΔP3 protein is similar to the GAP-negative mutant DLC1-R677E (Figure 3.13B). The RhoGAP activity of DLC1 was known to be essential for its function in inducing cell shrinkage and dissociation of stress fibers and focal adhesions (Wong *et al.,* 2005). The similar effect of the two mutants raises the issue whether P3 region could regulate the function of DLC1 by directly affecting its RhoGAP activity or through an unknown mechanism.
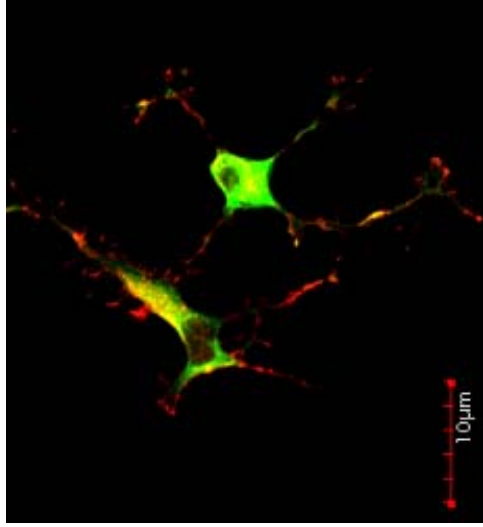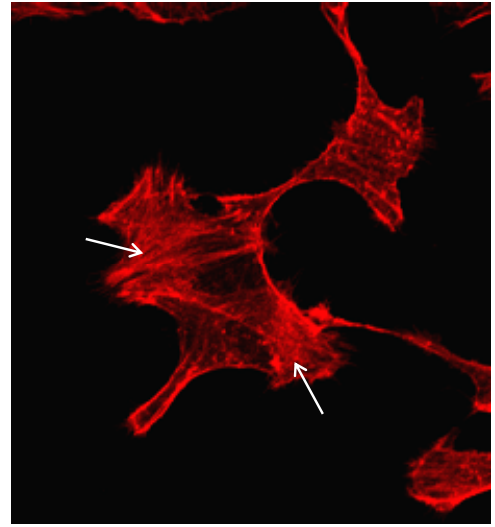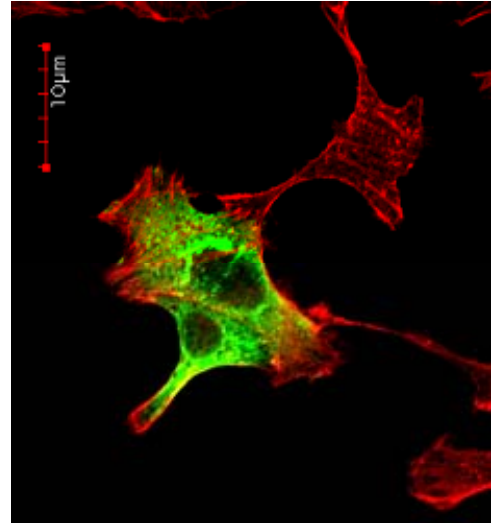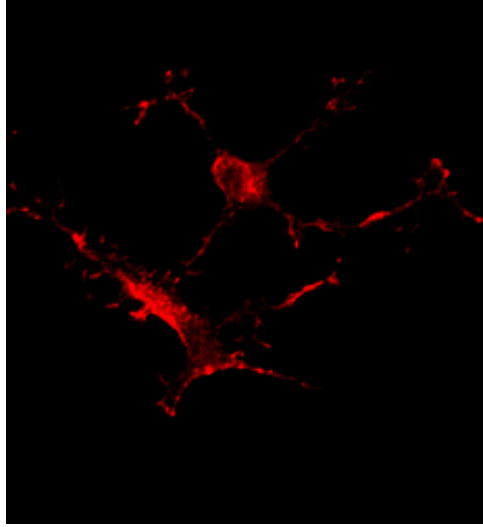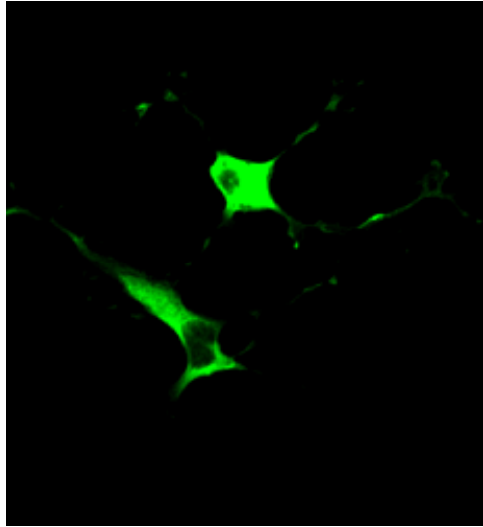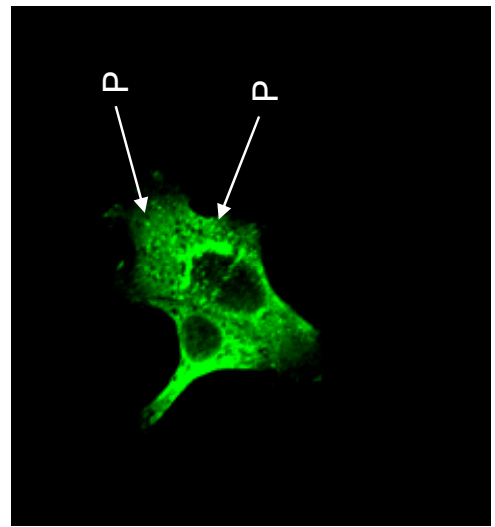
Figure 3.25 DLC1-ΔP3 could not induce stress fiber dissociation and cell shrinkage as DLC1 full length. NIH3T3 cells transfected with Flag-tagged DLC1 full length or ΔP3 constructs were fixed, permeabilized, stained and visualized under confocal immunofluorescent microcopy as described in "Materials and Methods". Ectopic expression of the proteins were detected by anti-Flag (green) followed by fluorophore-conjugated secondary antibodies. Cells were stained with TRITC-phalloidin (red) to label actin structures. Merged signals are presented as overlaid staining (yellow). *Short arrows* indicate intact stress fibers in transfected cells. *P labels* indicate large vesicular structures of DLC1-ΔP3 within the cytosol. *Red bars* indicate 10 µm.

3.4.2 DLC1-ΔP3 retains *in vivo* GAP activity towards RhoA

As cellular morphological changes caused by DLC1 (shrinkage of cell body and disruption of stress fibers and focal adhesions) are an indication of an active RhoGAP function, lost of function by deletion of P3 region indicates its role in regulating the RhoGAP function of DLC1. To address this issue, we compared the *in vivo* GAP activity of full length DLC1 and DLC1-ΔP3 towards RhoA in cells. Pull-down assay with GST-tagged RBD domain of rhotekin was used here to examine the endogenous RhoA activity of various DLC1 constructs. Rhotekin is an effector of RhoA. Its RBD domain can recognize and specifically bind to GTP-bound RhoA. Thus the in vivo activity of RhoA can be determined by its magnitude of binding to GST-RBD (Ren *et al.,* 1999; Wheeler and Ridley, 2004; Shang *et al.,* 2003). 293T Cells were transfected with Flag-tagged DLC1 full length (FL), ΔP3, R677E (GAP negative mutant), GC (N-terminal truncation

mutant), ΔSAM, or remained untransfected. Cells were also transfected with GFP-tagged wild-type BPGAP1 (WT) or its GAP negative mutant BPGAP1-A2, for which their GAP activity towards RhoA have been shown in GST-RBD pull down assay by our group (Shang *et al.*, 2003). Here the BPGAP1 constructs were used as controls for the assay. Cell lysates expressing various constructs were then mixed with GST-RBD purified on glutathione beads. The amount of endogenous GTP-bound RhoA pulled down by GST-RBD was then shown by SDS-PAGE and immunoblotting against RhoA. Figure 3.26 shows that BPGAP1 reduced the level of endogenous active RhoA, while cells expressing its GAP-negative mutant BPGAP1 A2 had more active RhoA, which level is similar to the level in the untranfected cells. Similarly, DLC1 full length reduced active RhoA level, showing its active GAP function towards RhoA. Consistently, DLC1-R677E mutant did not have active GAP function due to the mutation on the essential "Arginine finger". At the same time, SAM-deletion did not affect the GAP activity of DLC1. Surprisingly, what is different from our hypothesis is that ΔP3 could reduce GTP-RhoA to similar extent as DLC1 full length, showing that deletion in P3 region did not affect the RhoGAP activity directly. Interestingly, N-terminal deletion mutant (GC) lost its GAP activity, indicating unidentified regulatory module(s) in the N-terminus affecting the GAP activity directly.
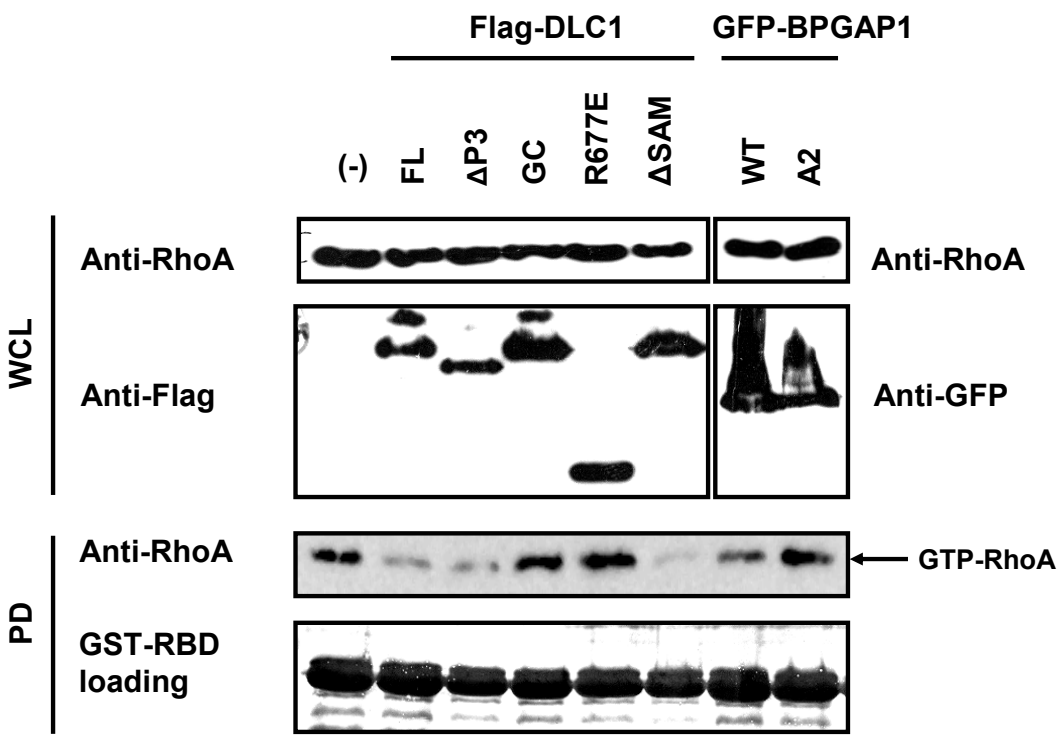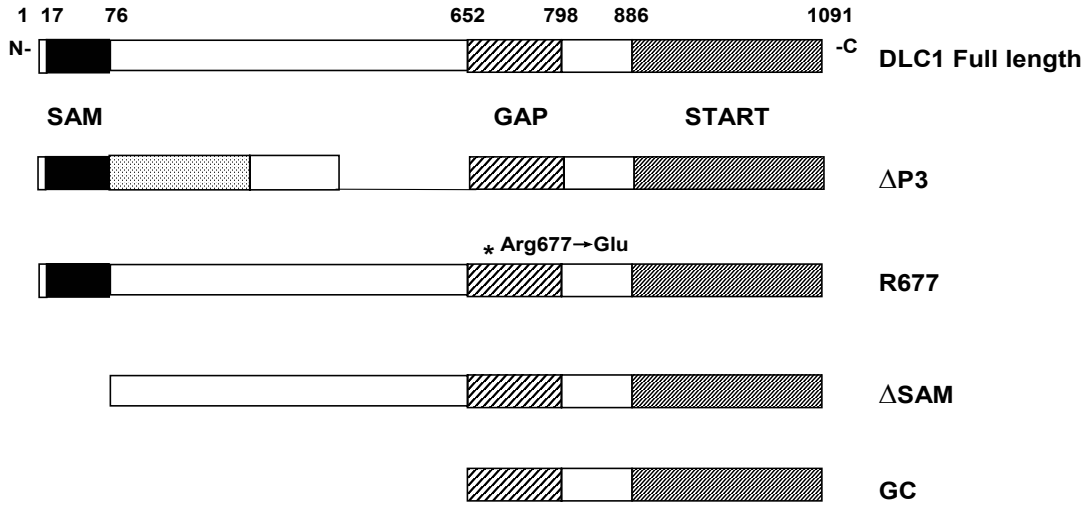
Figure 3.26 The *in vivo* GAP activity of different DLC1 mutants towards endogenous RhoA. Untransfected 293T cells or cells transfected with Flag-tagged DLC1 full length (FL), ΔP3, R677 (GAP negative mutant), GC or ΔSAM mutants, or GFP-tagged BPGAP1 full length, GFP-tagged BPGAP1 A2 (GAP negative mutant) were used for pull-down assay (PD) with GST-tagged RBD purified on glutathione-sepharose beads. Proteins in the whole cell lysate (WCL) and the pull-down complex were processed with SDS-PAGE and immunoblotting. Endogenous RhoA, ectopic expression of Flag-tagged or GFP-tagged proteins in the whole cell lysate and the active RhoA pulled down by GST-RBD were immunoblotted with indicated antibodies. Blot was stripped and stained with amido black to reveal loading of GST-RBD

3.4.3 Deletion in DLC1-P3 strongly affects its ability to suppress cell migration

DLC1 was known for its inhibitory function in cell migration and tumor metastasis (Goodison *et al.,* 2005). Cell migration is a biological process accompanied by dynamic changes of cytosketon and cell morphology. The phenomenon that deletion in DLC1-P3 lost the function of DLC1 in causing cell morphological changes (Figure 3.23B and 3.25) raises an interesting issue whether deletion in DLC1-P3 could also affect its suppressing function in cell migration. Boyden chamber migration assay was carried out to address this issue. Motile NIH3T3 cells were transiently transfected with cell marker pCMV-βGAL alone (Ctrl) or together with 4 times quantity of the wild-type/full length DLC1, the P3 deletion mutant (ΔP3), the N-terminal truncation mutant which contain the GAP domain and the START domain (GC) and the full length DLC1 GAP-negative

mutant (DLC1-R677E). Then the cells were allowed to migrate through a Boyden chamber for 12 hours. The proportions of all transfected cells were then scored for their ability to exert migration in 3 independent assays as described in "Materials and methods". Figure 3.27 shows that wild type DLC1 greatly inhibited the rate of migration by more than 70%. Meanwhile, GC construct, which is deleted in the entire N-terminus and does not have active GAP activity towards RhoA (Figure3.26), had lost the ability to suppress cell migration ($P<0.05$). In comparison, while DLC1-Arg677 is not as potent as full length in suppressing cell migration, Arg677 could still inhibit the cell migration by around 30%, though both Arg677 and GC lost GAP activity towards RhoA (Figure 3.26). The difference in their suppressing ability indicates that besides the GAP domain, an unidentified motif in the N-terminal region of DLC1 seems to play a role in the inhibition in cell migration. Consistent with this, DLC1-ΔP3, which retains *in vivo* GAP activity towards RhoA (Figure3.26), is greatly less potent in suppressing cell migration compared to full length DLC1 but could still inhibit cell migration but only by around 30% (Figure 3.27). It shows that the lost of function in cell morphological changes by P3-deletion could result in the decreased ability of DLC1 in migration suppression. Taken together, all these results strongly support the notion that P3 region is important to the function of DLC1 and P3 region collaborates with the GAP activity of DLC1 in the suppression of cell migration.
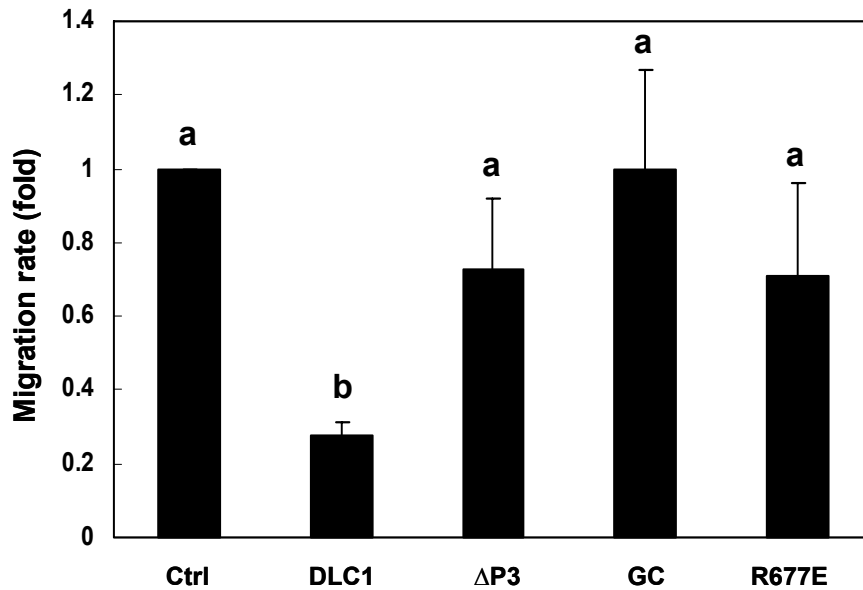
Figure 3.27 Effects of different DLC1 mutants on cell migration. NIH3T3 cells were transiently transfected with cell marker pCMV-βGAL alone (Ctrl) or together with 4 times quantity of Flag-tagged DLC1 full length, ΔP3, GC or R677 (GAP negative) mutants. The effects of different constructs on cell migration were assayed in Boyden chamber. Data were presented as the means +/- standard deviation (SD) compared with the control of 3 independent experiments. Statistical comparison was made using ANOVA and Newman-Keuls multiple comparisons. Data denoted by different letters indicate significant difference at *p* values of < 0.05.

Chapter 4

Discussion

4.1 A novel function for the SAM domain of DLC1

SAM domain represents an emerging class of important protein domain superfamily in which different members have been implicated in diverse cellular functions (Qiao and Bowie, 2005). The number of encoded SAM domains (in brackets) roughly correlates with the complexity of genomes in *S. cerevisiae* (4), *C.elegans* (26), *D. melanogaster* (42), mice (178) and the humans (206). It could serve as a docking site for kinase (e.g. ETS-1 transcriptional activator for ERK2 MAP kinase), as a polymeric device (e.g. for transcriptional repression function of TEL), as a RNA-binding domain (e.g. Smaug), or as a signaling scaffold through homophilic interactions (e.g. for Byr2 serine/threonine kinase, Eph receptor tyrosine kinase and diacylglycerol kinase). Some SAM domains also engage non-SAM proteins as their binding partners (e.g. interaction of BAR with Bcl-2 and Bcl-XL) (Qiao and Bowie, 2005). Given the uniformity in structural folds but diversity in their functions (Kim and Bowie, 2003), our understanding on the precise role(s) of more than 200 SAM domains possibly encoded by the human genome would require systematic and thorough examinations.

Combining proteomics, biochemical, structural and cellular studies, our current work had added yet another important aspect of SAM function for DLC1, a RhoGAP protein and a candidate tumor suppressor where it interacts specifically with an emerging multi-functional protein, the translational elongation factor EF1A1. Such interaction is specific and important as it provides the molecular basis for shuttling EF1A1 to membrane periphery and membrane ruffles upon FGF stimulation where it helps regulate

cell migration. In strong contrast, the homologous DLC2-SAM does not have any of such effects. This novel functional coupling immediately places the importance of DLC1-SAM in the context of actin-based cell dynamics control (as discussed below).

4.2 The molecular mechanism of the interaction between DLC1-SAM and EF1A1

DLC1- and DLC2-SAM adopts a unique fold with 4 nearly parallel helices, whereas most SAM domains consist of 5 helices organized in a globular manner. In this regard, we showed that DLC1-SAM does not self-associate. Instead, it utilizes mainly a unique hydrophobic patch to interact with EF1A1. Since DLC1-SAM does not bear significant resemblance to most of the other SAM domains (Figure 3.3A), it is possible that such sequence variability could give rise to target specificity as evidenced by the unique EF1A1-targeting dipeptide F38-L39 motif present only in the DLC1-SAM.

Interestingly, when DLC1-SAM or the EF1A1 were expressed as bacterial recombinants they failed to interact with one another. Instead, it required either one or both of them being expressed in eukaryotic cells. It seems likely that such interaction requires certain modification(s) on at least one of the two proteins. Furthermore, both the GTP-binding domain (Domain I) and the actin-binding domain (Domains I and III) of EF1A1 are important for its interaction with DLC1-SAM. Intriguingly, the binding by the GTP-binding domain is only apparent *in vivo* and it binds stronger than the full length EF1A1 or the actin-binding domain III. In contrast, only the actin-binding domain III of

EF1A1 interacts most strongly *in vitro*. The apparent dynamic nature of interaction is likely to be due to proper folding of EF1A1 in the Eukaryotic system or extrinsic regulation of EF1A1 *in vivo* through further conformational modifications. Several modifications of EF1A1 have been reported previously, including methylation and phosphorylation at different sites on the protein. Methylation of EF1A or its prokaryote homologue EF-Tu was reported in several species, including *E.coli.*, the fungus *Mucor*, mouse and rabbit. In contrast to the single methylation site in the prokaryote EF-Tu, methylation on multiple sites of EF1A was observed in eukaryote cells. The extent of methylation on eEF1A changes during different developmental stages and is different between SV40-transformed 3T3B and normal 3T3B mouse cells, suggesting methylation may be a novel mode of regulation of eEF1A activity or its interaction with G-actin, and a way to affect cell growth properties (Polevoda and Sherman, 2007). Phosphorylation of EF1A by several proteins was also reported as another potential way to regulate its activity. The F-actin-bundling activity of EF1A1 can be down-regulated as a result of direct phosphorylation on eEF1A1 by Rho-kinase, an important regulator of cytoskeleton and cell motility (Izawa *et al.,* 2000). C-Raf, a protein involved in the Ras antiapoptotic pathway, can bind to eEF1A and phospohorylate eEF1A on serine and threonine residues. Such phosphorylation was suggested in mediating the antiapoptotic effect of C-Raf (Lamberti *et al.,* 2007). Threonine phosphorylation on eEF1A1 by protein kinase Cδ was also reported, though the functional significance is unclear (Kielbassa *et al.,* 1995). Likewise, previous studies had shown that certain SAM domains are subjected to phosphorylation and also modification via the small ubiquitin-like modifiers (SUMO)

(Qiao and Bowie, 2005). Previous research together implicates that the variation of the modifications on EF1A1 in different cell physiology is a means of regulation to its cellular function. Consequently, the involvement of at least two distinct domains of EF1A1 suggest that while F38-L39 being the essential motif (possibly by initiating the interaction), it is plausible that other secondary binding sites on the SAM domain could still well exist to render further stabilization.

Notably, EF1A1 has a homologue, EF1A2, which is very similar to EF1A1 on amino-acid sequence, molecular weight and the function of peptide chain elongation in protein synthesis (Thornton *et al.*, 2003). At the same time, they have different expression profiles (Knudson *et al*., 1993), indicating that they might have different cellular roles. Thus it would be interesting to investigate the binding activity of DLC1-SAM towards EF1A2, which might shed light on the binding mechanism for EF1A1 towards DLC1-SAM, and help identify the specific functions of these two homologues. All these results imply a complex regulation of EF1A1 function and interaction, the mechanism of which awaits more detailed structural and mutational studies.

4.3 Implications of DLC1 interacting with EF1A1, a central regulator for cell metabolism and signaling

This study identified EF1A1 as the interacting partner of the SAM domain of DLC1, and suggested that SAM domain could regulate the function of DLC1 in cell dynamic control through the interaction with EF1A1. The results show for the first time that SAM domain of DLC1 binds specifically to EF1A1. Since DLC1 is a tumor suppressor, their interaction supports previous hypothesis that EF1A1 might be involved

in tumorigenesis and exert some unknown functions besides its well-known house-keeping function in protein translation elongation (Lamberti *et al.*, 2004).

Besides its earlier established role in transferring aminoacyl-tRNA to ribosome during protein synthesis (Lamberti *et al.*, 2004; Thornton *et al.*, 2003), EF1A1 has been shown to be involved either directly or indirectly in diverse cellular processes. These range from embryogenesis (Krieg *et al.*, 1989), oncogenic transformation (Tatsuka *et al.*, 1992), mitosis (Kuriyama *et al.*, 1990), cell proliferation (Gangwani *et al.*, 1998), transporting mRNA (Liu *et al.*, 2002), bundling of F-actin (Gross *et al.*, 2005), controlling microtubule dynamics (Moore *et al.*, 1998), conferring susceptibility to cell death induced by palmitate-overload (Borradaile *et al.*, 2006) or by hydrogen peroxide (Chen *et al.*, 2000), as well as conferring cyto-protection against ER stress-induced apoptosis (Talapatra *et al.*, 2002). Interestingly, EF1A1 also interacts with a zinc finger protein ZPR1 and both are co-translocated to the nucleus in response to EGF stimulation or nutrient stimulation to regulate normal cellular proliferation (Gangwani *et al.*, 1998), whereas plant EF1A1 acts as an activator of phosphatidylinositol 4-kinase (Yang *et al.*, 1993; Yang and Boss, 1994). Furthermore, EF1A1 binds to the split-Pleckstrin Homology domain of phospholipase Cγ1 to regulate IP$_3$ production (Chang *et al.*, 2002). This in turn helps increase their interaction. On the other hand, its expression is also elevated in melanomas and tumors of the pancreas, breast, lung, prostate and colon (Thornton *et al.*, 2003), with its expression levels correlated with metastasis (Taniguchi *et al.*, 1992) and increased susceptibility to oncogenic transformation (Tatsuka *et al.*, 1992). All these data point towards EF1A1 being an emerging key regulator of cell growth, cell death and cell dynamics control, the molecular mechanisms of which remain largely unknown.

Our current finding of DLC1 acting in concert with EF1A1 via its interaction with SAM domain thus opens up new possible mechanisms that could underlie many aspects of DLC1's effect on anti-metastatic (Yuan *et al.*, 2003; Goodison *et al.*, 2005), tumor-suppression (Yuan *et al.*, 2003; Goodison *et al.*, 2005; Wong *et al.*, 2005; Zhou *et al.*, 2004), or/and pro-apoptotic functions (Zhou *et al.*, 2004). Firstly, when stimulated with FGF, there was a concomitant re-localization of EF1A1 to DLC1 at the membrane ruffles and not to the focal adhesions, in a process that required the functional SAM domain. In the absence of such interactions, most of the EF1A1 was retarded in the perinuclear region. These results indicate an intricate control for the interaction between EF1A1 and DLC1, depending on the signaling input. Indeed, we further showed that the catalytic-inactive mutant of DLC1 did not allow their co-localization in quiescent cells unless it was relieved upon FGF treatment. This result supports the functional coupling between the SAM and GAP domains of DLC1 whereby inactivation of Rho signaling is necessary for the re-localization of DLC1 and EF1A1 together at membrane ruffles (Figure 4.1). Interestingly, wild type or FLF mutant of SAM domain could still be localized to those structures independent of other functional modules of DLC1. The basis for such autonomous translocation remains unknown. Given that these actin-rich structures are involved in cell locomotion (Rodriguez *et al.*, 2003), we propose that DLC1 interaction with EF1A1 at the membrane ruffles could serve to regulate the invasiveness and migratory nature of motile cells. Indeed, we later showed that the presence of SAM stimulates cell migration by sequestrating EF1A1 from interacting with endogenous DLC1. Consistently, SAM mutant devoid of EF1A1-binding fails to recruit EF1A1 to

these actin-rich sites where it also fails to affect cell migration. Consistently, corresponding DLC1 full length mutant also becomes less potent in suppressing cell migration. Together, we propose a model whereby the primary role of DLC1-SAM is to facilitate EF1A1 translocation to the sites of active actin assembly/disassembly *in vivo* during cell motility control (Figure 4.1). Meanwhile, DLC1 was previously reported to localize at focal adhesions through the linker region between SAM and RhoGAP domain, and it was recently shown to dramatically reduced RhoA activity at the leading edge of cellular protrusions (Liao *et. al..*, 2007; Qian *et. al..*, 2007; Healy *et. al..*, 2007). It is worth noting that the cellular relocalization of several other proteins, which are also found both at the membrane ruffles and at focal adhesions, was indicated as a key regulatory event in polarized cell migration (Wonzniak et. al.., 2004). As the effect of DLC1-SAM serves to recruit EF1A1 to the membrane periphery and ruffles and help suppressing cell motility, such auxiliary effect should ensure better control on DLC1 activity in cell migration during physiological conditions. Given that EF1A1 is involved in actin-mediated cell morphogenesis in yeast (Gross and Kinzy, 2005; Gross and Kinzy, 2007), our results provide the first evidence that EF1A1 is indeed important for cell migration by linking to a RhoGAP protein in the mammalian system.

Secondly, EF1A1 regulates phosphatidylinositol 4,5-bisphosphate via its interaction with phospholipase Cγ1 (Chang *et al.,* 2002). Recently, EF1A1 was identified as a binding partner of Akt2 (Lau *et al.,* 2006) while the other isoform of EF1A, EF1A2 was shown to bind and activate phosphatidylinositol 4 kinase (PI4K) and Akt, depending on the intracellular abundance of phosphatidylinositol 3,4,5-trisphosphate (Amiri *et. al..*,

2006; Jeganathan and Lee, 2007). In this regards, DLC1 has also been identified to be a target for Akt kinase signaling in response to insulin (Hers et. al.., 2006) and its rat homolog, p122RhoGAP was also shown to interact with phospholipase C (Homma and Emori, 1995; Sekimata *et al.*, 1999; Yamaga *et al.*, 2007), which helps in generating the IP$_3$. Based on these findings, it is likely that DLC1 and EF1A1 could act in concert to regulate PI(3,4,5)P3/Akt pathway and phosphoinositide metabolism which is necessary for cell growth, apoptosis and motility control. Furthermore, as indicated above, EF1A1 acts to either sensitize or protect against apoptosis and also engage in complexing with ZPR1 protein for proliferation. Therefore, interaction between DLC1 and EF1A1 could also indirectly serve to modulate the threshold of response simply by sequestering EF1A1 from their actions during protein synthesis or apoptosis induction. It remains an exciting prospect to further investigate just how these possible mechanisms operate and whether they are functionally linked.

Thirdly, the interaction between DLC1 and EF1A1 indicates the crosstalk between the EF1A1 signaling and the RhoA signaling pathways. In fact, EF1A1 had been implicated in the downstream pathways of the Rho signaling in previous work. In the yeast *Saccharomyces cerevisiae*, EF1A1 was find to interact with Bni1p, which inhibits the F-actin binding and bundling activities of EF1A1 (Umikawa *et al.,* 1998). Bni1p is the homologue of the mouse mDiaphanous, which is an effector of RhoA important for the regulation of actin and focal adhesion dynamics (Fukata *et. al.*, 2003). Furthermore, EF1A1 was shown to be phosphorylated *in vitro* by Rho kinase, another effector for RhoA, resulting in reduced actin binding and bundling (Izawa *et. al.*, 2000). Such

findings implicate that EF1A1 could be a common downstream target in the Rho signaling pathway that might participate in the Rho-regulated cytoskeletal reorganization. In our work, EF1A1 was identified as a novel interacting partner of DLC1. We further found that their interaction play an auxiliary role for the inhibition by DLC1 in cell migration. As DLC1 is an upstream regulator of RhoA, the interaction between EF1A1 and DLC1 suggests that down-regulation on the RhoA signaling by DLC1 might be mediated not only through direct negative regulation on RhoA but also through targeting its downstream substrate, EF1A1. Our work supports the notion that the RhoA pathway crosstalks with the EF1A1 pathway and EF1A1 is a common target of multiple molecules in the Rho pathway.

Taken together, our results provide the first evidence that the RhoGAP DLC1 can functionally interact with EF1A1 through its SAM domain towards sites of active actin assembly/disassembly and is involved in inhibiting cell migration. As DLC1 has been shown to exert its inhibition on cell migration at least via its GAP activity, such an auxiliary role by SAM could help modulate the actin-based dynamics. The complexity of function and regulation on DLC family proteins could now be further addressed by simple modularity and then validated in the context of the whole protein. Together with other common actions of EF1A1 and DLC1 in phosphoinositide metabolism and their ability to regulate apoptosis, it is envisaged that DLC1 could exert multiple levels of control over cell growth and cell motility (see model in Figure 4.1). It remains to be explored just what functions of each and every module confers towards the entire function and regulation of DLC family proteins.
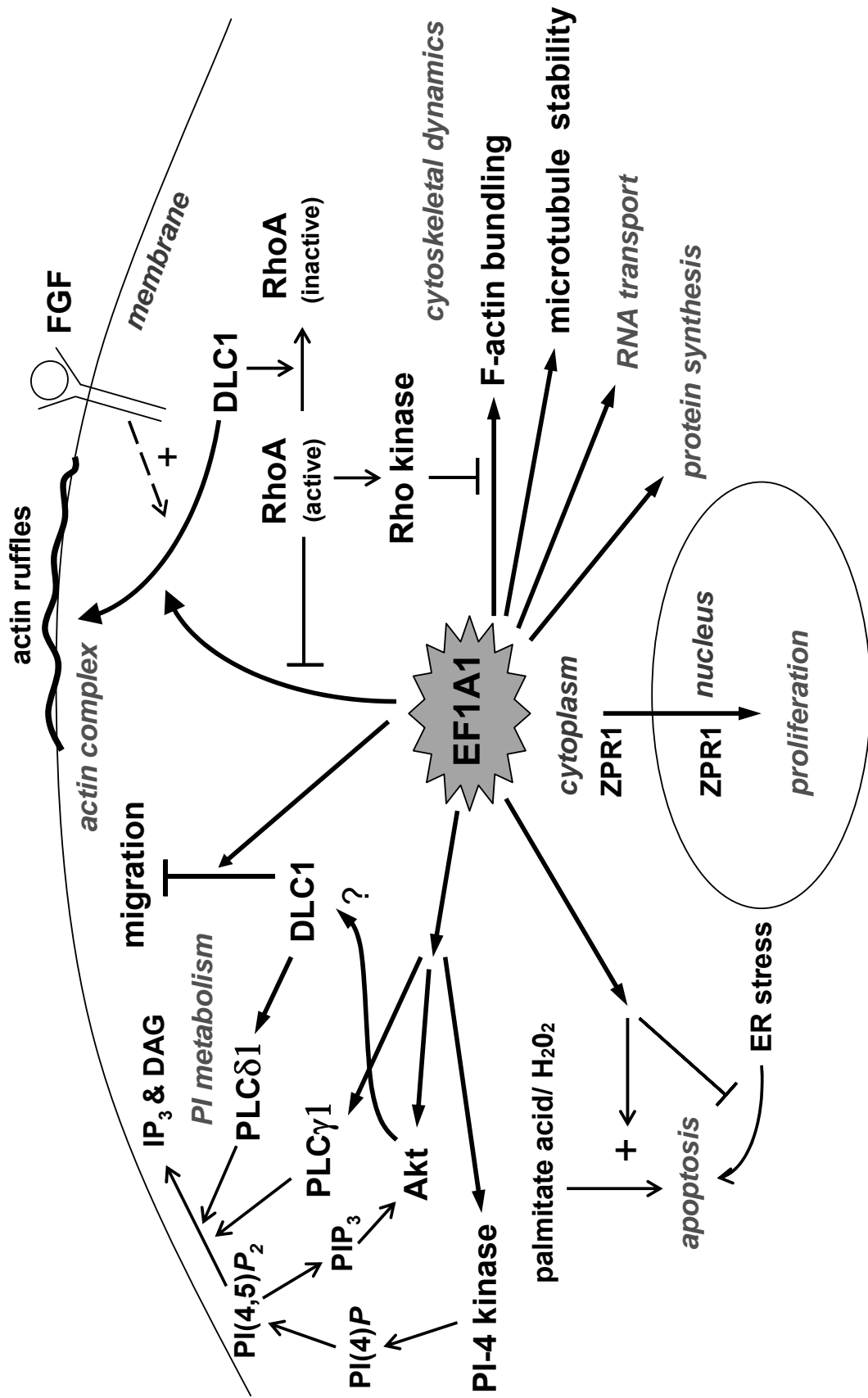
Figure 4.1 Implications of DLC1 and EF1A1 interaction on cell dynamics and cell growth control. EF1A1 regulate diverse cellular processes, ranging from long-established role in protein synthesis to promoting F-actin bundling and stabilizing microtubules, controlling normal cell proliferation, transporting β-actin mRNA, conferring susceptibility to or cyto-protection against cell death (please see text for more details). EF1A1 also activates phosphatidylinositol-4-kinase (at least in plant) and phospholipase Cγ1 to regulate PIP_2 and IP_3 production, similar to the action of PLCδ1 activation by DLC1. EF1A1 was found to a binding partner of Akt kinase. DLC1's rat homologue p122RhoGAP is also a target of Akt while the effect on p122's function is not clear. EF1A1 has also been shown to be phosphorylated *in vitro* by Rho kinase, an effector for RhoA, resulting in reduced F-actin bundling. At the present report, we show that DLC1-SAM domain EF1A1's translocation to membrane ruffles with DLC1 only after FGF stimulation. Furthemore, such translocation requires Rho to be inactivated by DLC1 or when FGF is present. As PIP_2 production and actin dynamics are both regulated by Rho signaling during cell migration and that cytoskeleton control is linked to susceptibility of apoptosis, it is plausible that DLC1 and EF1A1 could act in concert through a temporal-spatial control of the actin dynamics in order to exert its anti-metastasis or/and its pro-apoptotic functions, whose detailed molecular mechanisms require more extensive investigation. PLC, phospholipase C; PI(4)P, phosphatidylinositol-4-phopshate; PI(4,5)P_2, phosphatidylinositol-4,5-bisphopshate; IP_3, inositol-3,4,5-triphosphate; PIP_3, phosphatidylinositol-3,4,5-bisphopshate; DAG, diacylglycerol.

4.4 Implications of DLC1 as a novel BCH domain-interacting partner

In our study, DLC1 was identified as a novel interacting partner for the BNIP-2 family. Interestingly, the interaction is specific towards BNIP-2 and BNIP-Sα, but not BNIP-H. We also confirmed that such interaction with BNIP-Sα is mediated by its BCH domain. Since BNIP-2 has similar domain organization as BNIP-Sα, it is very possible that the interaction between DLC1 and BNIP-2 could also be mediated by the BCH domain. It is known that BCH domains are crucial for the diverse cellular effects of members in the BNIP-2 family (Zhou *et al.,* 2002; Zhou *et al.,* 2005; Zhou *et al.,* 2006; Buschdorf *et al.,* 2006). The newly identified interaction between BCH domain and DLC1 could shed light on the diverse mechanistic function of BNIP-2 family proteins in the complex signaling network inside the cell.

BCH domain was originally identified as the highly homologous sequence between the C-terminus of BNIP-2 and N-terminus of p50-RhoGAP (Low *et al.,* 2000A). Later research work demonstrates that BCH domains are protein-protein interaction domains, which can mediate homophilic interaction with the same protein and/or heterophilic interaction with another BCH-domain containing protein (Low *et al.,* 2000B; Zhou *et al.,* 2005; Zhou *et al.,* 2006). Meanwhile, BCH domain was also suggested as putative phospholipid-binding domain since it shares low homology with the lipid-binding Sec14 domain, though no similar property of BCH domains has been reported yet (Low *et al.,* 2000A). Proteins that contain a highly conserved BCH domain

in their C-terminus and share high homology to the human BNIP-2 protein are grouped in the BNIP-2 family, including BNIP-Sα, BNIP-2 and BNIP-H. Although members in the BNIP-2 family share very high homology, they have different and specific functions in cell dynamic regulation. For example, BNIP-2 can induce cell elongation and membrane protrusions (Zhou *et al.,* 2005). BNIP-H can cause similar cell elongation changes and play important roles for normal brain function (Buschdorf *et al.,* 2006). Differently, BNIP-Sα can lead to cell rounding and apoptosis eventually (Zhou *et al.,* 2002; Zhou *et al.,* 2006).

Recently, our group found that the BCH domains of BNIP-2 family proteins were able to target specific small Rho GTPases. Our coworkers show that the BCH domains of BNIP-Sα and BNIP-2 can bind to RhoA and Cdc42, respectively (Zhou *et al.,* 2006; Zhou *et al.,* 2005) while no interaction was found for BNIP-H towards RhoA, Cdc42 and Rac1 (Unpublished data of our group courtesy of Chew Li Li). Our group also found that the involvement of the different Rho GTPase pathways is required for the different cellular functions of BNIP-2 family proteins. BNIP-Sα can activate RhoA that lead to the apoptotic effect of BNIP-Sα (Zhou *et al.,* 2006). For BNIP-2, although it won't affect the net Cdc42 GTPase activity *in vivo*, the functional Cdc42 pathway is necessary for the morphological changes induced by BNIP-2 (Zhou *et al.,* 2005). Since RhoA and Cdc42 are also the targets of DLC1 (Wong *et al.,* 2003), the interaction between DLC1 and BNIP-2/BNIP-Sα indicates that the mechanism under the diverse functions of BNIP-2 family could be a cellular process with multiple-step control of different Rho GTPase pathways. BNIP-2 family members might exert their cellular effects not only by directly

binding and/or activating small Rho GTPases, but also through interaction with the regulator of Rho GTPases, DLC1. Since activate RhoA signaling is necessary for the apoptotic function of BNIP-Sα (Zhou *et al.,* 2006), the binding of BNIP-Sα to DLC1 may provide several effects: First, it might abolish the affinity of DLC1 towards RhoA, thus releasing RhoA from its negative regulator DLC1. As a result, RhoA could be free for the binding and activation by BNIP-Sα. Alternatively, BNIP-Sα might form a complex with DLC1 and RhoA together. Here DLC1 might act as a targeting signal instead. Their physiological interaction relationship and the underlying mechanistic function needs further detailed investigation including binding studies and functional assays.

4.5 The molecular mechanism of the interaction between DLC1 and BNIP-Sα

Our studies delineate three distinct regions on DLC1, *i.e.* DLC1-P1, -P3 regions and START domain, for the interaction with BNIP-Sα. We also confirmed that BNIP-Sα interacts with DLC1 through its BCH domain. Our findings in such regions may shed light on some possible mechanisms of how other modules besides the RhoGAP domain could contribute to the entire function and regulation of DLC1 protein.

DLC1-P1 and P3 regions are within the long sequence (around 600 amino-acid long) between the SAM domain and the GAP domain of DLC1. Although no conserved domain could be identified in such a long sequence, corresponding regions of this sequence are conserved with around 30−40% identity among the three human DLC

homologues, DLC1, DLC2 and DLC3 (Durkin *et al.,* 2007), which indicates the presence

of unknown motif(s) in it. Thus we hypothesized that this sequence might play a role in

the function of DLC1. Several recent founding supports our hypothesis by revealing some

functional motifs within this sequence. Serine 322 of the DLC1 rat homologue

p122RhoGAP (corresponding to the serine 329 within the P1 region of DLC1) was found

to be phosphorylated by Akt upon insulin stimulation, which was suggested as a

regulatory module by growth factors for its GAP activity towards Rho GTPases (Hers *et*

al., 2006). Another two residues serine 440 and tyrosine 442 (located between P1 and P3

region) could interact with the tensin family proteins that help locating DLC1 to focal

adhesions. Such interaction and localization is essential to the suppressive function of

DLC1 in colony formation and cell growth (Qian *et al.,* 2007; Liao *et al.,* 2007). Our

novel identified interactive activity of DLC1-P1 and -P3 regions towards BNIP-Sα could

also implicate the functional significance of this region. At the same time, it remains to be

deciphered how DLC1-P1/P3 could have affinity towards BNIP-Sα and whether they

could similarly interact with other BCH domain containing proteins. In our direct binding

studies, we already confirmed the direct and specific binding affinity of P3 region to

BNIP-Sα full length and its BCH domain, while whether the interaction between

DLC1-P1 and BNIP-Sα is direct or not remains to be elucidated by future research.

Interestingly, we also show that deletion in the P3 region lead to the lost of function of

DLC1 protein, indicating the functional importance of DLC1-P3. Whether there is any

special motif in P3 region that mediates the interaction with BNIP-Sα BCH domain and

whether such interaction confers to the functional importance of DLC1-P3 needs further

binding and functional studies combined with bioinformatic prediction.

We also show that there is binding affinity between the START domain of DLC1 and BNIP-Sα BCH domain. Work done by our co-worker show that DLC1-START domain could not bind to BNIP-Sα full length and BCH domain in *in vitro* direct binding studies (courtesy of Teo Ai Shi, Valerie). We speculate that the interaction between START domain of DLC1 and BNIP-Sα might be mediated by a third partner *in vivo*. Lipid could possibly mediate their interaction, since START domain and BCH domain are both putative lipid-binding domains. The START domain family has long been recognized as lipid-binding domain. The lipid-binding property of many START domains has already been demonstrated, such as cholesterol-binding by the START domains of STARD1 and MLN64, phophatidycholine-binding by the START domain of PCTP (Alpy and Tomasetto, 2005). Some of the functions from such lipid-binding property have also been shown in lipid trafficking, lipid metabolism, lipid-modulated signal transduction and transcriptional regulation (Alpy and Tomasetto, 2005). There is some evidence implicating the lipid-binding property of DLC1-START domain. An auxiliary role of the START domain of DLC1 rat homologue p122RhoGAP was suggested in its specific lipid raft caveola-localization, which is involved in cholesterol trafficking and Ca^{2+} mobilization (Yamaga *et al.*, 2004). A role of DLC1-START domain was also implicated in lipid-regulated pathway, since DLC1 had been identified as a binding partner of PLCδ1 and C-terminus half of DLC1 containing START domain is responsible for the activation of PLCδ1 by DLC1 (Homma and Emori, 1995; Sekimata *et al.*, 1999). Recently, it was shown that DLC1 could interact with PLCδ1 through the pleckstrin homology (PH)

domain, which binds PI(4,5)P$_2$, the phospholipid substrate of PLCδ1, with high affinity (Yamaga *et al.*, 2007). Such finding indicates that DLC1-START domain might interact with lipids *esp.* phospholipid. BCH domains of BNIP-2 family proteins might also have affinity towards phospholipids, since they share low degree of sequence homology to the phospholipid-binding Sec14 domain (Low *et al.*, 2000A) though there is no evidence to indicate lipid-interaction nature of any BCH domain yet. Our data showing the possibly indirect binding of DLC1-START and BNIP-Sα-BCH domains raises the possibility that phospholipids might help bring the two domains into proximity inside the cells, and lipid signals could regulate the functions of DLC1 and BNIP-Sα through modifying their interaction. At the same time, it remains to be explored whether the interaction between DLC1-START and BNIP-Sα-BCH domains could affect the affinity of DLC1-P1/P3 regions towards BNIP-Sα under physiological conditions. In future work, it will be interesting to investigate whether there is any lipid binding property of the START domain of DLC1, whether such property could regulate the function of DLC1 and how this is related to the interaction with BNIP-Sα.

4.6 Functional implications of DLC1 interacting with BNIP-Sα

BNIP-Sα is a pro-apoptotic protein (Zhou *et al.*, 2002). Work of our co-worker revealed that BNIP-Sα could bind to RhoA and trigger apoptosis by activating it (Zhou *et al.*, 2002; Zhou *et al.*, 2006). At the same time, BNIP-Sα could interact with a negative regulator of RhoA, p50-RhoGAP, and prevent p50-RhoGAP from inactivating RhoA. As

a result, BNIP-Sα suppresses p50-RhoGAP effects on cell protrusions while promoting

cell rounding through its interaction with RhoA. Here, we demonstrate that BNIP-Sα

could interact with DLC1, another RhoGAP of RhoA. Our finding implicates that

BNIP-Sα might exert its cellular effect through interaction with multiple RhoGAPs.

Although DLC1 itself could also induce apoptosis (Wong *et al.*, 2005; Zhou *et al.*,

2004; Syed *et al.*, 2005), its interaction with BNIP-Sα is not contradictory to the

proapoptotic function of each of the proteins. Apoptosis induced by DLC1 involves the

activated caspase-3 pathway. But such effect was only present in the cancerous cell lines

without endogenous DLC1 expression, not in the nontumorigenic cell line with similar

origin (Zhou *et al.*, 2004; Syed *et al.*, 2005). This shows that the proapoptotic effect of

DLC1 could be cell type-specific. In comparison, BNIP-Sα-induced apoptosis is not cell

type-specific and could be caspase-independent (Zhou *et al.*, 2002; Zhou *et al.*, 2006).

Together, it shows that DLC1 and BNIP-Sα use different mechanisms to induce apoptosis.

The interaction of BNIP-Sα and DLC1 could be a regulatory step on RhoGAPs in the

apoptosis process triggered by BNIP-Sα.

Both BNIP-Sα and DLC1 can induce apoptosis and target RhoA, a key

cytoskeleton regulator (Zhou *et al.*, 2002; Zhou *et al.*, 2006). Previously, it was known

that apoptosis can lead to cytoskeleton changes eventually. Now more and more findings

show that cytoskeleton changes can also be a regulatory step of apoptosis. Recently,

RhoA was known to be important in the regulation of various apoptosis processes. The

regulation of apoptosis by RhoA could be achieved either through its down-regulation or

up-regulation under different cellular conditions. For example, down-regulation of RhoA was shown to induce apoptosis in epithelianl cells (Fiorentini *et al.,* 1998), fibroblasts (Bobak *et al.,* 1997), lymphoma cells (Moorman *et al.,* 1999), endothelial cells (Hippenstiel *et al.,* 2002), osteosarcoma cells (Fromigué *et al.,* 2006) *etc*. Meanwhile, up-regulation of RhoA was reported to lead to apoptosis in some other cell types, such as phorbol ester-stimulated erythroblastic cell lines (Chang and Lee, 2006), fibroblasts induced by cellular cholesterol depletion (Calleros *et al.,* 2006), cardiomyocytes (Del Re *et al.,* 2007), and neurons treated with phenylalanine (Zhang *et al.,* 2007). The expression of RhoA could promote apoptosis in zebrafish embryogenesis as shown by the work of our co-worker (Zhu *et al.,* 2007). Altogether, these data demonstrates that a balanced cellular level of RhoA activity is essential for cell fate. As DLC1 can induce apoptosis and down-regulate RhoA, and BNIP-Sα can activate RhoA to induce apoptosis, our newly identified interaction between DLC1 and BNIP-Sα further supports the notion that the balance of RhoA activity in cell is crucial to cell survival. For future research, it would be interesting to further investigate the interaction mechanistic model of BNIP-Sα and DLC1, the regulation on RhoA by such interaction, and the downstream cellular effects.

4.7 DLC1-P3 region is a novel regulatory module for the function of DLC1

Our work identified DLC1-P3 region as a novel important region for the function of DLC1. We show that deletion in P3 region abrogates the ability of DLC1 in causing cell rounding and dissociation of stress fibers and focal adhesions, and lowers the

capacity of DLC1 in suppressing cell migration while not affecting the *in vivo* GAP activity of DLC1 towards RhoA. Most RhoGAPs contain multiple domains and they carry out their functions by integrating several signaling pathways through these functional modules. Currently, bioinformatic search shows no obvious motif within the P3 region to predict its functional mechanism. It raises an intriguing question about how DLC1-P3 region can play a role to the function of DLC1.

Protein/lipid interaction mediated by DLC1-P3 region could be one possible mechanism that leads to its role in the function of DLC1. Many RhoGAPs can interact with other proteins to mediate their functions (Tcherkezian and Lamarche-Vane, 2007). For example, our group has shown that the interaction between cortactin, a cortical actin binding protein and the proline-rich region of BPGAP1 is essential for the function of BPGAP1 in promoting cell migration (Lua and Low, 2004). Some RhoGAPs can also be directly regulated by lipid-binding (Tcherkezian and Lamarche-Vane, 2007). For example, β2-chimaerin, a GAP for Rac, can bind to the lipid second messenger DAG (diacylglycerol) that facilitates its RacGAP function by localizing β2-chimaerin to the plasma membrane site of active Rac1 (Wang and Kazanietz, 2006). In our current studies, we have identified the direct binding activity of DLC1-P3 region and the BNIP-Sα-BCH domain. It is possible that P3 region might regulate the function of DLC1 by integrating the BNIP-Sα signaling pathway with the Rho GTPase pathway. Given that BCH domain is a putative lipid-binding domain, interaction between DLC1-P3 and BNIP-Sα might facilitate the function of DLC1 by targeting it to the lipid rafts where active Rho GTPases are located.

Phosphorylation could be another possible regulatory mechanism for DLC1 by its P3 region. Many RhoGAPs can be regulated by phosphorylation which can affect the translocalization or protein-binding of the RhoGAPs and lead to either activation or inhibition of their functions (Tcherkezian and Lamarche-Vane, 2007). Our current studies show that deletion in DLC1-P3 region leads to the localization of DLC1 in large vascular structures instead of diffused localization. It raises the possibility that there might be some phosphorylation sites in the P3 region that affects the intracellular trafficking the DLC1 protein. Bioinformatic tools (such as Netphos 2.0 Server, http://www.cbs.dtu.dk/services/NetPhos/) identified several putative phosphorylation sites in P3 region (Figure 4.2). It remains to be elucidated whether these putative sites in DLC1-P3 region are phosphorylated and what is the regulation on DLC1 by such phosphorylation.

```
WSEKFSDEGDSDSALDSVSPCPSSPKQIHLDVDNDRTTPSDLDSTGNSLNEPEEPSEIPERRDSGVGASLTRSNR      560
HRLRWHSFQSSHRPSLNSVSLQINCQSVAQMNLLQKYSLLKLTALLEKYTPSNKHGFSWAVPKFMKRIKVPDYKDRSVFG   640
VPLTVNVQRTGQ                                                                     652
    .S...S....S.S.....S....S.............T.S...S...S......S.......S...........    560
......S...S...S...................................................Y...S...         640
............                                                                     652

Phosphorylation sites predicted:    Ser: 15   Thr: 1   Tyr: 1
```

Figure 4.2 Putative phosphorylation sites in DLC1-P3 region. Putative phosphorylation sites in DLC1-P3 region (corresponding to amino acid 485-652 in the sequence of DLC1) are predicted using Netphos 2.0 Server (http://www.cbs.dtu.dk/services/NetPhos/).

Earlier work on DLC1 or its rat homologue p122RhoGAP had only investigated their GAP activities towards RhoA, Cdc42 and Rac1 through *in vitro* GAP assays (Homma and Emori, 1995; Wong *et al.,* 2003). Our data show that deletion in DLC1-P3 region does not affect its *in vivo* GAP activity towards RhoA. Meanwhile, we can not rule out the possibility that P3 region could directly regulate the GAP activity of DLC1 on other Rho GTPases. Very recently, DLC1 was shown to downregulate RhoB and RhoC as well as RhoA and Cdc42 *in vitro* (Healy *et al.,* 2007). DLC1-P3 might play a role in the function of DLC1 through regulating its GAP activity towards RhoB or RhoC instead. Although RhoA, RhoB and RhoC share 85% identity on amino acid sequence, they have distinct cellular functions in the regulating cytoskeleton and cell motility, development and transcription (Wheeler and Ridley, 2004). RhoA plays a key role in controlling cell contractility. RhoB is important for the regulation of cytokine trafficking and cell survival. RhoC was shown to be important in cell locomotion. Besides, their patterns of altered expression and activity in cancers are very different. In cancers, RhoA and RhoC were found to be overexpressed especially in highly metastatic cancer cell lines. While RhoA can promote transformation in fibroblasts, RhoC doesn't have similar effect but it can promote metastasis. In contrast, the expression of RhoB was found to be decreased in more progressed cancers. Furthermore, RhoB can inhibit migration, invasion and metastasis. The different cellular roles of RhoA, RhoB and RhoC attribute to the binding specificity of their regulators and effectors, which is achieved through either different binding affinity or different cellular localization. Given that many RhoGAPs have different *in vivo* specificity of RhoGTPases from their *in vitro* activity, DLC1 might have

different specificity towards RhoA, RhoB and RhoC *in vivo,* though DLC1 was shown to have similar *in vitro* affinity towards them (Healy *et al.,* 2007). Since deletion in P3 region leads to the localization of DLC1 in large vascular structures in the cytosol instead of diffused localization in the cytosol in most of the cells, DLC1-P3 region might regulate the intracellular trafficking of DLC1 which would affect its *in vivo* RhoGAP activity towards RhoB/RhoC and affect the functions of DLC1 in regulating cell morphology and cell migration.

4.8 Conclusions and future perspectives

In this study, we have identified EF1A1 as a novel interacting partner for the SAM domain of DLC1, defined their interaction mechanism through identifying important motif/domain involved for their interaction and investigated the functional significance of their interaction in cell migration. Significantly, we have shown that hydrophobic residues F38 and L39 in DLC1-SAM form an indispensable interacting motif for the interaction with EF1A1. Using DLC1 mutants mutated at these residues, we demonstrated that SAM domain is necessary for DLC1 to translocate EF1A1 to the membrane periphery and ruffles upon fibroblast growth factor stimulation, and it acts as an auxiliary switch to the anti-metastastic RhoGAP domain.

We have also identified BNIP-Sα as another novel interacting partner for DLC1. We have shown that BNIP-Sα interacts with DLC1 through its BCH domain and the

GAP-binding motif within the BCH domain is essential for their interaction. On DLC1, multiple sites showed interaction affinity, including the P1, P3 regions and the START domain. Additionally, we have found that the P3 region is important for the function of DLC1 to change cell morphology and suppress cell migration, while not affecting the RhoGAP activity of DLC1.

The findings shown in this study have raised some interesting issues.

What signaling pathway is involved in the interaction of DLC1 and EF1A1 that help suppress cell migration?

Our data demonstrate that DLC1-SAM recruits EF1A1 to membrane periphery and ruffles and plays an auxiliary role in the suppression of cell migration by DLC1 while the mutant devoid of the binding with EF1A1 does not have such effects. It shows that the auxiliary effect of DLC1-SAM is mediated by its interaction of DLC1 with EF1A1 and the translocalization of EF1A1 to cell periphery. It is possible that the presence of SAM stimulates cell migration by sequestrating EF1A1 from interacting with endogenous DLC1. It implicates that not only the translocalization of EF1A1 but also an unknown signaling pathway coupled by the interaction of EF1A1 and DLC1 at cell periphery is necessary to modulate the function of DLC1 in migration. For future study, it would be interesting to investigate the signaling molecules downstream of the binding of DLC1 with EF1A1. The phospholipase C pathway might be the target coupled by DLC1 and EF1A1 (Figure 4.1). Previous research shows that EF1A1 binds to the split-Pleckstrin Homology (PH) domain of phospholipase C (PLC) $\gamma 1$ isoform to regulate IP$_3$ production

(Chang *et al.,* 2002), while its interaction activity towards other PLC isoforms has not been tested. Studies on DLC1 show that DLC1 rat homologue p122RhoGAP can specifically bind to the PH domain of PLCδ1 isoform but not PLCβ1 or PLCγ1 and activate PLCδ1 (Homma and Emori, 1995; Sekimata *et al.*, 1999; Yamaga *et al.*, 2007). PLC is a key molecule in the lipid metabolite signaling. Its PH domain is essential for its localization at plasma membrane where activated PLC hydrolyzes inositol phospholipid to generate two important lipid second messengers, diacylglycerol (DAG) and IP3. Recently, PLCδ1 was found to be a novel tumor suppressor that could inhibit tumor growth and cell migration (Fu *et al.*, 2007). Based on these findings, PLCδ1 could be the target downstream of the interaction of DLC1 and EF1A1 at cell periphery to regulate cellular activities especially cell growth and migration. To address this issue, biochemical assays of the activity of PLC in the presence of DLC1 and EF1A1 and functional studies of DLC1 using PLC pathway inhibitors could be carried out.

Does the interaction between DLC1 and EF1A1 also play a role in other cellular activities besides migration, such as cell growth, apoptosis and embryonic development, which is non-compensable by DLC1 homologues?

Previous research on DLC1 mainly focused on its tumor suppressor function while the role of DLC1 under physiological conditions in normal cellular activites has not been addressed. Recent finding with DLC1 knockout mice shows that homozygous DLC1 deletion is lethal to embryo development (Durkin *et al.*, 2005). It indicates that DLC1

also play other important cellular roles besides tumor suppression. Further more, the mouse orthologues for DLC2 and DLC3 have been identified (Durkin *et al.*, 2007B), implying that the functions of DLC2 and DLC3 can not compensate the functions of DLC1 or probably their expression profiles are different though they have very similar roles in tumor suppression. In our current study, we identified EF1A1 as a novel partner of DLC1, showing the role of their interaction in the regulation of cell migration. We further showed that the homologous DLC2-SAM could not interact with EF1A1 and did not have any of such effects. Given that EF1A1 is a central regulator for a variety of cell activities which is not confined to protein synthesis (as introduced previously in this chapter), its interaction with DLC1 could also regulate other cellular processes which could contribute to the specific functions of DLC1 compared with its homologues. Functional assays on cell growth, apoptosis, actin and microtubule dynamics, and embryonic development can be the focus for further investigation. DLC1 and its mutant devoid of EF1A1-interaction could also be used in these functional assays. For future studies, the *in vivo* molecular property of the proteins could be better studied under physiological conditions. Technique such as small interfering RNAs (RNAi) may be used to knock-down the expression of EF1A1 and DLC1 to investigate the cellular function of their interaction when these two proteins are lowly expressed. Zebrafish, a good animal model for development research, can also be used. Currently, DLC1 homologues in zebrafish are under investigation in our group. In future studies of DLC1, we can utilize the morpholino, tissue-specific and inducible knockdown/expression techniques in zebrafish. We have recently successfully employed such strategy to investigate the role of

RhoA to apoptosis in zebrafish embryogenesis (Zhu *et al.*, 2007). Significantly, it provides an excellent alternative to avoid lethal effect of DLC1 deletion in embryo development.

What is the function of the interaction between DLC1 and BNIP-Sα/BNIP-2?

Our current work have also identified BNIP-Sα and BNIP-2 as novel interacting partners for DLC1. It remains to be explored just what functions of such interactions confer towards the entire function and regulation of DLC1 protein. For BNIP-Sα, we have shown that the GAP-binding motif within its RhoA-binding region is essential for the binding with DLC1. Our group has previously shown that BNIP-Sα mediates apoptosis through the binding and activation of RhoA by displacing p50RhoGAP (Zhou *et al.*, 2002; Zhou *et al.*, 2006). Since RhoA is also a target of DLC1, it would be interesting to elucidate the interactive and functional relationship of BNIP-Sα, DLC1 and RhoA. Further binding studies for these three proteins and apoptosis assays could be carried out for future investigation. Further more, as both BNIP-Sα and DLC1 contain potential lipid-binding domains, *i.e.* BCH domain and START domain respectively, it remains to be seen whether lipid metabolites could affect their functions through regulating their interaction. For BNIP-2, we had only identified its interactive activity with DLC1. More binding studies are needed to explore their interaction mechanism. Work on BNIP-2 by our colleagues shows that it can induce cell elongation and membrane protrusions through the interaction with Cdc42 (Zhou *et al.*, 2005). Since

Cdc42 is also the target of DLC1 and DLC1 is a regulator of cell migration which involves actin-disassembly and cell morphological changes, the interaction of DLC1 and BNIP-2 raise an interesting question on whether their interaction could impact on the inhibitory effect of DLC1 in migration. Proper migration activity is also an essential process during embryonic development. Currently, BNIP-2 and DLC1 homologues in zebrafish are under investigation in our lab. Migration assays on cellular level and in zebrafish embryogenesis could be used for future research to explore the functional significance of the interaction between DLC1 and BNIP-2.

Chapter 5

References

Amiri A, Noei F, Jeganathan S, Kulkarni G, Pinke DE, Lee JM (2006) eEF1A2 activates Akt and stimulates Akt-dependent actin remodeling, invasion and migration. *Oncogene* **26**: 3027-3040

Alberts B, Johnson A, Lewis J, Raff M, Roberts K, Walter P (2002) *Molecular Biology of the cell 4th ed.* New York and London: Garland Science

Alpy F, Tomasetto C (2005) Give lipids a START: the StAR-related lipid transfer (START) domain in mammals. *J Cell Sci.* **118**: 2791-801

Alpy F, Tomasetto C (2006) MLN64 and MENTHO, two mediators of endosomal cholesterol transport. *Biochem. Soc. Trans*. **34**: 343-345

Awasthi S, Singhal SS, Sharma R, Zimniak P, Awasthi YC (2003) Transport of glutathione conjugates and chemotherapeutic drugs by RLIP76 (RALBP1): a novel link between G-protein and tyrosine kinase signaling and drug resistance. *Int. J. Cancer* **106**: 635-646.

Barfod ET, Zheng Y, Kuang WJ, Hart MJ, Evans T, Cerione RA, Ashkenazi A (1993) Cloning and expression of a human CDC42 GTPase-activating protein reveals a functional SH3-binding domain. *J Biol. Chem*. **268**: 26059-26062

Barrera FN, Poveda JA, González-Ros JM, Neira JL (2003) Binding of the C-terminal sterile alpha motif (SAM) domain of human p73 to lipid membranes. *J Biol. Chem.* **278**: 46878-46885

Bernards A, Settleman J (2005) GAPs in growth factor signalling. *Growth Factors* **23**: 143-149

Bishop AL, Hall A (2000) Rho GTPases and their effector proteins. *Biochem. J.* **348**: 241-255

Bobak D, Moorman J, Guanzon A, Gilmer L, Hahn C (1997) Inactivation of the small GTPase Rho disrupts cellular attachment and induces adhesion-dependent and adhesion-independent apoptosis. *Oncogene* **15**: 2179-2189

Borkhardt A, Bojesen S, Haas OA, Fuchs U, Bartelheimer D, Loncarevic IF, Bohle RM, Harbott J, Repp R, Jaeger U, Viehmann S, Henn T, Korth P, Scharr D, Lampert F (2000) The human GRAF gene is fused to MLL in a unique t(5;11)(q31;q23) and both alleles are disrupted in three cases of myelodysplastic syndrome/acute myeloid leukemia with a deletion 5q. *Proc. Natl. Acad. Sci. U. S. A.* **97**: 9168–9173

Borradaile NM, Buhman KK, Listenberger LL, Magee CJ, Morimoto ETA, Ory DS, Schaffer JE (2006) A critical role for eukaryotic elongation factor 1A-1 in lipotoxic cell death. *Mol. Biol. Cell* **17:** 770-778

Brouns MR, Matheson SF, Settleman J (2001) p190 RhoGAP is the principal Src substrate in brain and regulates axon outgrowth, guidance and fasciculation. *Nat. Cell Biol.* **3**: 361–367

Burridge K, Wennerberg K (2004) Rho and Rac take center stage. Cell **116**: 167-179

Buschdorf JP, Li Chew L, Zhang B, Cao Q, Liang FY, Liou YC, Zhou YT, Low BC (2006) Brain-specific BNIP-2-homology protein Caytaxin relocalises glutaminase to neurite terminals and reduces glutamate levels. *J. Cell. Sci.* **119**: 3337-3350

Calleros L, Lasa M, Rodriguez-Alvarez FJ, Toro MJ, Chiloeches A (2006) RhoA and p38 MAPK mediate apoptosis induced by cellular cholesterol depletion. *Apoptosis* **11**: 1161-1173

Case DA, Pearlman DA, Caldwell JW, Cheatham III TE, Wang J, Ross WS, Simmerling CL, Darden TA, Merz KM, Stanton RV, Cheng A, Bincent JJ, Crowley M, Tsui V, Gohlke H, Radmer RJ, Duan Y, Pitera J, Massova I, Seibel GL, Singh UC, Weiner PK, Kollman PA (2002) *AMBER 7* University of California, San Francisco

Chang JS, Seok H, Kwon TK, Min DS, Ahn BH, Lee YH, Suh JW, Kim JW, Iwashita S, Omori A, Ichinose S, Numata O, Seo JK, Oh YS, Suh PG (2002) Interaction of Elongation Factor-1α and Pleckstrin Homology domain of phospholipase Cγ1 with activating its activity. *J. Biol. Chem.* **277:** 19697-19702

Chang ZF, Lee HH (2006) RhoA signaling in phorbol ester-induced apoptosis. *J. Biomed. Sci.* **13**: 173-180

Chen E, Proestou G, Bourbeau D, Wang E (2000) Rapid up-regulation of peptide elongation factor EF-1α protein levels is an immediate early event during oxidative stress-induced apoptosis. *Exp. Cell Res.* **259:** 140-148

Chiang SH, Hwang J, Legendre M, Zhang M, Kimura A, Saltiel AR (2003) TCGAP, a multidomain Rho GTPase-activating protein involved in insulin-stimulated glucose transport. *EMBO J.* **22**: 2679-2691.

Ching YP, Wong CM, Chan SF, Leung TH, Ng DC, Jin DY, Ng IO. (2003)   Deleted in liver cancer (DLC) 2 encodes a RhoGAP protein with growth suppressor function and is underexpressed in hepatocellular carcinoma. *J. Biol. Chem.* **278**: 10824-10830

Cleverley SC, Costello PS, Henning SW, Cantrell DA. (2000) Loss of Rho function in the thymus is accompanied by the development of thymic lymphoma. *Oncogene* **19**: 13-20

Cornilescu G, Delaglio F, Bax A (1999) Protein backbone angle restraints from searching a database for chemical shift and sequence homology. *J. Biomol. NMR* **13:** 289-302

Delaglio F, Grzesiek S, Vuister GW, Zhu G, Pfeifer J, Bax A (1995) NMRPipe: a multidimensional spectral processing system based on UNIX pipes. *J. Biomol. NMR* **6:** 277-293

Del Re DP, Miyamoto S, Brown JH (2007) RhoA/Rho kinase up-regulate Bax to activate a mitochondrial death pathway and induce cardiomyocyte apoptosis. *J. Biol. Chem.* **282**: 8069-8078

DerMardirossian C, Bokoch GM (2005) GDIs: central regulatory molecules in Rho GTPase activation. *Trends Cell Biol.* **15**: 356-363

Durkin ME, Ullmannova V, Guan M, Popescu NC (2007A) Deleted in liver cancer 3

(DLC-3), a novel Rho GTPase-activating protein, is downregulated in cancer and inhibits tumor cell growth. *Oncogene* **26**: 4580-4589

Durkin ME, Yuan BZ, Zhou X, Zimonjic DB, Lowey DR, Thorgeirsson SS, Popescu NC (2007B) DLC-1:a Rho GTPase-activating protein and tumour suppressor. *J. Cell Mol. Med.* **11**: 1185-1207

Dvorsky R, Blumenstein L, Vetter IR, Ahmadian MR (2004) Structural insights into the interaction of ROCKI with the switch regions of RhoA. *J. Biol. Chem.* **279**: 7098-7104

Etienne-Manneville S, Hall A (2002) Rho GTPases in cell biology. *Nature* **420**: 629-635

Erickson JW, Cerione RA (2004) Structural elements, mechanism, and evolutionary convergence of Rho protein-guanine nucleotide exchange factor complexes. *Biochemistry* **43**:837-842

Fiorentini C, Matarrese P, Straface E, Falzano L, Fabbri A, Donelli G, cossarizza A, Boquet P, Malorni W (1998) Toxin-induced activation of Rho GTP-binding protein increases Bcl-2 expression and influences mitochondrial homeostasis. *Exp. Cell Res*. **242**: 341-350

Fromigué O, Haÿ E, Modrowski D, Bouvet S, Jacquel A, Auberger P, Marie PJ (2006) RhoA GTPase inactivation by statins induces osteosarcoma cell apoptosis by inhibiting p42/p44-MAPKs-Bcl-2 signaling independently of BMP-2 and cell differentiation. *Cell Death Differ.* **13**: 1845-1856

Fu L, Qin YR, Xie D, Hu L, Kwong DL, Srivastava G, Tsao SW, Guan XY (2007) Characterization of a novel tumor-suppressor gene PLC delta 1 at 3p22 in esophageal squamous cell carcinoma. *Cancer Res.* **67**: 10720-10726

Fukata M, Nakagawa M, Kaibuchi K (2003) Roles of Rho-family GTPases in cell polarisation and directional migration. *Curr. Opin. Cell Biol*. **15**: 590-597

Gangwani L, Mikrut M, Galcheva-Gargova Z, Davis RJ (1998) Ineraction of ZPR1 with translation elongation factor-1α in proliferating cell. *J. Cell Biol.* **143:** 1471-1484

Glass CA and Pollard KM (1990) Post-translational isoprenylation of human lamin B in the Reticulocyte Lysate In Vitro Translation System. *Promega Notes* **26**: 6-10

Goley ED, Welch MD (2006) The Arp2/3 complex: an actin nucleator comes of age. *Nat. Rev. Mol. Cell Biol.* **7**: 713-726

Gomes C, Oh SD, Kim JW, Chun SY, Lee K, Kwon HB, Soh J (2004) Expression of the putative sterol binding protein Stard6 gene is male germ cell-specific. *Biol. Reprod.* **72**: 651-658

Goodison S, Yuan J, Sloan D, Kim R, Li C, Popescu NC, Urquidi V (2005) The RhoGAP protein DLC-1 functions as a metastasis suppressor in breast cancer cells. *Cancer Res*. **65:** 6042-6053

Gross SR, Kinzy TG (2007) Improper actin organization of actin cytoskeleton affects protein synthesis at initiation. *Mol. Cell Biol.* **27**: 1974-1989

Gross SR, Kinzy TG (2005) Translation elongation factor 1A is essential for regulation of the actin cytoskeleton and cell morphology. *Nat. Struct. & Mol. Biol.* **12:** 772-778

Grzesiek S, Bax A (1993) Amino acid type determination in the sequential assignment procedure of uniformly ^{13}C/^{15}N-enriched proteins. *J. Biomol. NMR*, **3:** 185-204

Hakoshima T, Shimizu T, Maesaki R (2003) Structural basis of the Rho GTPases signaling. *J Biochem.* **134**: 327-331

Hall A (1998) Rho GTPases and the actin cytoskeleton. *Science* **279**: 509-514

Hall A (2005) Rho GTPases and the control of cell behaviour. *Biochem. Soc. Trans.* **33**: 891-895

Healy KD, Hodgson L, Kim TY, Shutes A, Maddileti S, Juliano RL, Hahn KM, Harden TK, Bang YJ, Der CJ (2007) DLC-1 suppresses non-small cell lung cancer growth and invasion by RhoGAP-dependent and independent mechanisms. *Mol. Carcinog.* **DOI**: 10.1002/mc.20389

Hakem A, Sanchez-Sweatman O, You-Ten A, Duncan G, Wakeham A, Khokha R, Mak TW. (2005) RhoC is dispensable for embryogenesis and tumor initiation but essential for metastasis. *Genes Dev.* **19**: 1974-1979

Herrmann T, Güntert P, Wüthrich K (2002) Protein NMR structure determination with automated NOE assignment using the new software CANDID and the torsion angle dynamics algorithm DYANA. *J. Mol. Biol.* **319:** 209-227

Hers I, Wherlock M, Homma Y, Yagisawa H, Tavare JM (2006) Identification of p122RhoGAP (deleted in liver cancer-1) serine-322 as a substrate for protein kinase B and RSK in insulin-stimulated cells. *J. Biol. Chem.* **281:** 4762-4770

Hippenstiel S, Schmeck B, N'Guessan PD, Seybold J, Krüll M, Preissner K, Eichel-Streiber CV, Suttorp N (2002) Rho protein inactivation induced apoptosis of cultured human endothelial cells. *Am. J. Physiol. Lung Cell Mol. Physiol.* **283**: L830-L838

Hoffman GR, Cerione RA (2000) Flipping the switch: the structural basis for signaling through the CRIB motif. *Cell* **102**: 403-406

Holm L, Sander C (1998) Touring protein fold space with Dali/FSSP. *Nucleic Acids Res*. **26:** 316–319

Homma Y, Emori Y (1995) A dual functional signal mediator showing RhoGAP and phospholipase C-delta stimulating activities. *EMBO J*. **14:** 286-91

Hu KQ, Settleman J (1997) Tandem SH2 binding sites mediate the RasGAP-RhoGAP interaction: A conformational mechanism for SH3 domain regulation. *EMBO J.* **16**: 473-483

Izawa T, Fukata Y, Kimura T, Iwamatsu A, Dohi K, Kaibuchi K (2000) Elongation Factor-1a is a novel substrate of Rho-Associated Kinase. *Biochem. Biophy. Res. Comm.* **278:** 72-78

Jaffe AB, Hall A (2005) Rho GTPases: biochemistry and biology. *Annu. Rev. Cell. Dev. Biol.* **21**: 247-269

Jeganathan S, Lee JM (2007) Binding of elongation factor eEF1A2 to phosphatidylinositol 4-kinase b stimulates lipid kinase activity and phosphatidylinositol 4-phosphate generation. *J. Biol. Chem.* **282:** 372-380

Jenna S, Hussain NK, Danek EI, Triki I, Wasiak S, McPherson PS, Lamarche-Vane N (2002) The activity of the GTPase-activating protein CdGAP is regulated by the endocytic protein intersectin. *J. Biol. Chem* **277**: 6366–6373.

Jiang W, Sordella R, Chen GC, Hakre S, Roy AL, Settleman J (2005) TSC2 is phosphorylated and inhibited by Akt and suppressed mTOR signaling. *Nat. Cell Biol.* **4**: 648-657

Johnson BA, Blevins RA (1994) NMRView: A computer program for the visualization and analysis of NMR data. *J. Biomol. NMR* **4**: 603–614

Joneson T, Bar-Sagi D (1999) Suppression of Ras-induced apoptosis by the Rac GTPase. *Mol. Cell. Biol.* **19**: 5892-5901

Kandpal RP (2006) Rho GTPase activating proteins in cancer phenotypes. *Curr. Protein Pept. Sci.* **7**: 355-365

Kay LE, Xu GY, Singer AU, Muhandiram DR, Forman-Kay JD (1993) A gradient-enhanced HCCH-TOCSY experiment for recording side-chain ^{1}H and ^{13}C correlations in H_2O samples of proteins. *J. Magn. Reson.* **B101:** 333-337

Khosravi-Far R, Solski PA, Clark GJ, Kinch MS, Der CJ (1995) Activation of Rac1, RhoA, and mitogen-activated protein kinases is required for Ras transformation. *Mol. Cell Biol.* **15**: 6443-6453

Kielbassa K, Müller HJ, Meyer HE, Marks F, Gschwendt M (1995) Protein kinase C delta-specific phosphorylation of the elongation factor eEF-alpha and an eEF-1 alpha peptide at threonine 431. *J. Biol. Chem.* **270:** 6156-6162

Kim TY, Jong HS, Song SH, Dimtchev A, Jeong SJ, Lee JW, Kim TY, Kim NK, Jung M & Bang YJ (2003) Transcriptional silencing of the DLC-1 tumor suppressor gene by epigenetic mechanism in gastric cancer cells. Oncogene 22: 3943-3951

Kim CA, Bowie JU (2003)SAM domains: uniform structure, diversity of function. *Trends in Biochem. Sci.* **28:** 625-628.

Knudson SM, Frydenberg J, Clark BF, Leffers H (1993) Tissue-dependent variation in the expression of elongation factor-1 alpha isoforms: isolation and characterization of a cDNA encoding a novel variant of human elongation-factor 1 alpha. *Eur. J. Biochem.* **215**: 549-554

Kobayashi H, Suzuki M, Kanayama N, Terao T (2004) Genetic down-regulation of phosphoinositide 3-kinase by bikunin correlates with suppression of invasion and metastasis in human ovarian cancer HRA cells. J. Biol. Chem. 279: 6371-6379

Koradi R, Billeter M, Wüthrich K (1996) MOLMOL: A program for display and. analysis of macromolecular structures. *J. Mol. Graphics* **14:** 51–55

Krieg PA, Varnum SM, Wormington WM, Melton DA (1989) The mRNA encoding elongation factor-1α (eEF-1α) is a major transcript at the midblastula transition in Xenopus. *Dev. Biol.* **133:** 93-100

Krugmann S, Williams R, Stephens L, Hawkins PT (2004) ARAP3 is a PI3K- and rap-regulated GAP for RhoA. *Curr. Biol.* **14**: 1380-1384

Kuriyama R, Savereide P, Lefebuve P, Dasgupta S (1990) The predicted amino acid sequence of a centrosphere protein in dividing sea urchin eggs is similar to elongation factor (EF-1a). *J. Cell Sci.* **95:** 231-236

Kwan JJ, Donaldson LW (2007) The NMR structure of the murine DLC2SAM domain reveals a variant fold that is similar to a four-helix bundle. *BMC Struct. Biol.* **7**: 34

Lamberti A, Caraglia M, Longo O, Marra M, Abbruzzese A, Arcari P (2004) The translation elongation factor 1A in tumorigenesis, signal transduction and apoptosis. *Amino Acids* **26:** 443-448

Lamberti A, Longo O, Marra M, Tagliaferri P, Bismuto E, Fiengo A, Viscomi C, Budillon A, Rapp UR, Wang E, Venuta S, Abbruzzese A, Arcari P, Caraglia M (2007) C-Raf antagonizes apoptosis induces by IFN-α in human lung cancer cells by phosphorylation and increase of the intracellular content of elongation factor 1A. *Cell Death Differ.* **14:** 952-962

Lancaster CA, Taylor-Harris PM, Self AJ, Brill S, van Erp HE, Hall A (1994) Characterization of rhoGAP. A GTPase-activating protein for rho-related small GTPases. *J Biol Chem.* **269**:1137-1142

Larsen TA, Olson AJ, Goodsell DS (1998) Morphology of protein–protein interfaces. *Structure (London)* **6:** 421–427

Laskowski RA, Rullmann JAC, MacArthur MW, Kaptein R, Thornton JM (1996) AQUA and PROCHECK-NMR: programs for checking the quality of protein structures solved by NMR. *J Biomol. NMR* **8:** 477–486

Lau J, Castelli LA, Lin EC, Macaulay SL (2006) Identification of elongation factor 1 alpha as a potential associated binding partner of Akt2. *Mol. Cell Biochem.* **286:** 17-22

Lee JS, Kamijo K, Ohara N, Kitamura T, Miki T (2004) MgcRacGAP regulates cortical activity through RhoA during cytokinesis. *Exp. Cell Res.* **293**: 275-282

Leung TH, Ching YP, Yam JW, Wong CM, Yau TO, Jin DY, Ng IO. (2005)   Deleted in liver cancer 2 (DLC2) suppresses cell transformation by means of inhibition of RhoA activity. *Proc Natl Acad Sci U S A* **102**:15207-15212

Li H, Fung KL, Jin DY, Chung SM, Ching YP, Ng OL, Sze KH, Ko CB, Sun H (2007) Solution structures dynamics and lipid-binding of the sterile a-motif domain of the deleted in liver cancer 2. *Proteins* **67**: 1154-1166

Li R, Zhang B, Zheng Y (1997) Structural determinants required for the interaction between Rho GTPase and the GTPase-activating domain of p190. *J. Biol. Chem.* **272**: 32830-32835

Liao YC, Lo SH (2007) Deleted in liver cancer-1 (DLC-1): A tumor suppressor not just for liver. *Int. J. Bioch. Cell Biol.* **Doi**: 10.1016/j.biocel.2007.04.008

Liao YC, Si L, White RWV, Lo SH. (2007) The phosphotyrosine-independent interactionof DLC-1 and the SH2 domain of cten regulates focal adhesion localization and growth suppression activity of DLC-1. *J. Cell Biol.* **176**: 43-49

Lin Z, Xu Y, Yang S, Yang D (2006) Sequence-specific assignment of aromatic resonances of uniformly ^{13}C, ^{15}N-labeled proteins with the use of ^{13}C- and ^{15}N-edited NOESY spectra. *Angew. Chem. Int. Ed.* **45:** 1960-1963

Liu G, Grant WM, Persky D, Latham VM, Singer RH Condeelis J (2002) Interaction of elongation factor 1α with F-actin and β-actin mRNA: Implications for anchoring mRNA in cell protrusions. *Mol. Biol. of the Cell* **13:** 579-592

Low BC, Seow KT, Guy GR (2000A) Evidence for a novel Cdc42GAP domain at the carboxyl terminus of BNIP-2. *J. Biol. Chem.* **275:** 14415-14422

Low BC, Seow KT, Guy GR (2000B) The BNIP-2 and Cdc42GAP Homology domain of BNIP-2 mediates itshomophilic association and heterophilic interaction with Cdc42GAP. *J. Biol. Chem.* **275:** 37742-37751

Lua BL, Low BC (2004) BPGAP1 interacts with cortactin and facilitates its translocation to cell periphery for enhanced cell migration. *Mol. Biol. Cell* **15:** 2873-2883

Lua BL, Low BC (2005) Activation of EGF receptor endocytosis and ERK1/2 signaling by BPGAP1 requires direct interaction with EEN/endophilin II and a functional RhoGAP domain. *J. Cell Sci.* **118**:2707-2721

Mackereth CD, Scharpf M, Gentile LN, MacIntosh SE, Slupsky CM, McIntosh LP (2004) Diversity in structure and function of the Ets family PNT domains. *J. Mol. Biol.* **342**: 1249-1264

Malliri A, van der Kammen RA, Clark K, van der Valk M, Michiels F, Collard JG (2002) Mice deficient in the Rac activator Tiam1 are resistant to Ras-induced skin tumours. *Nature* **417**: 867-871

Malliri A, Collard JG (2003) Role of Rho-family proteins in cell adhesion and cancer. *Current Opinion in Cell Biol.* **15**:583-589

Millard TH, Sharp SJ, Machesky LM (2004) Signalling to actin assembly via the WASP (Wiskott-Aldrich syndrome protein)-family proteins and the Arp2/3 complex. *Biochem. J.* **380**: 1-17.

Modarressi MH, Cheng M, Tarnasky HA, Lamarche-Vane N, de Rooij DG, Ruan Y, van der Hoorn FA (2004) A novel testicular RhoGAP-domain protein induces apoptosis. *Biol. Reprod.* **71**: 1980-1990

Montelione GT, Lyons BA, Emerson SD, Tashiro M (1992) An efficient triple resonance experiment using carbon-13 isotropic mixing for determining sequence-specific resonance assignments of isotopically-enriched proteins. *J. Am. Chem. Soc.* **114**, 10974 – 10975

Moon SY, Zheng Y (2003) Rho GTPases-activating proteins in cell regulation. *Trends in cell Biol.* **13**: 13-22

Moore RC, Durso NA, Cyr RJ (1998) Elongation factor-1alpha stabilizes microtubules in a calcium/calmodulin-dependent manner. *Cell Motil. Cytoskel.* **41:** 168-180

Moorman JP, Luu D, Wickham J, Bobak DA, Hahn Cs (1999) A balance of signaling by Rho family small GTPases RhoA, Rac1 and Cdc42 coordinates cytoskeletal morphology but not cell survival. *Oncogene* **18**: 47-57

Murray JW, Edmonds BT, Liu G, Condeelis J (1996) Bundling of actin filaments by elongation factor 1 α inhibits polymerization at filament ends. *J. Cell Biol.* **135:** 1309-1321

Nassar N, Hoffman GR, Manor D, Clardy JC, Cerione RA (1998) Structures of Cdc42 bound to the active and catalytically compromised forms of Cdc42GAP. *Nat. Struct. Biol.* **5**: 1047-1052

Ng IO, Liang Z, Cao L, Lee TK (2000) *DLC-1* is deleted in primary hepatocellular carcinoma and exerts inhibitory effects on proliferation of hepatoma cell lines with deleted *DLC-1*. *Cancer Research* **60**: 6581-6584

Nobes CD, Hall A (1995) Rho, Rac and Cdc42 GTPases regulate the assembly of multimolecular focal complexes associated with actin stress fibers, lamellipodia and filopodia. Cell 81: 53-62

Olofsson, B (1999) Rho guanine dissociation inhibitors: pivotal molecules in cellular signaling. Cell Signal. 11:545-554

Peck J, Douglas IVG, Wu CH, Burbelo PD (2002) Human RhoGAP domain-containing proteins: structure, function and evolutionary relationaships. FEBS Letters 528: 27-34

Ponting CP, Aravind L (1999) START: a lipid-binding domain in StAR, HD-ZIP and signaling proteins. *Trends Biochem. Sci.* 24: 130-132

Prendergast GC, Khosravi-Far R, Solski PA, Kurzawa H, Lebowitz PF, Der CJ (1995)
Critical role of Rho in cell transformation by oncogenic Ras. *Oncogene* **10**: 2289-2296

Qiao F, Bowie JU (2005) The many faces of SAM. *Sci. STKE* **286:** re7

Qian X, Li G, Asmussen HK, Asnaghi L, Vass WC, Braverman R, Yamada KM, Popescu
NC, Papageorge AG, Lowy DR (2007) Oncogenic inhibition by a deleted in liver cancer
gene requires cooperation between tensin binding and Rho-specific GTPase-activating
protein activities. *Proc Natl Acad Sci* U S A **104**: 9012-9017

Raya A, Revert-Ros F, Martinez-Martinez P, Navarro S, Rosello E, Vieites B, Granero F,
Forteza J, Saus J (2000) Goodpasture antigen-binding protein, the kinase that
phosphorylates the Goodpasture antigen, is an alternatively spliced variant implicated in
autoimmune pathogenesis. *J. Biol. Chem.* **275**: 40392-40399

Ren XD, Kiosses WB, Schwartz MA (1999) Regulation of the small GTP-binding protein
Rho by cell adhesion and the cytoskeleton. EMBO J. **18**: 578-585

Riento K, Ridley AJ (2003) Rocks: multifunctional kinases in cell behaviour. *Nat. Rev.
Mol. Cell. Biol.* **4**: 446-456.

Rohatgi R, Ma L, Miki H, Lopez M, Kirchhausen T, Takenawa T, Kirschner MW (1999)
The interaction between N-WASP and the Arp2/3 complex links Cdc42-dependent signals
to actin assembly. *Cell* **97**: 221-231

Rodriguez OC, Schaefer AW, Mandato CA, Forscher P, Bement WM, Waterman-Storer CM (2003) Conserved microtubule-actin interactions in cell movement and morphogenesis. Nat. Cell Biol. **5:** 599-609

Roof RW, Dukes BD, Chang JH, Parsons SJ (1998) Phosphotyrosine (p-Tyr)-dependent and -independent mechanisms of p190 RhoGAP-p120 RasGAP interaction: Tyr 1105 of p190, a substrate for c-Src, is the sole p-Tyr mediator of complex formation. *Mol. Cell. Biol.* **18**: 7052-7063

Scheffzek K, Ahmadian MR (2005) GTPase activating proteins: structural and functional insights 18 years after discovery. *Cell. Mol.Life Sci.* **62**: 3014-3038

Sekimata M, Kabuyama Y, Emori Y, Homma Y (1998) Morphological changes and detachment of adherent cells induced by p122, a GTPase-activating protein for Rho. *J. Biol. Chem.* **274:** 17757-17762

Seng TJ, Low JS, Li H, Cui Y, Goh HK, Wong ML, Srivastava G, Sidransky D, Califano J, Steenbergen RD, Rha SY, Tan J, Hsieh WS, Ambinder RF, Lin X, Chan AT, Tao Q (2007) The major 8p22 tumor suppressor DLC1 is frenquently silenced by methylation in both endemic and sporadic nasopharyngeal, esophageal, and cervical carcinomas, and inhibits tumor cell colony formation. *Oncogene*, **26**: 934-944

Shang X, Zhou YT, Low BC (2003) Concerted regulation of cell dynamics by BNIP-2 and Cdc42GAP homology/Sec14-like, proline-rich, and GTPase-activating protein domains of a novel Rho GTPase-activating protein, BPGAP1. *J Biol. Chem.* **278**: 45903-45914

Shi H, Guo J, Duff DJ, Rahmatpanah F, Chitima-Matsiga R, Al-Kuhlani M, Taylor KH, Sjahputera O, Andreski M, Wooldridge JE, Caldwell CW (2007A) discovery of novel epigenetic markers in non-Hodgkin's lymphoma. *Carcinogenesis* **28**: 60-70

Shi L, Fu WY, Hung KW, Porchetta C, Hall C, Fu AK, Ip NY (2007B) Alpha2-chimaerin interacts with EphA4 and regulates EphA4-dependent growth cone collapse. *Proc. Natl. Acad. Sci. U. S. A.* **104**: 16347-16352

SmallaM, Schmieder P, Kelly M, Ter Laak A, Krause G, Ball L, Wahl M, Bork P, Oschkinat H (1999) Solution structure of the receptor tyrosine kinase EphB2 SAM domain and identification of two distinct homotypic interaction sites. *Protein Sci.* **8**: 1954-1961

Soccio RE, Breslow JL (2003) StAR-related lipid transfer (START) proteins: mediators of intracellular lipid metabolism. *J. Biol. Chem.* **278**: 22183-22186

Sordella R, Classon M, Hu KQ, Matheson SF, Brouns MR, Fine B, Zhang L, Takami H, Yamada Y, Settleman J (2002) Modulation of CREB activity by the Rho GTPase regulates cell and organism size during mouse embryonic development. *Dev. Cell.* **2**: 553-565

Sordella R, Jiang W, Chen GC, Curto M, Settleman J (2003) Modulation of Rho GTPase signaling regulates a switch between adipogenesis and myogenesis. *Cell* **113**: 147-158

Stapleton D, Balan I, Pawson T, Sicheri F (1999) The crystal structure of an Eph receptor SAM domain reveals a mechanism for modular dimerization. *Nat. Struct. Biol.* **6**: 44-49

Su L, Agati JM, Parsons SJ (2003) p190RhoGAP is cell cycle regulated and affects cytokinesis. *J. Cell Biol.* **163**: 571-582

Syed V, Mukherjee K, Lyons-Weiler J, Lau KM, Mashima T, Tsuruo T, Ho SM (2005) Identification of ATF-3, caveolin-1, DLC-1, and NM23-H2 as putative antitumorigenic, progesterone-regulated genes for ovarian cancer cells by gene profiling. *Oncogene* **24**: 1774-1787

Talapatra S, Wagner JDO, Thompson CB (2002) Elongation factor-1 alpha is selective regulator of growth factor withdrawal and ER stress-induced apoptosis. *Cell Death Differ*. **9:** 856-861

Taniguchi S, Miyamoto S, Sadano H, Kobayashi H (1992) Rat elongation factor 1 alpha: sequence of cDNA from a highly metastatic fos-transferred cell line. *Nucleic Acids Res.* **19:** 6949

Tatsuka M, Mitsui H, Wada M, Nagata A, Nojima H, Okayama H (1992) Elongation factor-1α gene determines susceptibility to transformation. *Nature* **359:** 333-336

Tcherkezian J, Lamarche-Vane N (2007) Current knowledge of the large RhoGAP family of proteins. *Biol. Cell* **99**:67-86

Thornton S, Anand N, Purcell D, Lee J (2003) Not just for housekeeping: protein initiation and elongation factors in cell growth and tumorigenesis. *J. Mol. Med.* **81:** 536-548

Umikawa M, Tanaka K, Kamei T, Shimizu K, Imamura H, Sasaki T, Takai Y (1998) Interaction of Rho1p target Bni1p with F-actin-binding elongation factor 1alpha: implication in Rho1p-regulated reorganization of the actin cytoskeleton in *Saccharomyces cerevisiae*. *Oncogene* **16:** 2011-2016

van Leeuwen FN, van der Kammen RA, Habets GG, Collard JG (1995) Oncogenic activity of Tiam1 and Rac1 in NIH3T3 cells. *Oncogene* **11**:2215-2221

Vetter IR, Wittinghofer A (2001) The guanine nucleotide-binding switch in three dimensions. *Science* **294**: 1299-1304

Villalonga P, Ridley AJ (2006) Rho GTPases and cell cycle control. *Growth Factors* **24**: 159-164

Wang DZ, Nur-E-Kamal MS, Tikoo A, Montague W, Maruta H (1997) The GTPase and Rho GAP domains of p190, a tumor suppressor protein that binds the M_r 120,000 Ras GAP, independently function as anti-Ras tumor suppressors. *Cancer Res.* **57**: 2478–2484

Wang H, Kazanietz MG (2006) The lipid second messenger diacylglycerol as a negative regulator of Rac signaling. *Biochem. Soc. Trans.* **34**:855-857

Wennerberg K, Der CJ (2004) Rho-family GTPases: it's not only Rac and Rho (and I like it). *J. Cell Sci.* **117:** 1301-1312

Wennerberg K, Rossman KL, Der CJ (2005) The RAS superfamily at a glance. *J. Cell Sci.* **118**: 843-846

Wheeler AP, Ridley AJ (2004) why three Rho proteins? RhoA, RhoB, RhoC, and cell motility. *Exp. Cell Res.* **301**: 43-49

Wittekind M, Mueller L (1993) HNCACB, a high-sensitivity 3D NMR experiment to correlate amide-proton and nitrogen resonances with the alpha- and beta-carbon resonances in proteins. *J. Magn. Reson., Ser.* B **101:** 201-205

Wong CM, Lee JMF, Ching YP, Jin DY, Ng IO (2003) Genetic and epigenetic alterations of DLC-1 gene in hapatocellular carcinoma. *Cancer Res*. **63:** 7646-7651

Wong CM, Yam JWP, Ching YP, Yau TO, Leung THY, Jin DY, Ng IO (2005) Rho GTPase-Activating protein deleted in liver cancer suppresses cell proliferation and invasion in hepatocellular carcinoma. *Cancer Res.* **65:** 8861-8868

Wong K, Ren XR, Huang YZ, Xie Y, Liu B, Saito H, Tang H, Wen L, Brady-Kalnay SM, Mei L, Wu JY, Xiong WE, Rao Y (2001) Signal transduction in neuronal migration: roles of GTPase activating proteins and the small GTPase Cdc42 in the Slit-Robo pathways. Cell **107**: 209-221

Yam JW, Ko FC, Chan CY, Jin DY, Ng IO (2006) Interaction of deleted in liver cancer 1 with tensin2 in caveolae and implications in tumor suppression. *Cancer Res.* **66**: 8367-8372

Yamada T, Sakisaka T, Hisata S, Baba T, Takai Y (2005) RA-RhoGAP, Rap-activated Rho GTPase-activating protein implicated in neurite outgrowth through Rho. *J. Biol. Chem.* **280**: 33026-33034

Yamaga M, Sekimata M, Fujii M, Kawai K, Kamata H, Hirata H, Homma Y, Yagisawa H (2004) A PLCdelta1-binding protein, p122/RhoGAP, is localized in caveolin-enriched membrane domains and regulates caveolin internalization. *Genes Cells* **9**: 25-37

Yamaga M, Kawai K, Kiyota M, Homma Y, Yagisawa H (2007) Recruitment and activation of phospholipase C (PLC)-delta(1) in lipid rafts by muscarinic stimulation of PC12 cells: Contribution of p122RhoGAP/DLC1, a tumor-suppressing PLCdelta(1) binding protein. *Adv. Enzyme Regul.* [Epub ahead of print]

Yamanaka M, Koga M, Tanaka H, Nakamura Y, Ohta H, Yomogida K, Tsuchida J, Iguchi N, Nojima H, Nozaki M, Matsumiya K, Okuyama A, Toshimori K, Nishimune Y (2000) Molecular cloning and characterization of phosphatidylcholine transfer protein-like protein gene expressed in murine haploid germ cells. *Biol.Reprod.* **62**: 1694-1701

Yang W, Boss WF (1994) Regulation of phosphatidylinositol 4-kinase by the protein activator PIK-A49. Activation requires phosphorylation of PIK-A49. *J. Biol. Chem.* **269**: 3852-3857

Yang W, Burkhart W, Cavallius J, Merrick WC, Boss WF (1993) Purification and characterization of a phosphatidylinositol 4-kinase activator in carrot cells. *J. Biol. Chem.* **268**: 392-398

Yuan BZ, Miller NJ, Keck CL, Zimonjic DB, Thorgeirsson SS, Popescu NC (1998) Cloning, characterization, and chromosomal localization of a gene frequently deleted in human liver cancer (*DLC-1*) homologous to rat RhoGAP. *Cancer Res*. **58:** 2196-2199

Yuan BZ, Zhou X, Durkin ME, Zimonjic DB, Gumundsdottir K, Eyfjord JE, Thorgeirsson SS, Popescu NC (2003) *DLC-1* gene inhibits human breast cancer cell growth and *in vivo* tomorigenecity. *Oncogene* **22:** 445-450

Zhang Y, Gu X, Yuan X (2007) Phenylalanine activates the mitochondria-mediated apoptosis through the RhoA/Rho-associated kinase pathway in cortical neurons. *Eur. J. Neurosci.* **25**: 1341-1348

Zhao WM, Fang G (2005) MgcRacGAP controls the assembly of the contractile ring and the initiation of cytokinesis. *Proc. Natl. Acad. Sci. U S A* **102**: 13158-13163.

Zhou X, Thorgeirsson SS, Popescu NC (2004) Restoration of *DLC-1* gene expression induces apoptosis and inhibits both cell growth and tumorigenicity in human hepatocellular carcinoma cells. *Oncogene* **23:** 1308-1313

Zhou YT, Soh UJK, Shang X, Guy GR, Low BC (2002) The BNIP-2 and Cdc42GAP homology/Sec14p-like domain of BNIP-Sa is a novel apoptosis-inducing sequence. *J. Biol. Chem.* **277**: 7483-7492

Zhou YT, Guy GR, Low BC (2005) BNIP-2 induces cell elongation and membrane protrusions by interacting with Cdc42 via a unique Cdc42-binding motif within its BNIP-2 and Cdc42GAP homology domain. *Exp. Cell Res.* **303**: 263-274

Zhou YT, Guy GR, Low BC (2006) BNIP-Salpha induces cell rounding and apoptosis by displacing p50-RhoGAP and facilitating RhoA activation via its unique motifs in the BNIP-2 and Cdc42GAP homology domain. *Oncogene* **25**: 2393-2408

Zhu S, Korzh V, Gong Z, Low BC (2007) RhoA prevents apoptosis during zebrfish embryogenesis through activation of Mek/Erk pathway. *Oncogene* **DOI**: 10.1038/sj.onc.1210790